Preliminary Investigation of the Seismic Vulnerability of the Alaskan Way Viaduct

WA-RD 265.1

Final Technical Report
April 1992

Washington State Department of Transportation
Washington State Transportation Commission
in cooperation with the
United States Department of Transportation
Federal Highway Administration

TECHNICAL REPORT STANDARD TITLE PAGE

1. REPORT NO.	2. GOVERNMENT ACCESSION NO.	3. RECIPIENT'S CATALOG NO.
WA-RD 265.1		

4. TITLE AND SUBTITLE

PRELIMINARY INVESTIGATION OF THE SEISMIC VULNERABILITY OF THE ALASKAN WAY VIADUCT

5. REPORT DATE

April 1992

6. PERFORMING ORGANIZATION CODE

7. AUTHOR(S)

Colin B. Brown, Marc O. Eberhard, Steven L. Kramer, Charles W. Roeder, and John F. Stanton

8. PERFORMING ORGANIZATION REPORT NO.

9. PERFORMING ORGANIZATION NAME AND ADDRESS

Washington State Transportation Center (TRAC)
University of Washington, JE-10
The Corbet Building, Suite 204; 4507 University Way N.E.
Seattle, Washington 98105

10. WORK UNIT NO.

11. CONTRACT OR GRANT NO.

GC8719, Task 43

12. SPONSORING AGENCY NAME AND ADDRESS

Washington State Department of Transportation
Transportation Building, MS: 7370
Olympia, Washington 98504-7374

13. TYPE OF REPORT AND PERIOD COVERED

Final technical report

14. SPONSORING AGENCY CODE

15. SUPPLEMENTARY NOTES

This study was conducted in cooperation with the U.S. Department of Transportation, Federal Highway Administration.

16. ABSTRACT

The University of Washington (UW) team reviewed the Washington State Department of Transportation (WSDOT) report titled "Earthquake Analyses of the Alaskan Way Viaduct" and performed an independent assessment of two typical sections of the structure. Additional analyses were performed to investigate the influence of some factors that were not considered in the WSDOT report.

The input motion and geotechnical characteristics assumed in the WSDOT report were consistent with the information available to the WSDOT and to the UW. However, the paucity of information available regarding the seismological risk and the subsoil conditions precluded the possibility of reliably estimating the input motion, foundations stiffnesses, foundation capacities, and potential for liquefaction. Inspection of the structural plans suggested that timber-concrete spliced piles in the section of the structure built by the WSDOT might be particularly vulnerable.

The elastic dynamic models generated by WSDOT and those constructed for this study were found to give comparable natural periods in the first three modes. Those in the higher modes differed because of the disparate ways in which the structures were modelled. However, the higher modes provided only a small portion of the total response, so the differences in calculated response were small.

For the WSDOT designed part of the structure, g-ratings and dynamic code ratios were established by assuming that the reinforcement would reach its yield strength. The present study found the structure to be generally weaker than did the WSDOT study. Some of the ratings showed a consistent relationship with those given by the WSDOT sutdy, while others showed considerable scatter. Regardless of the resolution of the discrepancies, both analyses indicated that the demands on structural members would be likely to greatly exceed their capacities. The main shortcomings in the structure appeared to be inadequate confinement steel and development lengths that were too short. Because no distress was observed after the 1965 Seattle earthquake, these calculations are undoubtedly conservative. However, the response of these brittle details cannot be predicted reliably without further investigation. The University of Washington team is proposing further study to verify the seismic safety of the structure.

17. KEY WORDS	18. DISTRIBUTION STATEMENT
Bridge, reinforced concrete, earthquakes, foundations	No restrictions. This document is available to the public through the National Technical Information Service, Springfield, VA 22616

19. SECURITY CLASSIF. (of this report)	20. SECURITY CLASSIF. (of this page)	21. NO. OF PAGES	22. PRICE
None	None	84	

Rev. 6/12/92

Final Technical Report

Research Project GC 8719, Task 43
Alaskan Way Viaduct Seismic Vulnerability

PRELIMINARY INVESTIGATION OF THE SEISMIC VULNERABILITY OF THE ALASKAN WAY VIADUCT

by

Colin B. Brown
Marc O. Eberhard
Steven L. Kramer
Charles W. Roeder
John F. Stanton

Washington State Transportation Center (TRAC)
University of Washington, JE-10
The Corbet Building, Suite 204
4507 University Way N.E.
Seattle, Washington 98105

Washington State Department of Transportation
Technical Monitor
Myint Lwin
Bridge and Structures Office
Washgington State Department of Transportation

Prepared for

Washington State Transportation Commission
Department of Transportation
and in cooperation with
U.S. Department of Transportation
Federal Highway Administration

April 1992

DISCLAIMER

The contents of this report reflect the views of the authors, who are responsible for the facts and the accuracy of the data presented herein. The contents do not necessarily reflect the official views or policies of the Washington State Transportation Commission, Department of Transportation, or the Federal Highway Administration. This report does not constitute a standard, specification, or regulation.

TABLE OF CONTENTS

Section		Page
Summary		**1**
Chapter 1. Introduction		**4**
1.1	Context	4
1.2	Description of Structure	5
Chapter 2. Procedures for UW Evaluation		**8**
2.1	Inspection	8
2.2	Geotechnical Aspects	8
2.3	Structural Analyses	9
2.4	Required and Computed Strengths	10
Chapter 3. Comparison of UW Evaluation with WSDOT Evaluation		**15**
3.1	Inspection	15
3.2	Geotechnical Aspects	19
3.3	Structural Analyses	25
3.4	Required and Computed Strengths	32
Chapter 4. Discussion		**42**
4.1	Structural Safety	42
4.2	Geotechnical Aspects	45
4.3	Structural Analyses	48
4.4	Required and Computed Strengths	68
Chapter 5. Recommendations/Implementation		**83**
5.1	Criteria	83
5.2	Geotechnical Information	83
5.3	Details	83
5.4	Material Properties	84
5.5	Atypical Frames	84

LIST OF FIGURES

Figure		Page
1.1.	Elevation of WSDOT Section Bent	6
1.2.	Elevation of Seattle Section Bent	7
3.1.	Load-Deflection Curves for Piles (Missing Fig.)	22
3.2.	Mode Shapes 1 and 2 of WSDOT Model	28
3.3.	Mode Shapes 3 and 4 of WSDOT Model	29
3.4.	Mode Shapes 1 and 2 of Seattle Model	30
3.5.	Mode Shapes 3 and 4 of Seattle Model	31
3.6.	Transverse g-Ratings	33
3.7.	Longitudinal Code Ratios	37
3.8.	Transverse Code Ratios	38
4.1.	Mode Shapes 1 and 2 of Pinned-Base Model	53
4.2.	Mode Shapes 3 and 4 of Pinned-Base Model	54
4.3.	Mode Shapes 1 and 2 of Outrigger Model	57
4.4.	Mode Shapes 3 and 4 of Outrigger Model	58
4.5.	Moment Diagrams for WSDOT Section Model with Applied Forces	60
4.6.	Transverse-Loading Moment Envelopes for WSDOT Section Model from Spectral Analysis	61
4.7.	Transverse-Loading Shear Envelopes for WSDOT Section Model from Spectral Analysis	62
4.8.	Longitudinal-Loading Moment Envelopes for WSDOT Section Model from Spectral Analysis	64
4.9.	Transverse-Loading Moment Envelopes for Pinned-Base Model from Spectral Analysis	66
4.10.	Longitudinal-Loading Moment Envelopes for Pinned-Base Model from Spectral Analysis	67
4.11.	Transverse-Loading Moment Envelopes for Outrigger Model from Spectral Analysis	69
4.12.	Longitudinal-Loading Moment Envelopes for Outrigger Model from Spectral Analysis	70
4.13.	Moment-Axial Load Interaction Diagram	72
4.14.	Section of Longitudinal Girder	79

LIST OF TABLES

Table		Page
2.1.	Calculation of Weight of Structure	11
2.2.	Calculation of Flexural Strengths	13
3.1.	Dynamic Properties of WSDOT Section Model	26
3.2.	Dynamic Properties of Seattle Section Model	27
3.3.	Calculation of Flexural g-Ratings	34
3.4.	Calculation of Shear g-Ratings	35
3.5.	Calculation of Flexural Code Ratios	39
3.6.	Calculation of Shear Code Ratios	40
4.1.	Dynamic Properties of Pinned-Base Model	52
4.2.	Dynamic Properties of Outrigger Model	56
4.3.	Development Lengths	77
4.4.	Influence of Debonding on g-Rating	81

SUMMARY

The University of Washington (UW) team reviewed the Washington State Department of Transportation (WSDOT) report titled "Earthquake Analyses of the Alaskan Way Viaduct" and performed an independent assessment of two typical sections of the structure. Additional analyses were performed to investigate the influence of some factors that were not considered in the WSDOT report. These factors included the unreliability of the calculated foundation stiffnesses, the presence of outrigger bents, differences between nominal and actual material strengths, inadequate confinement, joint shear and inadequate development lengths for reinforcement.

As to be expected in a reinforced concrete structure, many cracks were found in a brief field inspection. The cracks were, in general, consistent with the effects of gravity loads. Diagonal cracks in the joints suggested inadequate detailing of the joint. The inspection team encountered several regions in which the structure differed greatly from the typical bents. These regions included the north and south ends of the structure, locations at which off-ramps connected to the main structure, and the interface between sections constructed by the City of Seattle and the WSDOT.

The input motion and geotechnical characteristics assumed in the WSDOT report were consistent with the information available to the WSDOT and to UW. However, the paucity of information available regarding the seismological risk and the subsoil conditions precluded the possibility of reliably estimating the input motion, foundations stiffnesses, foundation capacities, and potential for liquefaction. Inspection of the structural plans suggested that timber-concrete spliced piles in the section of the structure built by the WSDOT might be particularly vulnerable.

The elastic dynamic models generated by WSDOT and those constructed for this study were found to give comparable natural periods in the first three modes. Those in the higher modes differed because of the disparate ways in which the structures were

modelled. However, the higher modes provided only a small proportion of the total response, so the differences in calculated response were small.

The great uncertainty in foundation stiffness and flexural capacity prompted the development of a pinned-base model. In comparison with the basic model, the pinned-base model had an increased period, and more importantly, had larger moments at the top of the first story columns. Additional analyses found that a single outrigger would induce asymmetrical response and a redistribution in column demands.

For the WSDOT designed part of the structure, g-ratings and dynamic code ratios were established by assuming that the reinforcement would reach its yield strength. The present study found the structure to be generally weaker than did the WSDOT study. The minimum g-rating for flexural failure was 0.09 g, whereas, for shear failure, it was 0.29g. Some of the ratings showed a consistent relationship with those given by the WSDOT study, while others showed considerable scatter. Regardless of the resolution of the discrepancies, both analyses indicated that the demands on structural members would be likely to greatly exceed their capacities.

The structural details were reviewed. The main shortcomings in the structure appeared to be inadequate confinement steel and splice and development lengths that were too short. The detail where the cross beam joined the column would be likely to fail by debonding at a stress well below the steel yield strength and warrants closer investigation. Simple calculations suggested that the bottom #17 bars would start to pull out at a base shear of 0.017 W. The connection between the longitudinal girder and the column is also a cause for concern.

Because no distress was observed after the 1965 Seattle Earthquake, these calculations are undoubtedly conservative. Material strengths may be greater than were assumed in the analyses, and development length provisions are conservative by intent. However, the response of these brittle details cannot be predicted reliably without further

investigation. The University of Washington team is proposing further study to verify the seismic safety of the structure.

CHAPTER 1

INTRODUCTION

1.1 CONTEXT

The Washington State Department of Transportation (WSDOT) is in the process of implementing an expanded seismic retrofit program for state bridges constructed before 1981. This program is predicated on seismic studies performed by WSDOT in 1987 and 1990. In these studies, researchers identified major bridges with unique structural features that required more detailed analysis with current seismic design criteria to determine what, if any, seismic retrofitting should be considered. The Alaskan Way Viaduct was one of these major bridges. It is a double-deck structure built to 1950s design standards, and it is located in an area typified by variable soil conditions.

The Bridge and Structures Office of the Washington State Department of Transportation (WSDOT) performed a series of analyses of the Alaskan Way Viaduct to provide a preliminary assessment of its seismic vulnerability. The analyses were summarized in a report by Jerald Dodson, Steven G. Rochelle, and Richard B. Stoddard, titled "Earthquake Analyses of the Alaskan Way Viaduct," dated May 31, 1990. The report presented the results of static and dynamic structural analyses of two typical sections of the Alaskan Way Viaduct. One of the sections, located around Bents 106 to 109, was designed by the City of Seattle and constructed in 1950. The other section, located around Bents 148 to 151, was designed by WSDOT and constructed in 1956. These sections will be referred to hereafter as the "Seattle" and "WSDOT" sections, respectively.

The procedure WSDOT followed to perform the static analysis was similar to that followed by researchers who studied the Cypress Viaduct in Oakland, California. Horizontal forces were applied to a linear model of the structure to estimate the base shear at which a structural member reached its capacity. Shear failure of a member was predicted

at a base shear of 0.34W for the Seattle section and 0.42W for the WSDOT section, where W is the weight of the structure. The base shear at which the first member reached its flexural capacity was 0.29W for the Seattle section and 0.18W for the WSDOT section. The three-dimensional dynamic analyses of both typical three-span sections of the Alaskan Way Viaduct were performed according to the *AASHTO Guide Specifications for Seismic Design of Highway Bridges* and current WSDOT design procedure.

This report reviews the WSDOT report and provides an independent assessment of the sections of the Alaskan Way Viaduct that were considered in the WSDOT study. The procedures followed by the University of Washington (UW) team are outlined in Chapter 2. The results of the evaluation are compared with those reported in the WSDOT study in Chapter 3, and the significance of the results are discussed in Chapter 4. Chapter 5 presents recommendations for further research.

1.2 DESCRIPTION OF STRUCTURE

The Alaskan Way Viaduct is an extremely complex structure. The double-deck structure is approximately 1-1/2 miles long, and runs north-south along the Elliot Bay waterfront in Seattle. The northern two-thirds of it, from Bent 1 to Bent 121, were designed by the City of Seattle, and, the southern one-third, from Bent 121 to Bent 183, was designed by the WSDOT. Both regions consist of typical 3-bay sections with spans of approximately 50, 70, and 50 feet. Where necessary, these sections change to accommodate off ramps, city streets, railroad lines, etc.

In both sections of the structure, the primary longitudinal support is provided by two exterior girders that are approximately 7 feet deep and 1 foot, 7 1/2 inches wide. The WSDOT section (Fig. 1.1) has an additional four identical interior stringers, which are supported on major cross beams at each bent and by floor beams at third points within each span. In the Seattle section (Fig. 1.2), a major crossbeam at every bent supports two heavy haunched longitudinal stringers and one lighter one in the center.

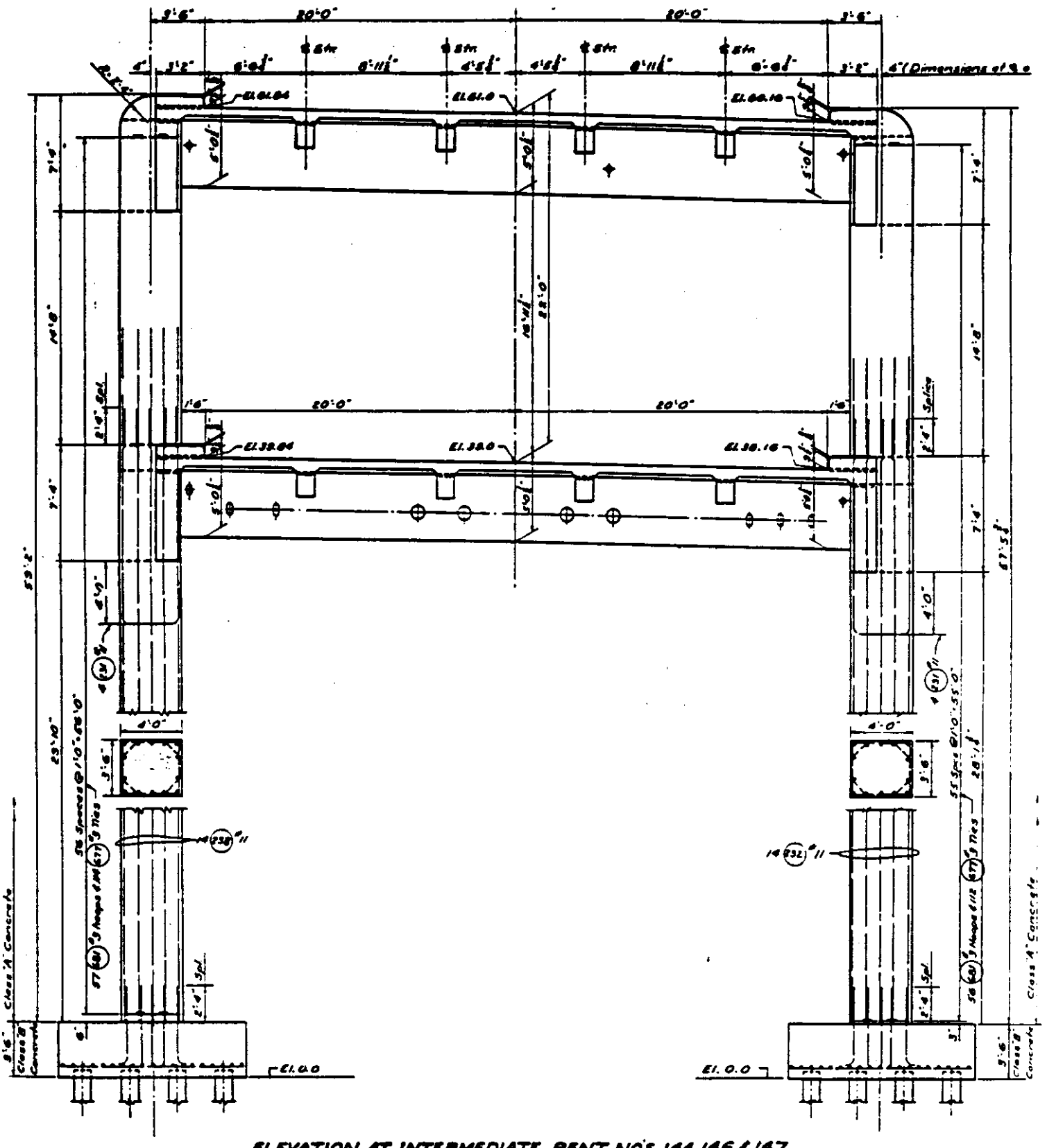

Figure 1.1 Elevation of WSDOT Section Bent

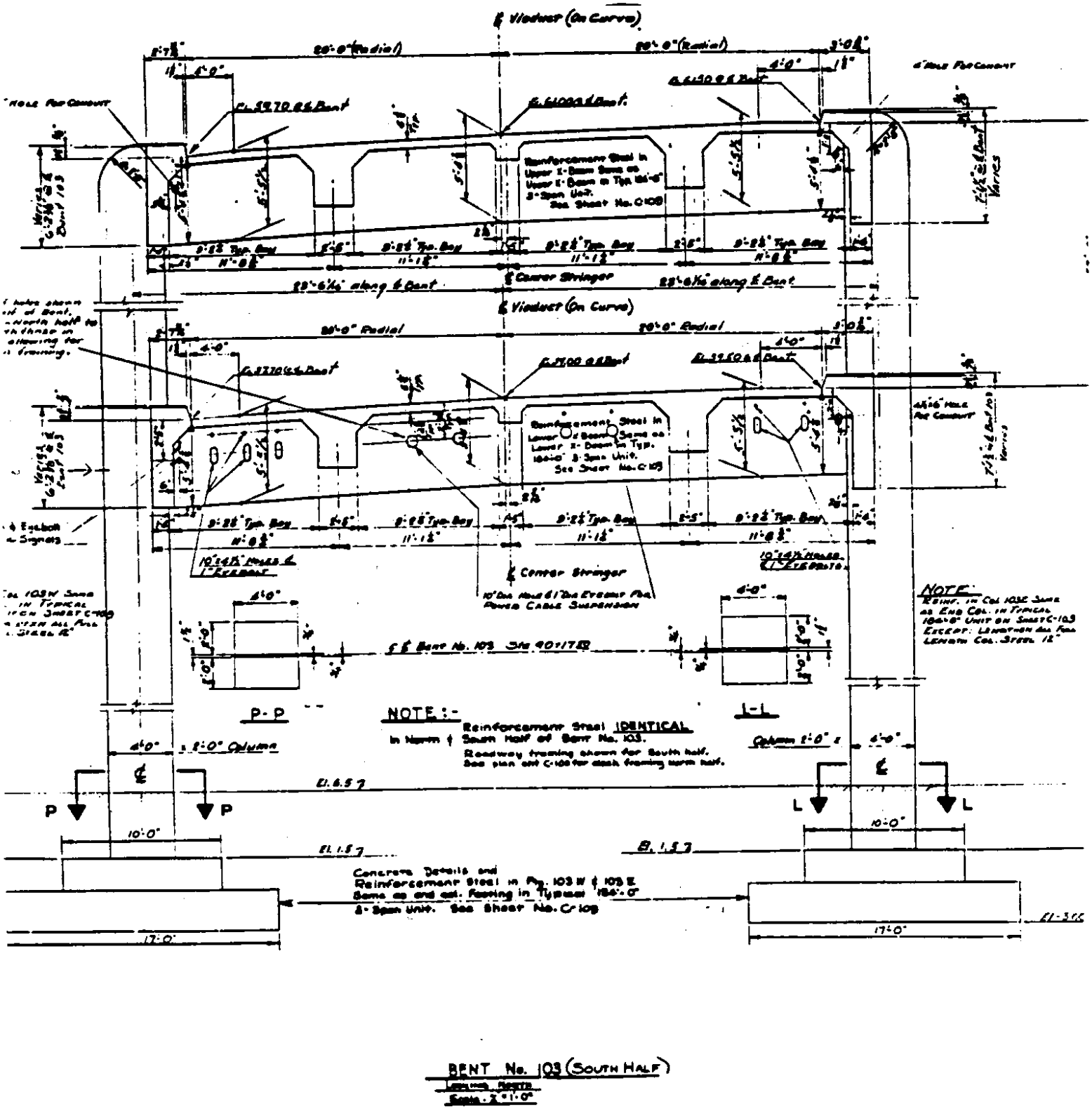

BENT No. 103 (SOUTH HALF)

Figure 1.2 Elevation of Seattle Section Bent

CHAPTER 2

PROCEDURES FOR UW EVALUATION

2.1 INSPECTION

Researchers conducted a 4-hour inspection of the Alaskan Way Viaduct by walking at ground level from the south end at Bent 183 to the north end where the northbound and southbound lanes separate. A summary of their observations is provided in Section 3.1.

2.2 GEOTECHNICAL ASPECTS

Geotechnical input for the static and dynamic analyses was provided by a February 20, 1990, intra-departmental memo from John Strada and Todd Harrison of the Materials Laboratory to Al Walley and George Markich of the Bridge and Structures office. The memo, titled "C.S. 1781, SR 99, XL-0450, Alaskan Way Viaduct, Bents 106 to 109 and 145 to 154, Earthquake Engineering Study," was included without attachments as Appendix A of the WSDOT report. A copy of the memo with attachments was provided to this project's researchers by Todd Harrison.

The available geotechnical information at the locations of the two typical sections was very sparse. Furthermore, construction records detailing the installation of the piles in the foundations at the two sections introduced uncertainty about the installed characteristics of the piles, particularly for the WSDOT section, where spliced composite piles were used. Environmental effects during the foundations' service period introduced further uncertainty about the current physical characteristics of these foundations.

The geotechnical aspects of the Alaskan Way Viaduct evaluation concentrated on review of the input motion, foundation stiffnesses, foundation capacities, and liquefaction potential. The as-built foundation conditions were determined from a review of the field records for piling contracts 3935 and 5262 provided by Todd Harrison. Contract 3935 covered the area of the Seattle section and contract 5262 the area of the WSDOT section.

The liquefaction potential of the soils that support the two typical sections was evaluated on the basis of the limited geotechnical information in the February 20, 1990, intra-departmental memo.

2.3 STRUCTURAL ANALYSES

The SAP-90 computer program was used to construct complex analytical models of the Seattle and WSDOT sections. The models included the membrane and bending stiffness of the slab, as well as the bending and axial stiffness of the heavy longitudinal edge girders, the transverse cross-beams, the intermediate transverse floor beams, and the interior stringers. These models also included the stiffness of the curb and composite interaction among elements. Deformation compatibility among elements was enforced by modeling the deck structure with an overlay of three joint depths and by generous use of rigid links and constraints. Joints were placed at critical locations so that additional springs or member releases could be inserted to model design variations, deterioration, or cracking. The member properties were input as uncracked sections. The models included the mass of the pile caps. Foundation flexibility was modeled with springs placed at the top of the piles (i.e., at the bottom of the pile cap). The foundation spring stiffness values used in the analyses were those reported in the WSDOT report.

In the static analyses, the member forces resulting from application of a 400-kip force at the lower deck and an 800-kip force at the upper deck were determined to permit calculation of g-ratings. For the dynamic analyses, the models were used to compute the first eight periods, frequencies, and mode shapes for both of the three-span sections. The same model was then used in conjunction with the Hart-Crowser spectrum to generate shear and moment demands for members. Additional dynamic analyses were performed to observe the influence of foundation flexibility and of outrigger columns on computed response.

2.4 REQUIRED AND COMPUTED STRENGTHS

The results of the SAP-90 analyses were used to compare the estimated seismic demands on the structure with its strength. The objective was to try to obtain a picture of the seismic vulnerability of the structure and to identify the locations at which damage would be the most likely to occur. Because the results of the computer analyses for the WSDOT and Seattle sections of the viaduct were similar, comparisons of demands with strengths were performed in depth only for the WSDOT section. G-ratings calculated from static analyses and code ratios calculated from dynamic spectral analyses that used Hart-Crowser's spectrum were compared with those the WSDOT had calculated.

Material Properties

To be consistent with the assumptions WSDOT used in its analyses, the researchers assumed a concrete compressive strength, f'_c=3000 psi, and a steel yield stress, fy=40 ksi. These values were believed to represent the specified strengths at the time of construction.

Member Weights

The weights of the elements of the typical module are shown in Table 2.1. The weight of the structure was calculated for a unit weight of 150 pcf for reinforced concrete and was found to be approximately 800 kips per column for interior columns and 400 kips for exterior (end) columns. Gravity loads were assigned on a tributary area basis, assuming that one half of the end span loads were carried by the exterior frame. Only loads above the pile cap level were considered. Though the researchers tried to avoid counting material twice where the major members crossed, some material was inevitably counted twice, but the weight of the railings was not included. Thus, the calculated weights should have been close to their true values.

Column Flexural Strengths

The flexural strengths of the columns in the WSDOT section of the viaduct were computed with conventional methods of strength analysis. A typical calculation of flexural

		ALASKAN WAY VIADUCT - SELF WEIGHTS									
Conc wt (kcf)	0.15										
WSDOT model (End frames, both decks)									no cols	2	
		net	net					tot. end			
Member	no	height	width	fillet	area	klf	gross L	dims.	net L	tot wt	wt/col
		(in)	(in)	(in)	(in^2)		(ft)	(ft)	(ft)	(kip)	
slab	2	6.5	516	0	3354	3.494	28.42	1	29.42	205.6	102.8
kerb	4	9.5	38	0	361	0.376	28.42	1	29.42	44.25	22.13
stringers	8	22	13.5	3.5	309.3	0.322	28.42	-1	27.42	70.66	35.33
Floor beams	2	54	17.5	3.5	957.3	0.997	43	0	43	85.75	42.88
Cross Beams	2	54	17.5	3.5	957.3	0.997	43	0	43	85.75	42.88
Long. Girders	4	88	17.5	3.5	1552	1.617	28.42	-1.75	26.67	172.5	86.25
Columns	2	48	24	0	1152	1.2	57.5	0	57.5	138	69
Total										802.5	401.2
WSDOT model (Interior frames, both decks, both frames)									no cols	4	
		net	net					tot. end			
Member	no	height	width	fillet	area	klf	gross L	dims.	net L	tot wt	wt/col
		(in)	(in)	(in)	(in^2)		(ft)	(ft)	(ft)	(kip)	
slab	2	6.5	516	0	3354	3.494	127.2	0	127.2	888.6	444.3
kerb	4	9.5	38	0	361	0.376	127.2	0	127.2	191.3	95.64
stringers	8	22	13.5	3.5	309.3	0.322	127.2	-2.92	124.3	320.2	160.1
Floor beams	8	54	17.5	3.5	957.3	0.997	43	0	43	343	171.5
Cross Beams	4	54	17.5	3.5	957.3	0.997	43	0	43	171.5	85.75
Long. Girders	4	88	17.5	3.5	1552	1.617	127.2	-3.5	123.7	799.9	399.9
Columns	4	48	42	0	2016	2.1	57.5	0	57.5	483	241.5
Total										3197	799.4

Table 2.1 Calculation of Weight of Structure

strength is shown in Table 2.2. Strengths were calculated for exterior and interior columns, in the transverse and longitudinal directions, and at four locations along the height of each column. The locations were as follows:

Location 1: Directly above the pile cap.

Location 2: Directly below the lower cross beam.

Location 3: Directly above the lower cross beam.

Location 4: Directly below the upper cross beam.

Where bars were spliced, the strength of a single bar was assumed. The number of bars that would be effective at location 4 was not easy to determine from the plans because the reinforcement in that region was quite heavy. Furthermore, some questions existed regarding the available anchorage for the bars and their effectiveness at the critical section because many of the bars there did not run the full height of the column.

The main longitudinal reinforcement specified on the plans were #11 for the interior columns and #13 for the exterior columns. A #13 bar does not exist today, but it was assumed to have a cross-sectional area of 2.075 in^2, corresponding to a circular section with a diameter of 13/8 inches. The ties usually consisted of #3 stirrups, in pairs, at 12-inch centers. This arrangement did not satisfy the minimum general (i.e., not even seismic) requirements of ACI 318-89, which require that #4 ties be used with #11 or larger bars, and that every other longitudinal bar be enclosed within a 135° tie bend. This latter requirement was violated only at location 4.

G-Ratings

The static g-ratings for the structural members were obtained by applying to the structure lateral loads of 800 kips to the top deck and 400 kips to the lower deck, as described in Section 2.3. Because a three-span section of the structure weighed 4,800 kips, rather than 1,200 kips, the moments and shears caused by this loading were

		Rectangular Column Strength								
TITLE:	WSDOT/ Interior/ Loc 1/Transverse									
Note: All strains are in .001 in/in										
b =	42	f'c =	3	fy =	40					
h =	48	beta1 =	0.85	Es =	29					
		eps u =	3	rho =	1.08%					
For c =	55	a =	46.75	curv =	0.0545	ept =	-0.382			
	total	Conc	bars 1	bars 2	bars 3	bars 4	bars 5	bars 6	bars 7	bars 8
dist from cg		-0.625	-21	-10.5	0	10.5	21	0	0	0
area		1963.5	6.24	3.12	3.12	3.12	6.24	0	0	0
strain			-2.836	-2.264	-1.691	-1.118	-0.545	-1.691	-1.691	-1.691
stress		-2.55	-40	-40	-40	-32.43	-15.82	-40	-40	-40
force	-5706	-5007	-249.6	-124.8	-124.8	-101.2	-98.71	0	0	0
Mcgc (in-k)	6546.2	3129.3	5241.6	1310.4	0	-1062	-2073	0	0	0
Mcgc (ft-k)	545.52	260.78	436.8	109.2	0	-88.53	-172.7	0	0	0
e (in) =	-1.147									
e/h =	-0.024									
c	P	M	e/h	est M(0)	est c(0)					
55	5706	545.52	0.002							
2	-692	351	-0.011							
4	-124	1351	-0.227	1517.8	4.4376					
6	172	1850	0.2243	1649.4	4.8389					
8	354	2124	0.125	1591.5	4.1127					
10	566	2398	0.0883	1665.9	4.6594					
12	809	2674	0.0689	1756.4	5.3464					
14	1035	2908	0.0586	1832.7	4.832					
16	1249	3108	0.0518	1810.6	4.3665					
18	1491	3275	0.0458	2244.1	5.6677					
20	1730	3412	0.0411	2419.2	5.5014					
22	1958	3520	0.0374	2594.4	4.8485					
24	2185	3594	0.0343	2877.1	4.7224					
25	2308	3610	0.0326	3316	6.3155					
26	2424	3615	0.0311	3509.1	5.0079					
27	2538	3614	0.0297	3625	4.6736					
28	2650	3608	0.0284	3752.3	4.3516					
30	2869	3579	0.026	3962.1	3.8998					
35	3495	3237	0.0193	5147.7	7.055					
40	4094	2756	0.014	6040.5	5.8354					
45	4659	2155	0.0096	7112	3.7888					
50	5189	1420	0.0057	8606.9	1.0688					
55	5706	546	0.002	10209	-0.224					
60	5891	208	0.0007	10965	-99.15					
70	5959	98	0.0003	9797.3	-811.4					
80	6002	21	7E-05	10525	-1296					
100	6014	0	0	10525	-9849					

Table 2.2 Calculation of Flexural Strengths

multiplied by four to obtain the equivalent of 1.0g acceleration of the structure. The ratio of the member capacity to the moment or shear corresponding to a base shear equal to the weight of the structure, W, is defined as the static g-rating.

Code Ratios

The analyses were repeated for the loads from the spectral analysis with the period-varying spectrum supplied by Hart-Crowser. Results were expressed in terms of a code ratio, instead of a g-rating. The code ratio is the internal action (moment or shear) caused by the applied spectral loads, divided by the strength for that same section, calculated according to standard code principles.

Because

$$\text{Code Ratio} = \frac{\text{Load}}{\text{Strength}}$$

a value less than 1.0 implies that the structure has adequate strength. Whereas a low g-rating indicates that a member may be vulnerable, a low code ratio indicates that the member is unlikely to be vulnerable.

Several calculations were then performed to investigate the effects of varying some of the assumptions made in the analyses. These calculations included estimates of bond strength, material properties, and the effects of axial load on flexural strength. The results of these additional analyses are presented in Section 4.4.

CHAPTER 3

COMPARISON OF UW EVALUATION WITH WSDOT EVALUATION

In this chapter, the results of the evaluation described in Chapter 2 are presented and compared with the results of the WSDOT evaluation.

3.1 INSPECTION

The structure was inspected to determine the extent of visible damage to the viaduct and to identify regions of the structure that were not typical.

Typical Sections

In general, the WSDOT section of the structure appeared to have been constructed better than the Seattle section. The Seattle section demonstrated some poor concrete work, particularly at its southernmost end. Many cracks were visible in the structure, but none appeared to pose an immediate threat to the structural integrity of the viaduct under gravity loads alone.

Slabs

Extensive cracking of the slab in the transverse direction was easily visible by virtue of calcium leaching out of the cracks. These cracks were most closely spaced and were most extensive near the major crossbeams and columns. Extensive slab cracking was visible also in the corners of the panels bounded by crossbeams and stringers. These cracks are to be expected in a bridge and were not expected to influence the seismic resistance of the Alaskan Way Viaduct.

Interior Stringers

No obvious damage or cracking was visible in the interior stringers. This was attributed to the fact that the stringers are not primary lateral-load-resisting members.

Main Crossbeams

The main crossbeams in the Seattle section of the structure had a large number of holes running north-south through them just below the slab. In the crossbeams at the end

bents of each frame, major shear cracks went downwards and outwards towards the columns at approximately 45° from these conduit holes. They were visible at almost every bent at the end of a frame and were easy to see because of the leaching calcium. This action was probably promoted by water dripping through the deck joint. The two major crossbeams at the interior bents of each three-bay frame also had some cracks in the same position. However, they were much harder to see because little calcium had leached through them. These cracks were visible in only some of the interior crossbeams.

At several bents, access for trains crossing underneath the viaduct and accommodation of off-ramps required the columns to be located outside the exterior girder line so the beams became outriggers. Many of these outrigger beams had significant shear cracks, and in some, the shear cracks penetrated across the underside of the beams. These cracks were visible on both the upper and lower levels of the structure.

In the upper levels of the structure, diagonal cracks went through the column-to-beam joint. These appeared similar to those observed in the San Francisco double-deck structures after the Loma Prieta earthquake, except that the cracks in the Alaskan Way Viaduct were much smaller. They suggested joints that either are inadequately reinforced in shear or whose reinforcement details do not provide sufficient development length.

Edge Girders

Almost all of the exterior girders displayed some flexural or shear cracks or both. In particular, in the WSDOT section, where the crossbeams were relatively heavy, the exterior girders had diagonal cracks that started at the two bottom edges of the junction of the crossbeam and the exterior girder and propagated to the bottom of the exterior girder. These cracks appeared to be caused by gravity loads. In the Seattle section of the structure, another type of crack was observed. It ran vertically for the full height of the exterior girder, where it met the column and continued up into the slab above. The cause of the cracks was not clear, although differential thermal movements between the upper and lower decks could have been partly responsible. The cracks were easily visible from underneath

the structure because of a significant amount of leaching. In some cases the cracks were judged to be approximately 1/8-in. wide.

Columns

With few exceptions, the columns appeared to be in good condition. Some columns contained diagonal cracks in the joint where the main crossbeams were connected. There were usually two or three per joint, starting at the outside of the longitudinal girders and proceeding upwards at approximately 45°. The orientation of the cracks was consistent with the effect of joint shear caused by negative moments imposed by the cross beam on the column.

A large number of the columns contained what appeared to be a crack just below the exterior girder. It started where the outside bottom edge of the exterior girder joined the column and then propagated downwards and inwards towards the inside face of the column, stopping approximately 2 ft. below the exterior girder. These cracks were first noticed because they appeared to be caused by leaching. However, in most cases, a crack was hard to see, and it is possible that the markings observed were just the edges of the weathering patterns.

Reinforcement

Reinforcement was visible in a few locations. In the worst case (the underside of the east girder between Bents 118 and 119), the main reinforcement in the exterior girders was clearly visible. In other cases stirrup reinforcement could be seen.

In both sections of the viaduct, rust marks were visible on the underside of the crossbeams. They suggested that some light steel structure had at one time been attached to the underside of the crossbeams. Inspection records should be checked to determine whether this was the cause, or the rust came from reinforcing bars.

Atypical Sections

Slender Columns at the North End of the Structure

North of the location where the two roadways separated, the supporting structure becomes relatively slender. In addition, the longitudinal exterior girders do not line up with the columns, and therefore, the longitudinal framing is relatively ineffective. The natural frequency of this system would be very different from that in other parts of the structure. In addition, this section was built on fairly steeply sloping ground, and therefore, the column lengths differ significantly, which would induce asymmetry and torsional response.

Off-ramps

Several of the off-ramps create major asymmetries in the structure. In some cases, the off-ramps are separated from the main structure. The Seneca St. off-ramp, which runs approximately east-west and comes in from the east, appeared to have been built at a later date because the form of construction was quite different. It was made from precast, prestressed girders that appeared to be seated on elastomeric bearing pads. A gap of approximately 2 in. separates this structure from the main Alaskan Way Viaduct. The off-ramp rests on relatively tall piers, and it appeared likely that pounding could occur between the two structures if major motions occurred in the east-west direction.

South End Abutments

In the southernmost frame of the structure, extending from Bents 180 to 183, several features were observed. First, the columns in Bent 180 exhibited flexural cracking near the base. This was attributed to the fact that the columns at the southernmost end, at Bent 183, are much shorter and stiffer than the others in the frame. Therefore, the longitudinal thermal expansion and contraction of the frame had to be accommodated entirely by deformation of the northernmost columns, namely at Bent 180. These thermal cracks were not seen as a serious problem for seismic resistance.

The short columns in Bents 183 and 182 had the same plan dimensions as the other columns. It is possible that these columns would attract large shear forces and might be vulnerable to shear failure. In the frame between Bents 179 and 175 the two roadways become a double-deck rather than a side-by-side system. In this area, some of the columns were built into walls at the lower roadway, again raising the possibility that the stocky columns might fail in shear.

Interface between the Seattle and WSDOT Sections

This region of the structure is extremely complex because, not only do the two different designs meet, but an on-ramp also enters from First Avenue. The quality of the construction of the Seattle portion was also poor in this region. This region deserves closer study.

3.2 GEOTECHNICAL ASPECTS

The results of the comparisons of the input motions, foundation stiffnesses, foundation capacities, and liquefaction potential are presented in this section.

Input Motion

Hart-Crowser performed a seismic risk analysis to develop design ground motion parameters with a 10 percent probability of exceedance in a 50-year period. This level of risk, which corresponds to a return period of 475 years, is commonly accepted for the seismic design of structures. The risk analysis was performed with the EQRISK program. This program, developed by the USGS, implements standard techniques to calculate a design bedrock acceleration. Hart-Crowser computed anticipated ground surface motions through one-dimensional ground response analyses, using the complex response (frequency domain) program SHAKE and the direct integration (time domain) program TESS1.

Five seismic source zones were specified in the model, and Gutenberg-Richter recurrence relationships were assigned to each. The source zones did not overlap in plan

view and covered a wide area, extending approximately from longitude 120°40'W to 126°50'W and from latitude 46°40'N to 49°20'N. The recurrence relationships assigned to each source zone appeared to be consistent with regional historical seismicity. However, the source zones were assumed to be horizontal and without thickness at a depth of 15 km. Most Puget Sound earthquakes, particularly the larger ones of primary engineering interest, have been generated at depths considerably greater than 15 km. The researchers believe that the reason for the selection of this relatively shallow depth was to attempt to counteract the effects of using an attenuation relationship developed predominantly from California (shallow focus) earthquakes. Because seismic waves from deep focus Puget Sound earthquakes travel through deeper, more intact materials than shallow focus California earthquakes, ground motion parameters would be expected to attenuate more slowly than predicted by attenuation relationships based on California data. While a shallower focal depth should counteract this trend, the selection of an "equivalent" focal depth for use in such an analysis is not clear. Using this approach, Hart-Crowser obtained peak rock outcrop accelerations of 0.24-0.26 g. They increased these by an arbitrary factor of 1.2 to account for the potential effects of focusing to arrive at a recommended design value of 0.30 g.

Using SHAKE and TESS1, Hart-Crowser performed one-dimensional ground response analyses to develop site-specific response spectra for various input motions scaled to an equivalent peak rock outcrop acceleration of 0.30g. They developed these spectra for two different soil profiles in the Seattle Transit Access site area, a soft-soil profile and a hard-soil profile. These spectra were used to develop a smoothed design response spectrum that had spectral values approximately equal to or slightly greater than the average of the values produced by the individual analyses. Interestingly, the low period spectral accelerations were set equal to 0.25g, even though a peak ground acceleration of 0.30g was used. The reason for this discrepancy is not known.

The description of the design earthquake in the WSDOT report stated that "the design earthquake is expected to produce peak bedrock accelerations of about .25g and amplified ground accelerations as high as .66g." This statement appears to misinterpret Hart-Crowser's results. The Hart-Crowser design response spectrum implied a peak ground surface (rather than bedrock) acceleration of 0.25g. The peak spectral acceleration was 0.66g, but this was not a ground acceleration. Though the design response spectral values may have been described incorrectly in the WSDOT report, they were used correctly in the analyses.

Foundation Stiffness

The researchers calculated single pile translational stiffnesses for assumptions of both fixed and pinned conditions at the connection between the pile and the pile cap. The analyses were performed with the hyperbolic tangent method to develop p-y curves for the sands and integrated clay criterion method to produce p-y curves for the clays. These criteria were different than those used in the WSDOT COM624 analyses, and were selected to provide an independent check of the computed pile stiffnesses.

Because the soil mobilizes its strength nonlinearly, single pile stiffnesses decrease with increasing pile displacement. Interpreting the results of the analyses in terms of a secant pile stiffness corresponding to a lateral pile head displacement of 0.25 in., the computed single pile stiffnesses were as follows:

Head Fixity	Seattle Section	WSDOT Section
Fixed	96 k/in.	68 k/in.
Pinned	40 k/in	27 k/in

Load deflection curves for each of these conditions are shown in Figure 3.1. This figure may be used to estimate secant stiffnesses for deflection levels other than that assumed above. However, note that these stiffnesses are only approximate, since they are based on parameters estimated from very little supporting information.

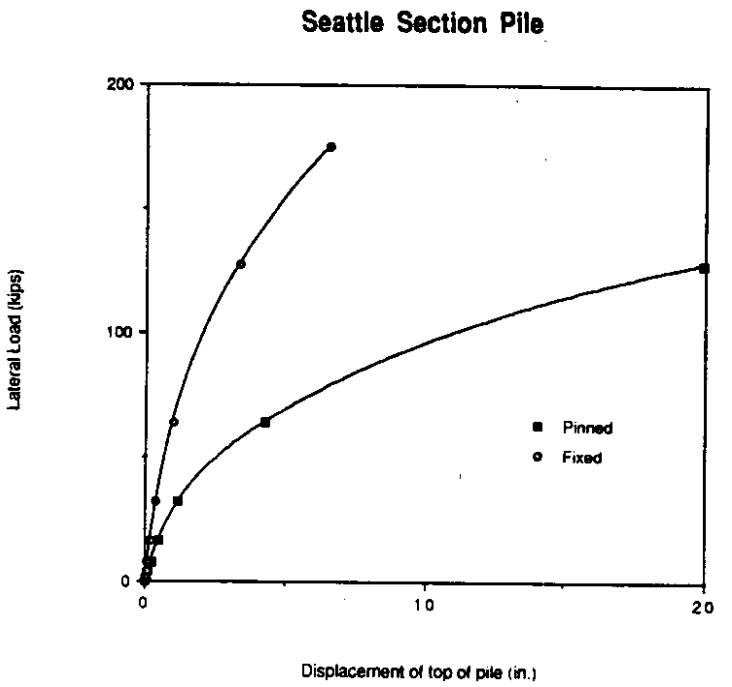

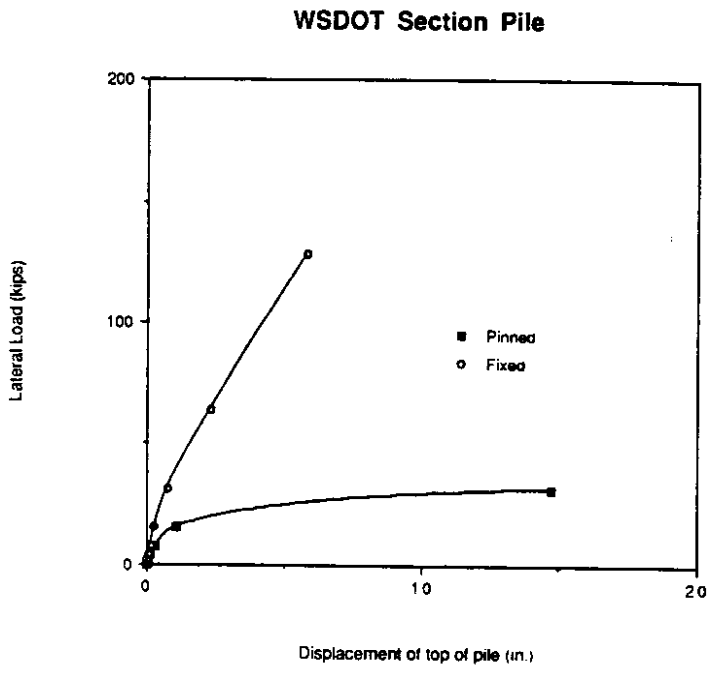

Figure 3.1 Load-Deflection Curves for Piles

Computation of dynamic pile group stiffness is a very complicated, and poorly understood, problem. Generally, group interaction effects cause lateral loads to be unevenly distributed within a pile group. Piles at the corners resist more than the average load and piles in the center resist less than the average load. These effects, and the interaction between displacement fields of closely spaced piles, typically produce a pile group stiffness that is less than the sum of the stiffnesses of the individual piles. However, the effects of densification of loose, granular soils during pile driving increase the stiffness of the soil above that which would influence the lateral load response of a single pile. As a result of these competing factors, it is often considered acceptable to compute the pile group stiffness as the sum of the pile stiffnesses.

In the Seattle section, the footings at the exterior bents (i.e., 106 and 109) had 14 piles in each group, and the footings at the interior bents (i.e., 107 and 108) each had 20 piles per group. In the WSDOT section, the footings at the interior bents (i.e., 145, 148, and 151) had 11 piles per group, whereas the footings for the interior bents (i.e., 146, 147, 149, 150, 152, 153) had 16 piles per group.

Foundation Capacities

The evaluation of foundation capacities was divided into two parts because different foundation elements were used for the Seattle and WSDOT sections. Evaluation of these capacities was difficult, primarily because of the lack of detailed information on the as-constructed characteristics of the foundations.

Seattle Section

Project history records indicated that foundation construction on the Seattle section of the viaduct began March 13, 1951. The foundations were designed to be supported on groups of piles extending through the loose surficial fills to the firmer material below. The piles were originally intended to be steel H piles; however, the project history states that "at the contractor's request and because of the slow rate of delivery on "H" beam piles, the Bridge Department agreed to use cast-in-place piles in lieu of "H" beams wherever

possible." Groundwater levels were not indicated in the available material but were likely to be at depths of about 7 feet.

The COM625 analyses indicated that the ultimate lateral load capacity of a single 18-inch diameter pile at the Seattle section would be about 120 kips. It is the doubtful that the piles are structurally strong enough to carry such a load. However, large displacements would be required to mobilize this resistance. At a pile head displacement of 4 inches, the lateral load resistance would be about 60 kips.

WSDOT Section

Construction of foundations for the WSDOT section began July 10, 1956. The foundations consisted of groups of 9 to 16 composite timber/concrete piles. The composite piles were apparently constructed by driving timber piles (13-inch tips) to depths of approximately 40 to 50 feet. The butt ends of the timber piles were typically at depths of 6 to 12 feet below the bottom of the pile cap. These timber piles were spliced to a concrete-filled steel pipe pile that extended up to the bottom of the pile cap. The splice was apparently accomplished by trimming the butt of the pile to allow placement of a 3-foot long, 12-inch diameter steel pipe over its end, secured with four spikes driven through holes in the side of the pipe, before filling the pipe pile with concrete.

Records do not reveal whether the timber piles were treated with creosote or other preservatives. The groundwater level at this location appeared to be about 6 feet deep, which was about 1 to 7 feet above the timber/concrete splices. Given these circumstances, it is likely that untreated timber piles were used and installed at such depths with the intent that they remain below the groundwater level.

The COM625 analyses indicated that the ultimate lateral load capacity of a single 14-inch diameter, composite pile at the Seattle section would be about 32 kips, provided that the splice was able to resist the induced bending moments. However, large displacements would be required to mobilize this resistance. At a pile head displacement of 4 inches, the lateral load resistance would be about 24 kips.

Liquefaction Potential

An evaluation of liquefaction potential was extremely difficult because of the paucity of information on subsurface soil gradation and density. As a result, the evaluation had to be subjective. The available information led the researchers to conclude that the conclusions of the Materials Lab personnel were appropriate. Additional subsurface investigation is required.

3.3 STRUCTURAL ANALYSES

The periods, frequencies, and mode shapes for the first eight modes of the WSDOT and Seattle section models are shown in Tables 3.1 and 3.2. The first four mode shapes for the two models are shown in Figures 3.2 to 3.5. These results can be compared directly with the mode shapes, frequencies, and periods reported in the WSDOT report. Some similarities are apparent from this comparison. The first mode for both the UW and WSDOT models was the longitudinal mode. Also, in both sets of analyses, the second and third modes consisted primarily of transverse translation and rotation about a vertical axis.

There were some differences between the UW and WSDOT models. First, though the second and third modes consisted of transverse displacement and rotation about a vertical axis, the order of the second and third modal frequencies were different in the two sets of analyses. Second, the natural periods computed in this study were typically 5 percent to 15 percent longer than those reported in the WSDOT study. Third, there were differences in the higher modes. The fourth and fifth modes of the WSDOT study consisted of frame deformation, with considerable bending of the deck. The fourth and fifth modes of this study involved local deformation of the columns of the bents. Deck bending action did not appear until the seventh to tenth modes.

BASE FORCE REACTION FACTORS

Mode #	Period (sec)	X Direction	Y Direction	Z Direction	X Moment	Y Moment	Z Moment
1	1.176	.122E+02	-.108E-05	-.580E-04	-.143E-02	.551E+03	-.286E+03
2	1.121	-.490E-05	.122E+02	.932E-06	-.550E+03	.386E-03	.111E+04
3	.978	-.819E-06	-.388E-02	-.790E-06	.171E+00	.913E-03	-.724E+03
4	.240	.208E+01	.972E-02	.426E-01	.206E+01	-.630E+02	-.475E+02
5	.239	.261E+00	.428E-03	-.531E+00	-.123E+02	.417E+02	-.353E+01
6	.239	-.845E-02	.664E-01	-.281E-01	.511E+01	.321E+01	-.309E+02
7	.239	.400E-01	-.644E-01	-.385E-02	-.582E+01	-.789E+00	-.435E+02
8	.222	-.768E-02	.201E+01	.124E-01	.155E+03	-.962E+00	.191E+03

PARTICIPATING MASS - (percent)

Mode #	X Direction	Y Direction	Z Direction	X Sum	Y Sum	Z Sum
1	95.867	0.000	0.000	95.867	0.000	0.000
2	0.000	96.604	0.000	95.867	96.604	0.000
3	0.000	0.000	0.000	95.867	96.604	0.000
4	2.797	0.000	0.001	98.664	96.604	0.001
5	0.044	0.000	0.183	98.708	96.604	0.184
6	0.000	0.003	0.001	98.708	96.607	0.184
7	0.001	0.003	0.000	98.709	96.610	0.184
8	0.000	2.862	0.000	98.709	99.472	0.185

Table 3.1 Dynamic Properties of WSDOT Section Model

BASE FORCE REACTION FACTORS

Mode #	Period (sec)	X Direction	Y Direction	Z Direction	X Moment	Y Moment	Z Moment
1	1.168	.124E+02	.469E-03	-.445E-03	-.355E-01	.563E+03	-.292E+03
2	1.086	-.468E-03	.125E+02	-.292E-02	-.555E+03	.239E+00	.111E+04
3	.935	-.218E-01	-.540E-02	-.398E-03	.224E+00	-.899E+00	-.713E+03
4	.241	.217E+01	.287E-02	.220E-01	.753E+00	-.798E+02	-.509E+02
5	.240	.493E-03	-.112E-02	-.672E+00	.157E+02	-.604E+02	.722E+00
6	.239	-.247E-02	-.115E-01	-.220E-01	-.297E+01	.210E+01	.300E+02
7	.239	.404E-01	-.934E-02	.216E-01	-.174E+01	-.419E+01	-.339E+02
8	.218	-.747E+00	.860E-02	.250E+01	.597E+02	-.575E+03	-.217E+02

PARTICIPATING MASS - (percent)

Mode #	X Direction	Y Direction	Z Direction	X Sum	Y Sum	Z Sum
1	96.085	0.000	0.000	96.085	0.000	0.000
2	0.000	97.425	0.000	96.085	97.425	0.000
3	0.000	0.000	0.000	96.085	97.425	0.000
4	2.934	0.000	0.000	99.019	97.425	0.000
5	0.000	0.000	0.283	99.019	97.425	0.283
6	0.000	0.000	0.000	99.019	97.425	0.283
7	0.001	0.000	0.000	99.020	97.426	0.284
8	0.349	0.000	3.917	99.369	97.426	4.200

Table 3.2 Dynamic Properties of Seattle Section Model

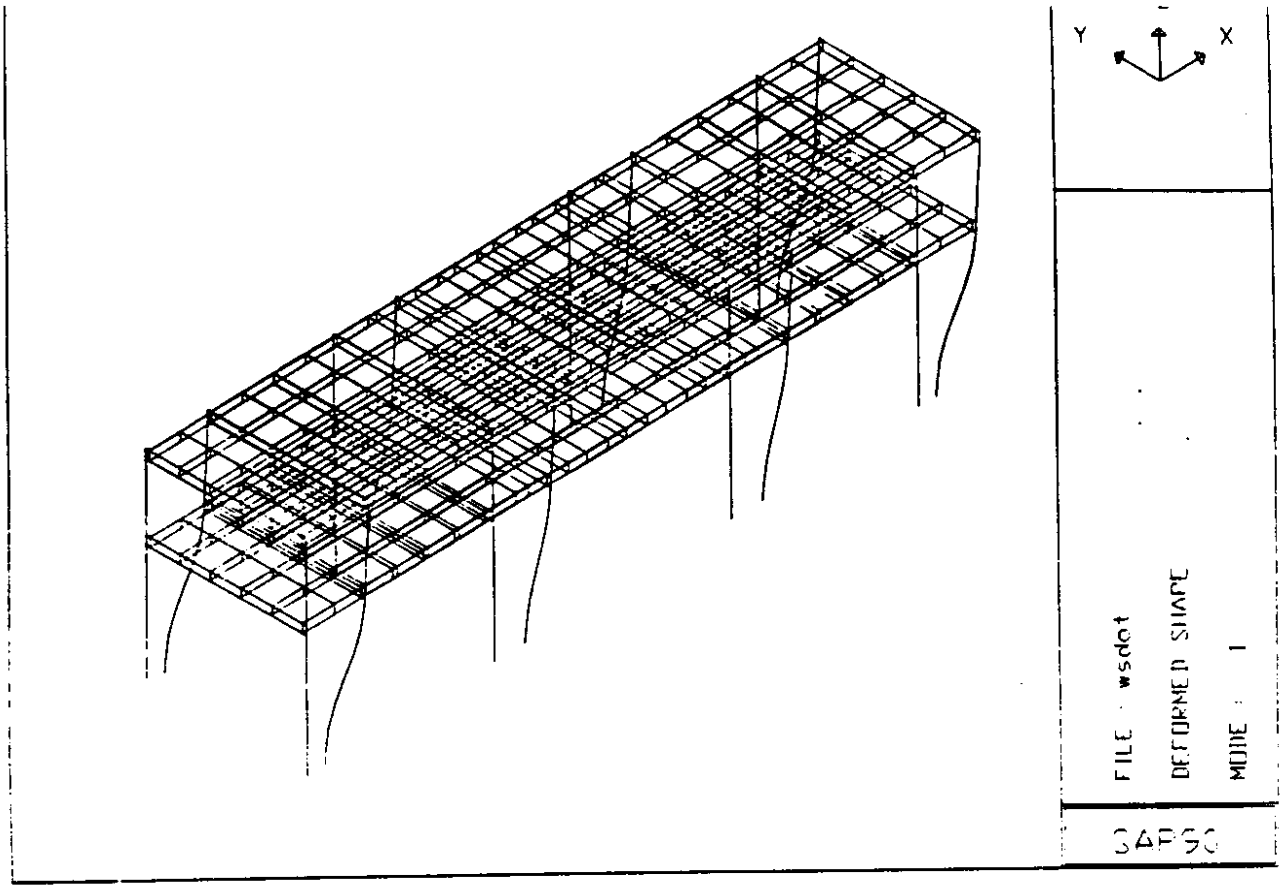

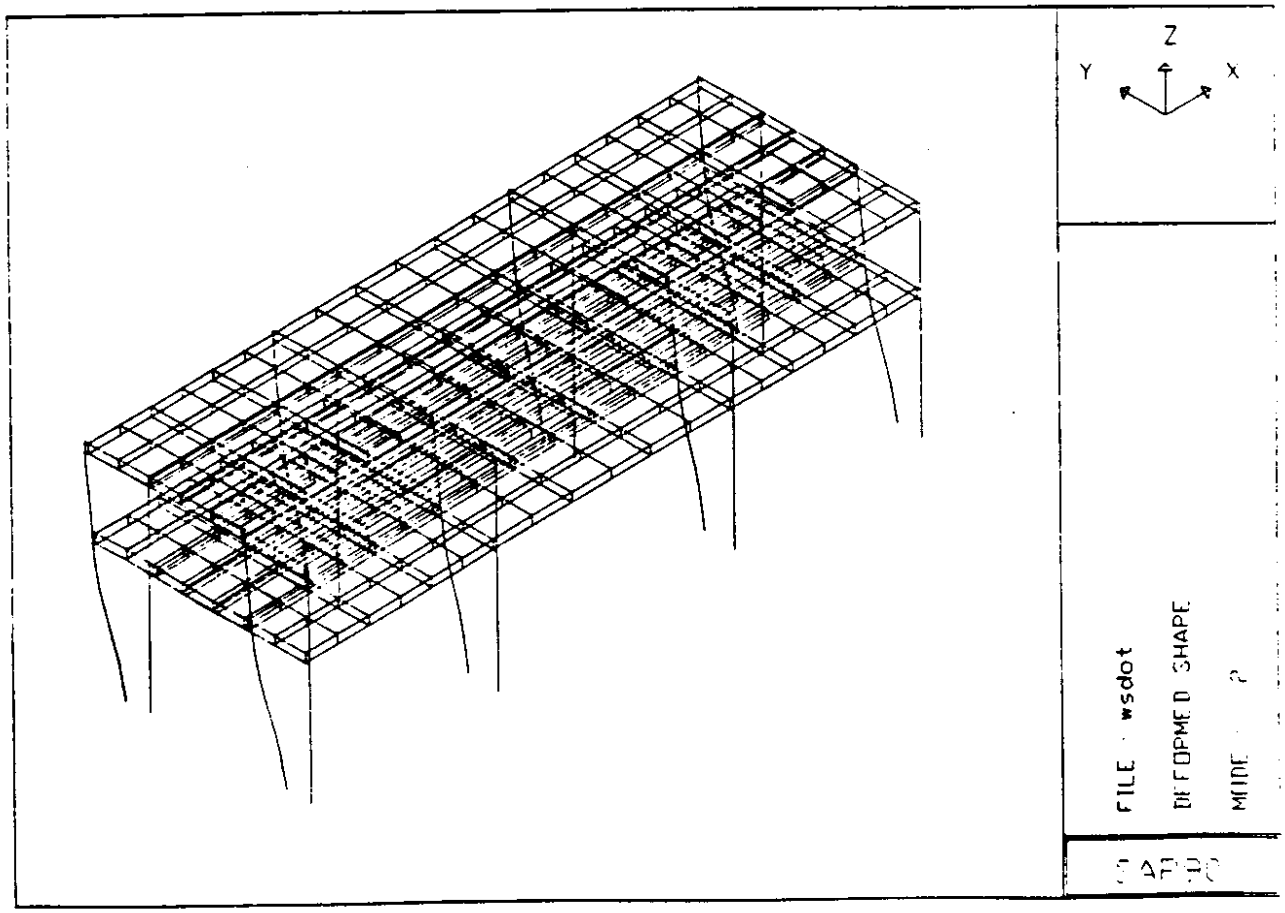

Figure 3.2 Mode Shapes 1 and 2 of WSDOT Model

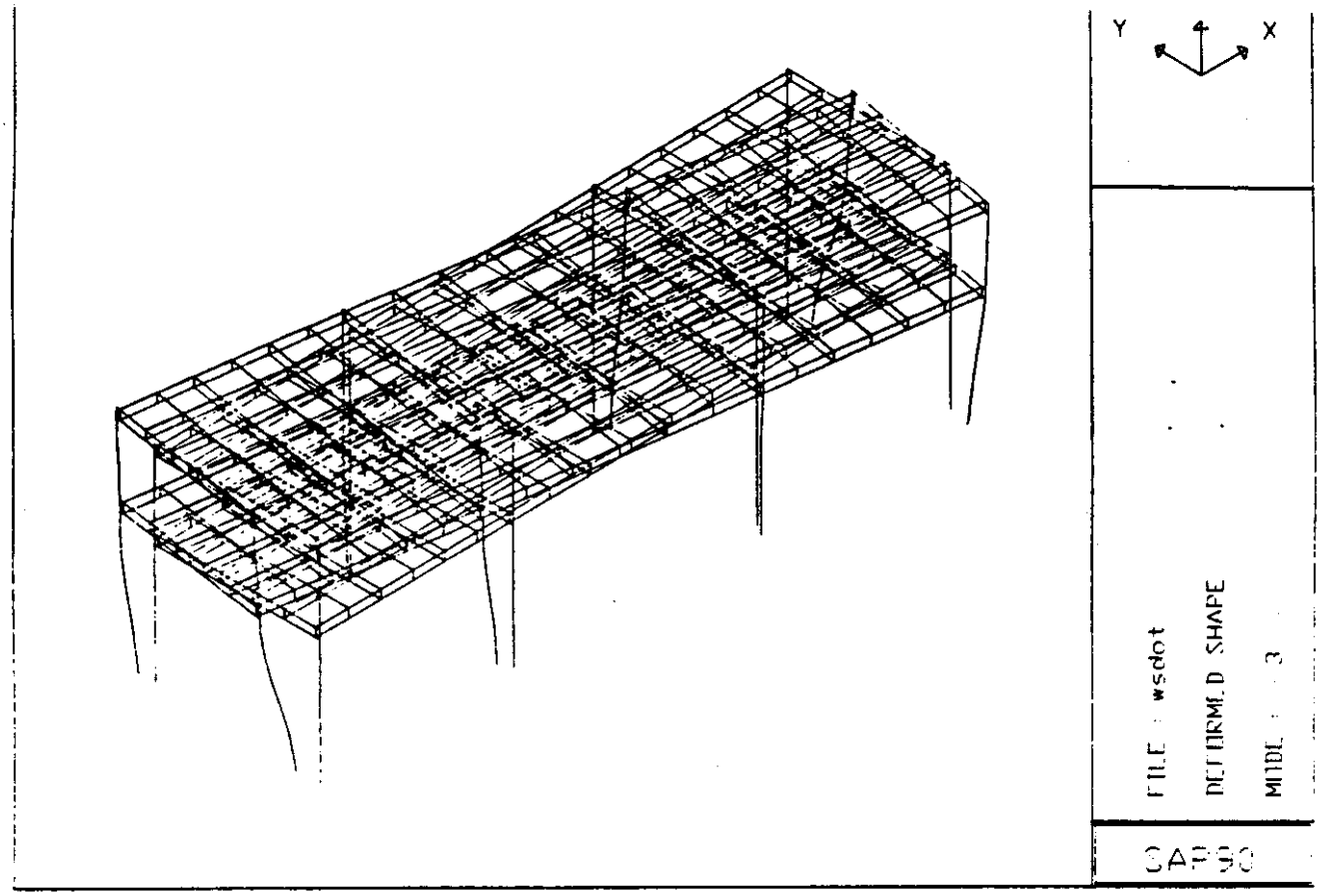

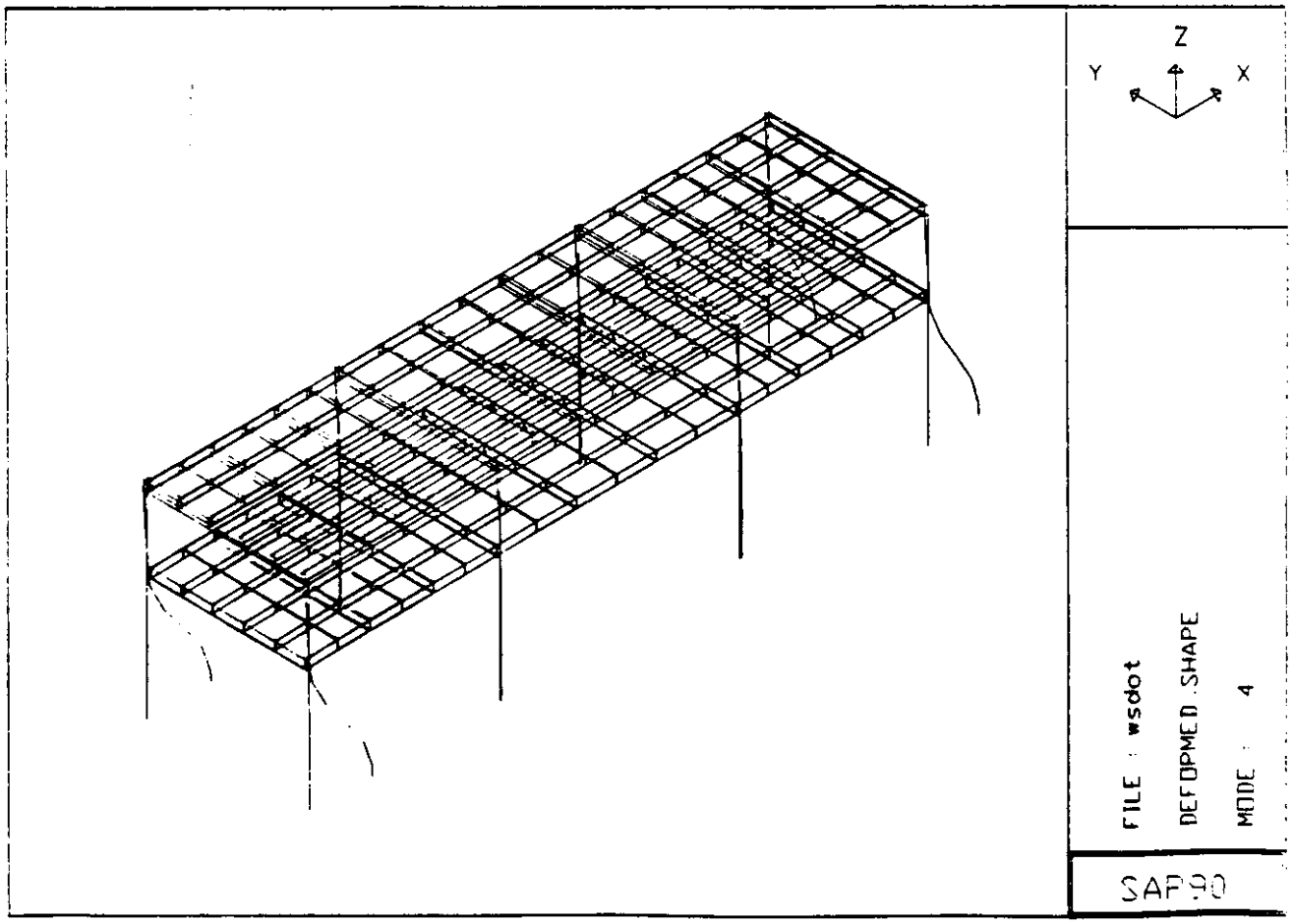

Figure 3.3. Mode Shapes 3 and 4 of WSDOT Model

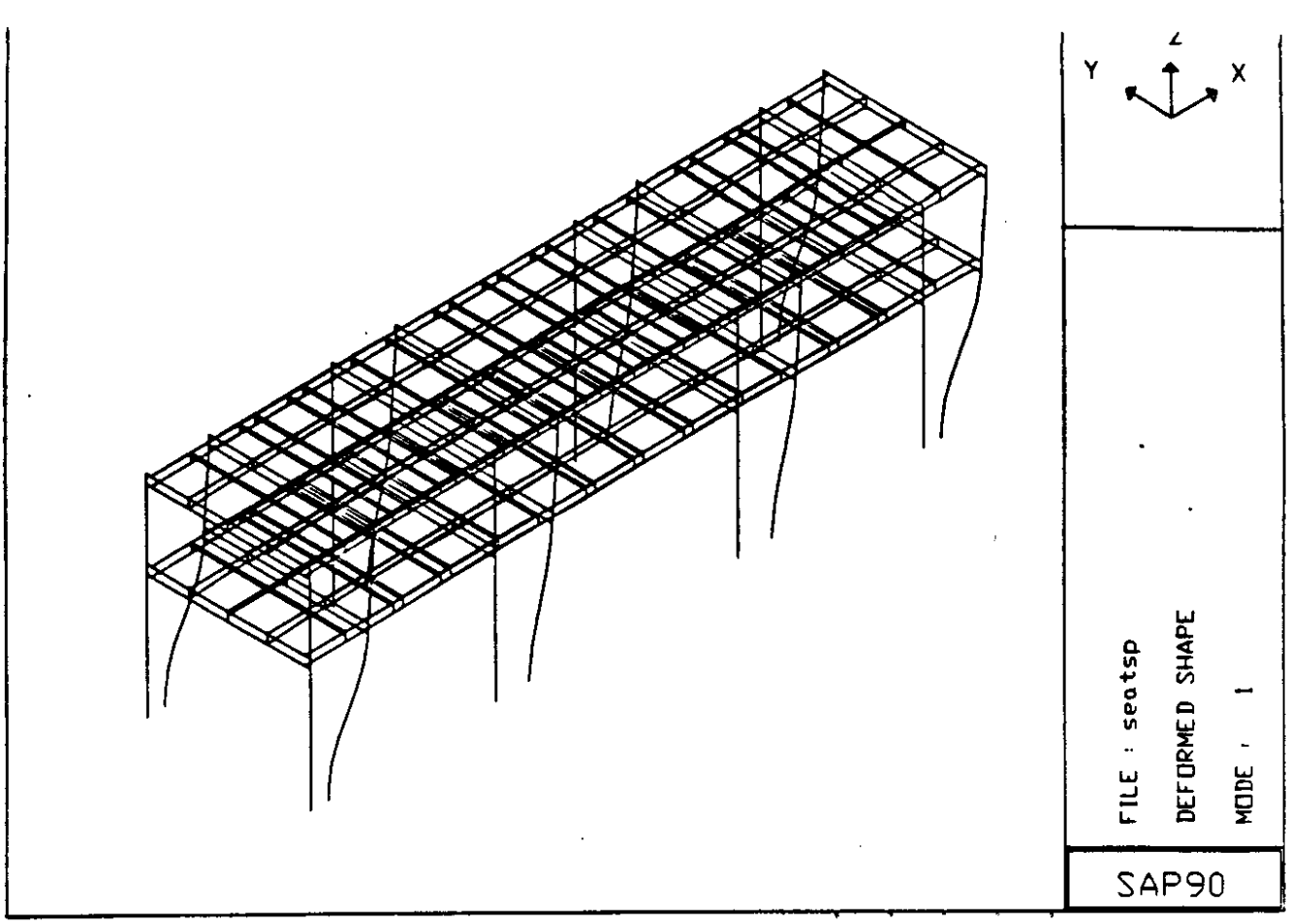

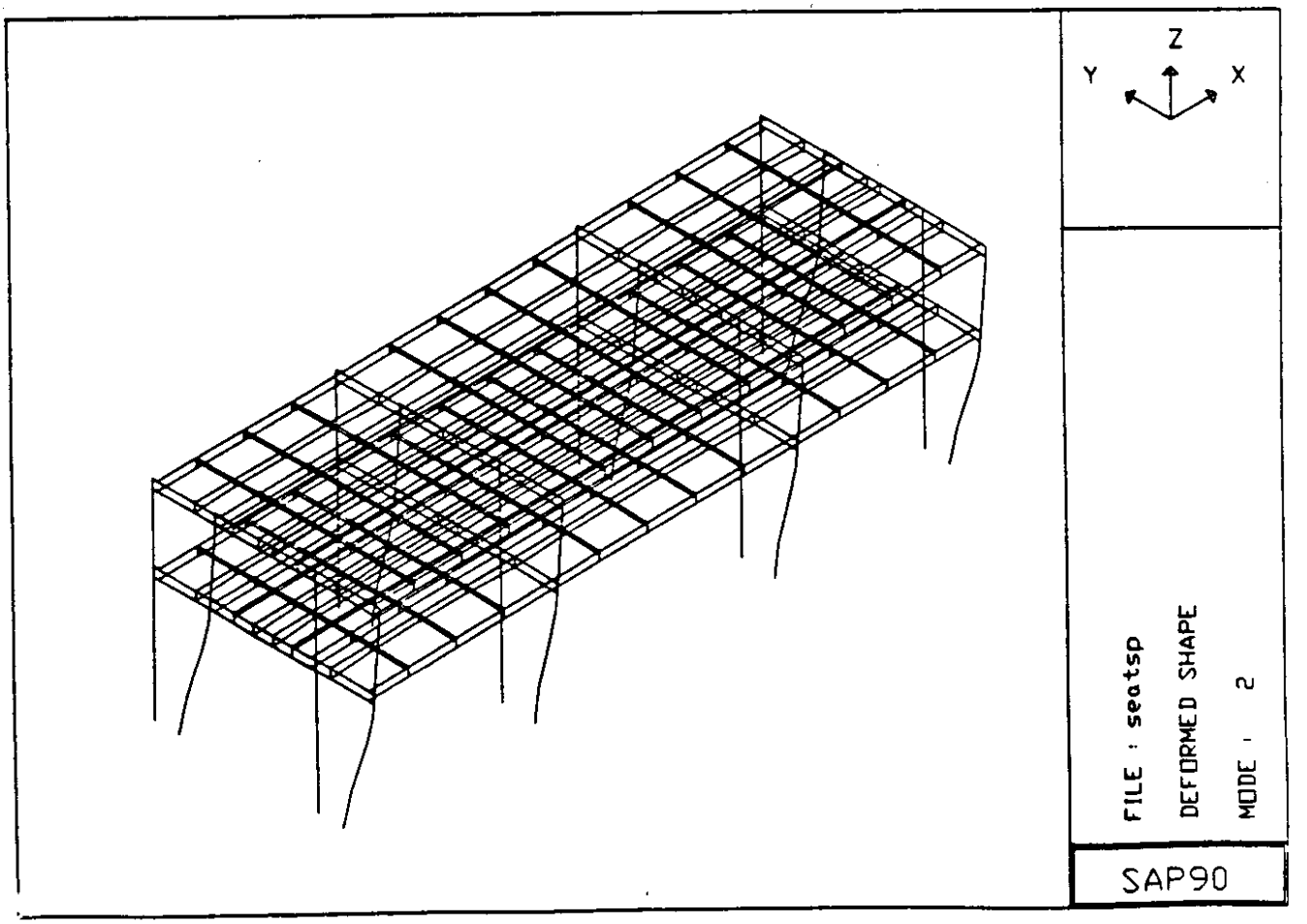

Figure 3.4. Mode Shapes 1 and 2 of Seattle Model

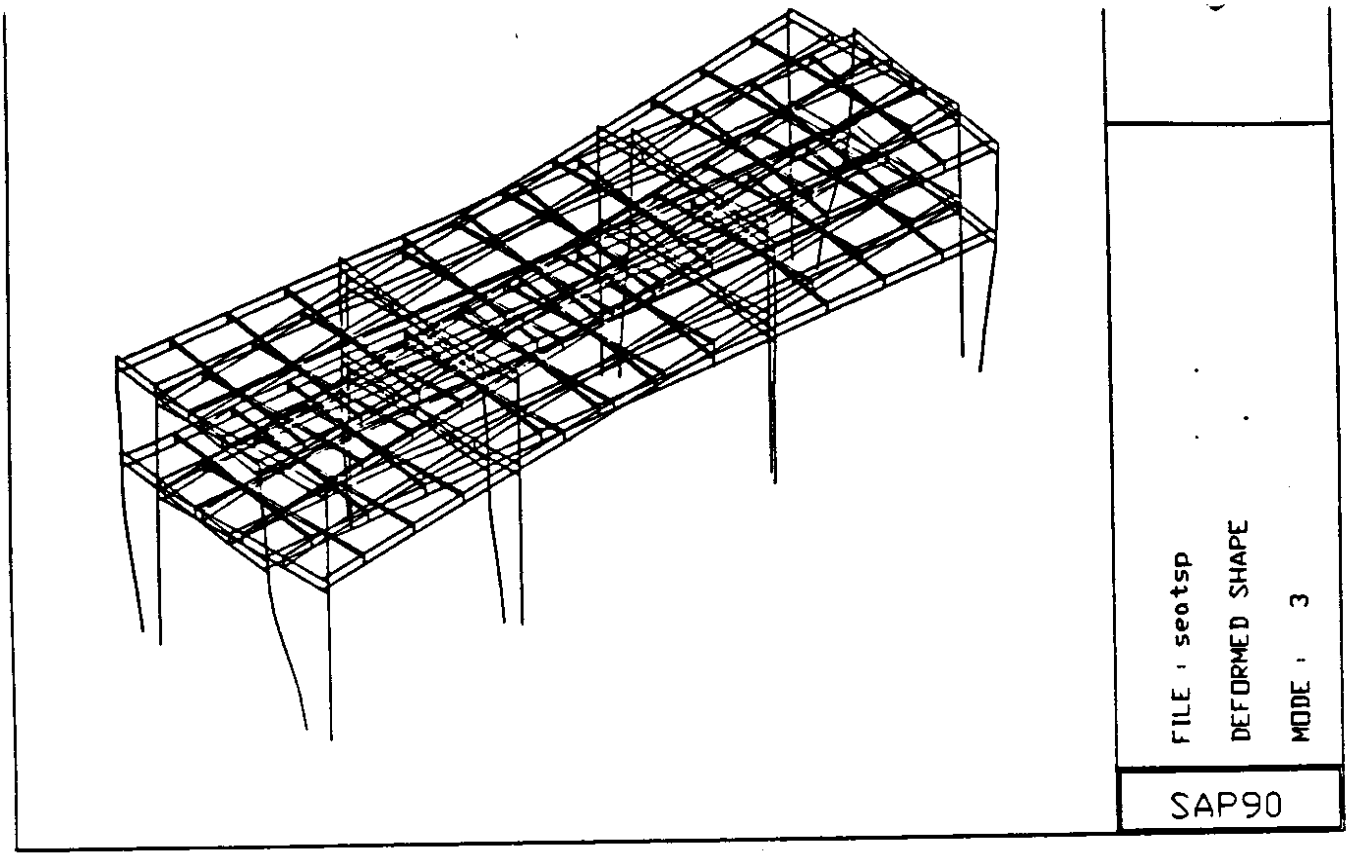

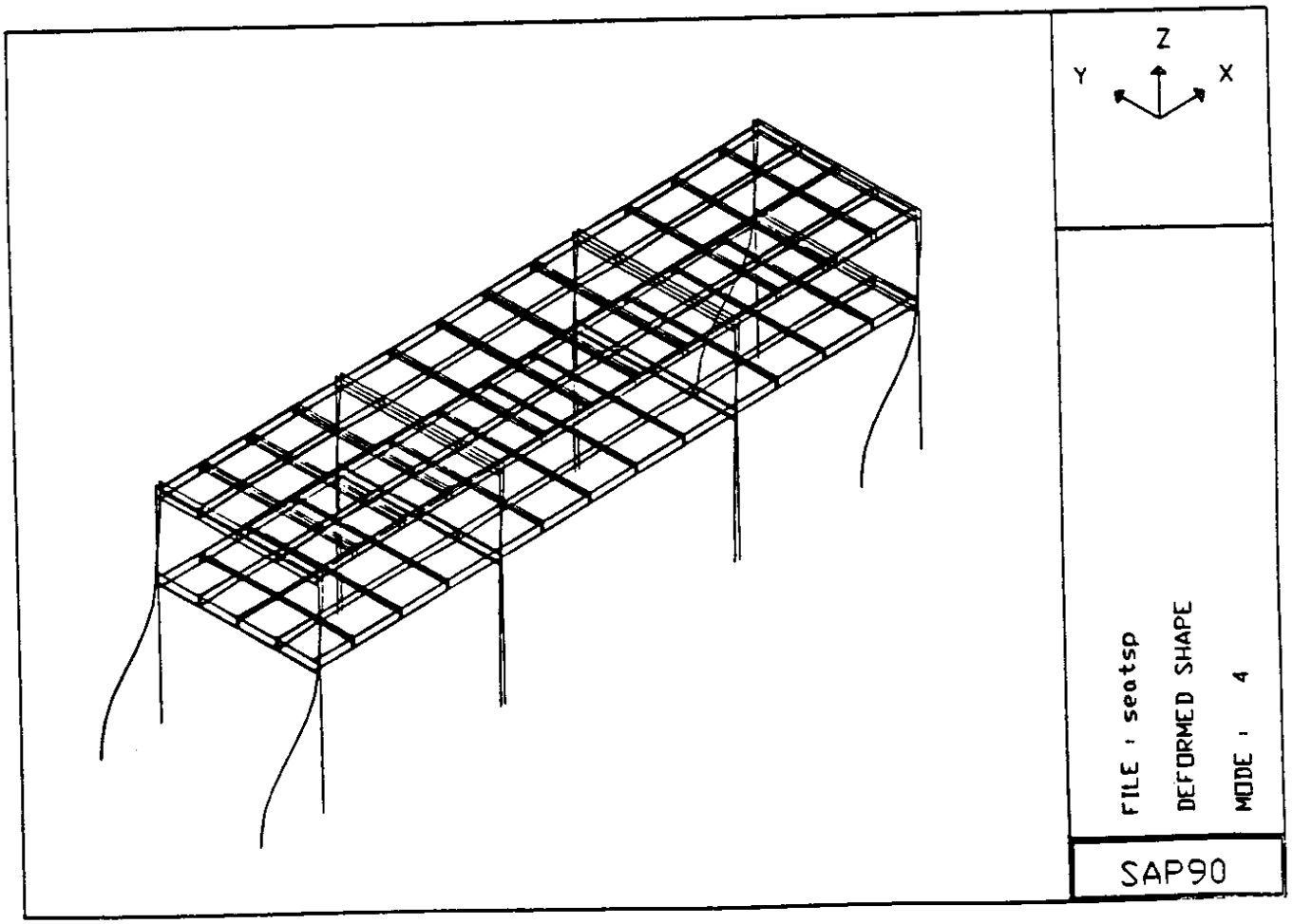

Figure 3.5. Mode Shapes 3 and 4 of Seattle Model

3.4 REQUIRED AND COMPUTED STRENGTHS

Static g-Ratings

The static g-ratings for each location, column, and direction are given in Figure 3.6 for flexure and shear. Details of the calculations are shown in Table 3.3 and 3.4. Two estimates of the flexural strength were computed. The first, $M_n(0)$, is the value obtained if the flexural strength is calculated with the assumption that no axial load acts concurrently. The second, $M_n(P)$, is calculated with the assumption that the columns carry the dead load of the structure. The associated g-ratings are called g-r(0) (no axial load) and g-r(P) (with axial load).

The g-ratings for flexure obtained by WSDOT for the transverse frames are included in Figure 3.6 and are compared with the g-ratings g-r(0) and g-r(P) obtained in this study. Several trends can be seen.

- At locations 1-3, the present study rated the columns as weaker than did the WSDOT study. The g-ratings lay between 37 percent and 49 percent of the WSDOT values, if axial load is ignored, and between 53 percent and 83 percent if the axial load is included.
- The present study attributed a much higher strength to the column at location 4 than did the WSDOT study. This difference may have been caused by different assumptions about the effectiveness of longitudinal reinforcement at that location.
- In this study the minimum g-rating, 0.09, was found at location 1 of the interior frames. The WSDOT study also found the minimum g-rating at this location, but the rating was 0.18. In either case, the rating was very low.

Similar comparisons could not be made in the longitudinal direction because no WSDOT figures were available. However, the UW analysis suggested that, for longitudinal moments, the lower column lifts were critical, since locations 1 and 2 had significantly lower static g-ratings than locations 3 and 4.

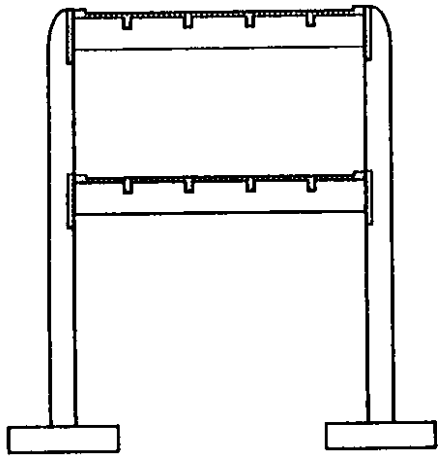

Interior Frame

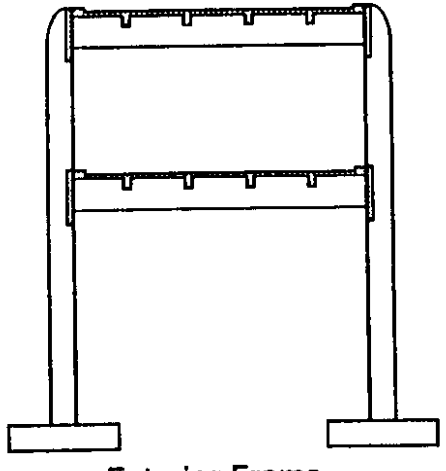

Exterior Frame

Locn.	Flexural g-ratings UW g-r(0)	UW g-r(P)	DOT g-r	UW(0) DOT	UW(P) DOT	Shear g-ratings UW g-r	DOT g-r	UW DOT
4	0.30	0.43	0.22	1.36	1.97	0.45	0.61	0.73
3	0.24	0.38	0.57	0.43	0.67	0.45	0.61	0.73
2	0.11	0.17	0.27	0.41	0.64	0.29	0.42	0.69
1	0.09	0.15	0.18	0.49	0.83	0.29	0.42	0.69

Locn.	Flexural g-ratings UW g-r(0)	UW g-r(P)	DOT g-r	UW(0) DOT	UW(P) DOT	Shear g-ratings UW g-r	DOT g-r	UW DOT
4	0.58	0.66	0.30	1.94	2.21	0.46	0.77	0.60
3	0.27	0.38	0.63	0.42	0.60	0.46	0.77	0.60
2	0.10	0.14	0.27	0.37	0.53	0.29	0.55	0.53
1	0.15	0.21	0.32	0.47	0.66	0.29	0.55	0.53

Figure 3.6. Transverse g-Ratings

SUMMARY OF FLEXURAL g-RATINGS

Phi= 0.7 (columns)

Frame	Int Ext	V Loc	Dirn.	b	h	bars	As	Mn(0)	Mn/Asfyh	P	Mn(P)	M(1g)	UW gr(0)	UW gr(P)	DOT gr	UW0 WSDOT	UWP WSDOT
				(in)	(in)		(in2)	(ft-k)	(-)	(k)	(ft-k)	(ft-k)	(g)	(g)	(g)		
WSDOT	Int	1	Trans	42	48	14#11	21.84	1565	0.448	800	2664	12500	0.088	0.149	0.180	0.487	0.829
WSDOT	Int	2	Trans	42	48	18#11	28.08	2000	0.445	800	3100	12628	0.111	0.172	0.270	0.411	0.636
WSDOT	Int	3	Trans	42	48	18#11	28.08	2000	0.445	800	3100	5720	0.245	0.379	0.570	0.429	0.666
WSDOT	Int	4	Trans	42	48	22#11	34.32	2436	0.444	800	3537	5720	0.298	0.433	0.220	1.355	1.967
WSDOT	Int	1	Long	48	42	14#11	21.84	1356	0.443	800	2396	15247	0.062	0.110	N.A.		
WSDOT	Int	2	Long	48	42	18#11	28.08	1722	0.438	800	2614	15247	0.079	0.120	N.A.		
WSDOT	Int	3	Long	48	42	18#11	28.08	1722	0.438	800	2614	6292	0.192	0.291	N.A.		
WSDOT	Int	4	Long	48	42	22#11	34.32	2046	0.426	800	2849	6292	0.228	0.317	N.A.		
WSDOT	Ext	1	Trans	24	48	8#13	16.6	1170	0.441	400	1654	5460	0.150	0.212	0.320	0.469	0.663
WSDOT	Ext	2	Trans	24	48	8#13	16.6	1170	0.441	400	1654	8120	0.101	0.143	0.270	0.374	0.528
WSDOT	Ext	3	Trans	24	48	8#13	16.6	1170	0.441	400	1654	3080	0.266	0.376	0.630	0.422	0.597
WSDOT	Ext	4	Trans	24	48	20#13	41.5	2563	0.386	400	2913	3080	0.583	0.662	0.300	1.942	2.207
WSDOT	Ext	1	Long	48	24	8#13	16.6	543	0.409	400	839	6053	0.063	0.097	N.A.		
WSDOT	Ext	2	Long	48	24	8#13	16.6	543	0.409	400	839	6053	0.063	0.097	N.A.		
WSDOT	Ext	3	Long	48	24	8#13	16.6	543	0.409	400	839	2508	0.152	0.234	N.A.		
WSDOT	Ext	4	Long	48	24	20#13	41.5	1286	0.387	400	1535	2508	0.359	0.428	N.A.		

Table 3.3 Calculation of Flexural g-Ratings

SUMMARY OF SHEAR g-RATINGS

Phi= 0.85 (columns, shear)

CR = spectral load / Code design strength

Frame	Int Ext	V Loc	Dirn.	b	h	Eff tie legs	Vs	Vc	Vn	Vu (1 g)	UW gr	DOT gr	UW DOT
				(in)	(in)		(k)	(k)	(k)	(k)			
WSDOT	Int	1	Trans	42	48	4#3@12"	66	207	273	806	0.288	0.420	0.685
WSDOT	Int	2	Trans	42	48	4#3@12"	66	207	273	806	0.288	0.420	0.685
WSDOT	Int	3	Trans	42	48	4#3@12"	66	207	273	520	0.446	0.610	0.732
WSDOT	Int	4	Trans	42	48	4#3@12"	66	207	273	520	0.446	0.610	0.732
WSDOT	Int	1	Long	48	42	4#3@12"	57	205	262	859	0.259	N.A.	
WSDOT	Int	2	Long	48	42	4#3@12"	57	205	262	859	0.259	N.A.	
WSDOT	Int	3	Long	48	42	4#3@12"	57	205	262	572	0.389	N.A.	
WSDOT	Int	4	Long	48	42	4#3@12"	57	205	262	572	0.389	N.A.	
WSDOT	Ext	1	Trans	24	48	2#3@12"	33	118	151	437	0.294	0.550	0.534
WSDOT	Ext	2	Trans	24	48	2#3@12"	33	118	151	437	0.294	0.550	0.534
WSDOT	Ext	3	Trans	24	48	2#3@12"	33	118	151	280	0.458	0.770	0.595
WSDOT	Ext	4	Trans	24	48	2#3@12"	33	118	151	280	0.458	0.770	0.595
WSDOT	Ext	1	Long	48	24	None	0	110	110	341	0.274	N.A.	
WSDOT	Ext	2	Long	48	24	None	0	110	110	341	0.274	N.A.	
WSDOT	Ext	3	Long	48	24	None	0	110	110	228	0.410	N.A.	
WSDOT	Ext	4	Long	48	24	None	0	110	110	228	0.410	N.A.	

Table 3.4 Calculation of Shear g-Ratings

Static g-ratings for shear failure are also given in Figure 3.6. Shear strengths were calculated under the assumption that the concrete contribution was $2\sqrt{f'_c}$. The ties were light and they contributed only a small amount to the shear strength. In the exterior columns under longitudinal load, the tie spacing was greater than d/2, so there was a high probability that shear cracks could miss the ties altogether. Those ties were therefore ignored.

Again, the WSDOT analysis included only the transverse direction. This study's minimum g-rating was 0.29, as compared to 0.42 in the WSDOT study. The values obtained in this study were 53 percent to 73 percent of those obtained by WSDOT, meaning that the loads were higher or the strengths were lower than those calculated by the WSDOT. Differences between the two models, such as the way in which the girder depths were modelled, could account for at least some of the differences in g-ratings.

The calculated shear strength of the columns would increase about 20 percent if the beneficial effect of axial compression were taken into account, although the effects of rocking and vertical acceleration would have to be included in the predicted axial load. Axial load effects on shear strength were not included in the present analysis, but if they were, the values from the two studies would have been closer.

Dynamic Code Ratios

Code ratios were obtained from the dynamic analyses and are shown in Figure 3.7 for the longitudinal direction and Figure 3.8 for the transverse direction. The calculations, summarized in Tables 3.5 and 3.6, were similar to those for the g-ratings, except that the demands at each location were taken from the spectral analyses rather than the static analyses. The following trends can be seen for the flexural code ratios.

- At locations 1-3, the ratio between the code ratios found in the two studies did not fall into a narrow band, as was the case for the static g-ratings; rather, values less than and greater than 1.0 existed at different locations. It

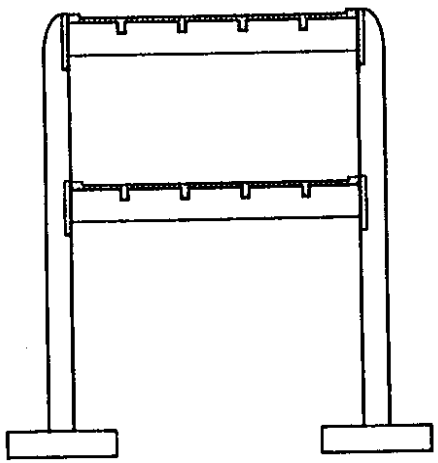

Interior Frame

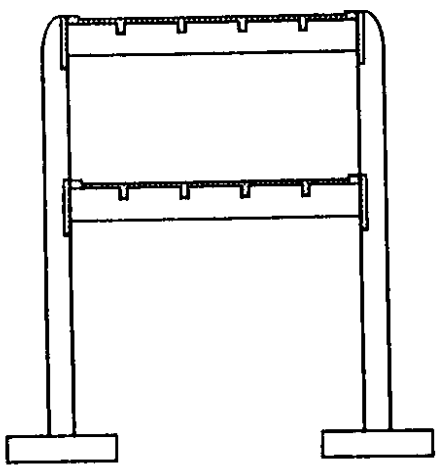

Exterior Frame

Locn.	Flexural Code Ratios					Shear Code Ratios		
	UW CR(0)	UW CR(P)	DOT CR	UW(0) / DOT	UW(P) / DOT	UW CR	DOT CR	UW / DOT
4	1.36	0.98	1.70	0.80	0.58	0.79	0.55	1.45
3	1.62	1.07	1.03	1.57	1.03	0.79	0.52	1.53
2	4.55	2.99	2.97	1.53	1.01	1.49	0.39	3.82
1	5.18	2.93	2.27	2.28	1.29	1.49	0.37	4.03

Locn.	Flexural Code Ratios					Shear Code Ratios		
	UW CR(0)	UW CR(P)	DOT CR	UW(0) / DOT	UW(P) / DOT	UW CR	DOT CR	UW / DOT
4	0.72	0.60	1.86	0.39	0.33	0.63	0.63	1.00
3	1.71	1.11	1.78	0.96	0.62	0.63	0.65	0.97
2	5.42	3.51	5.80	0.93	0.60	1.41	0.75	1.88
1	5.39	3.49	2.53	2.13	1.38	1.41	0.78	1.81

Figure 3.7. Longitudinal Code Ratios

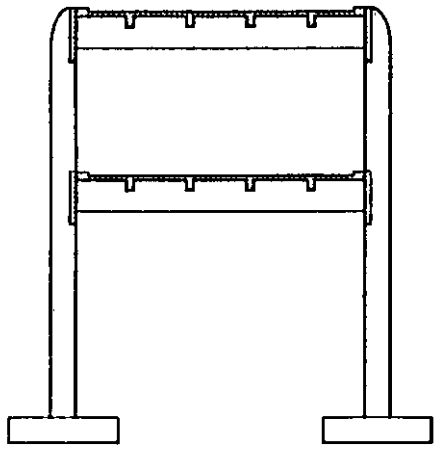

Interior Frame

Locn.	Flexural Code Ratios					Shear Code Ratios		
	UW CR(0)	UW CR(P)	DOT CR	UW(0) / DOT	UW(P) / DOT	UW CR	DOT CR	UW / DOT
4	1.18	0.82	2.12	0.56	0.38	0.61	0.84	0.73
3	0.39	0.25	0.67	0.58	0.37	0.61	0.88	0.70
2	3.58	2.31	2.44	1.47	0.95	1.37	0.96	1.43
1	4.47	2.63	2.28	1.96	1.15	1.37	1.02	1.34

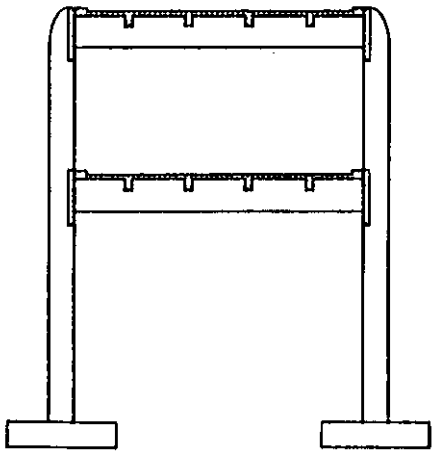

Exterior Frame

Locn.	Flexural Code Ratios					Shear Code Ratios		
	UW CR(0)	UW CR(P)	DOT CR	UW(0) / DOT	UW(P) / DOT	UW CR	DOT CR	UW / DOT
4	0.70	0.61	2.28	0.31	0.27	0.76	0.88	0.87
3	0.48	0.34	0.85	0.57	0.40	0.76	0.88	0.87
2	3.91	2.76	4.10	0.95	0.67	1.39	0.86	1.61
1	2.60	1.84	1.30	2.00	1.42	1.39	0.90	1.54

Figure 3.8. Transverse Code Ratios

SUMMARY OF FLEXURAL CODE RATIOS

Phi= 0.7 (columns, P&M)
CR = spectral load / Code design strength

Frame	Int Ext	V Loc	Dirn.	b	h	bars	As	Mn(0)	Mn / Asfyh	P	Mn(P)	M Spec	UW CR(0)	UW CR(P)	DOT CR	UW0 / DOT	UWP / DOT
				(in)	(in)		(in2)	(ft-k)	(-)	(k)	(ft-k)	(ft-k)					
WSDOT	Int		1 Trans	42	48	14#11	21.84	1565	0.448	800	2664	4900	4.473	2.628	2.280	1.962	1.152
WSDOT	Int		2 Trans	42	48	18#11	28.08	2000	0.445	800	3100	5012	3.580	2.310	2.440	1.467	0.947
WSDOT	Int		3 Trans	42	48	18#11	28.08	2000	0.445	800	3100	545	0.389	0.251	0.670	0.581	0.375
WSDOT	Int		4 Trans	42	48	22#11	34.32	2436	0.444	800	3537	2020	1.185	0.816	2.120	0.559	0.385
WSDOT	Int		1 Long	48	42	14#11	21.84	1356	0.443	800	2396	4915	5.178	2.930	2.270	2.281	1.291
WSDOT	Int		2 Long	48	42	18#11	28.08	1722	0.438	800	2614	5480	4.546	2.995	2.970	1.531	1.008
WSDOT	Int		3 Long	48	42	18#11	28.08	1722	0.438	800	2614	1950	1.618	1.066	1.030	1.571	1.035
WSDOT	Int		4 Long	48	42	22#11	34.32	2046	0.426	800	2849	1950	1.362	0.978	1.700	0.801	0.575
WSDOT	Ext		1 Trans	24	48	8#13	16.6	1170	0.441	400	1654	2130	2.601	1.840	1.300	2.001	1.415
WSDOT	Ext		2 Trans	24	48	8#13	16.6	1170	0.441	400	1654	3200	3.907	2.764	4.100	0.953	0.674
WSDOT	Ext		3 Trans	24	48	8#13	16.6	1170	0.441	400	1654	395	0.482	0.341	0.850	0.567	0.401
WSDOT	Ext		4 Trans	24	48	20#13	41.5	2563	0.386	400	2913	1254	0.699	0.615	2.280	0.307	0.270
WSDOT	Ext		1 Long	48	24	8#13	16.6	543	0.409	400	839	2050	5.393	3.491	2.530	2.132	1.380
WSDOT	Ext		2 Long	48	24	8#13	16.6	543	0.409	400	839	2060	5.420	3.508	5.800	0.934	0.605
WSDOT	Ext		3 Long	48	24	8#13	16.6	543	0.409	400	839	650	1.710	1.107	1.780	0.961	0.622
WSDOT	Ext		4 Long	48	24	20#13	41.5	1286	0.387	400	1535	650	0.722	0.605	1.860	0.388	0.325

Table 3.5 Calculation of Flexural Code Ratios

SUMMARY OF SHEAR CODE RATIOS

Phi= 0.85 (columns, shear)

CR = spectral load / Code design strength

Frame	Int Ext	V Loc	Dirn.	b	h	Eff tie legs	Vs	Vc	Vn	Vu Spec	UW CR	DOT CR	UW DOT
				(in)	(in)		(k)	(k)	(k)	(k)			
WSDOT	Int	1	Trans	42	48	4#3@12"	66	207	273	318	1.370	1.020	1.344
WSDOT	Int	2	Trans	42	48	4#3@12"	66	207	273	318	1.370	0.960	1.427
WSDOT	Int	3	Trans	42	48	4#3@12"	66	207	273	142	0.612	0.880	0.695
WSDOT	Int	4	Trans	42	48	4#3@12"	66	207	273	142	0.612	0.840	0.728
WSDOT	Int	1	Long	48	42	4#3@12"	57	205	262	332	1.491	0.370	4.029
WSDOT	Int	2	Long	48	42	4#3@12"	57	205	262	332	1.491	0.390	3.823
WSDOT	Int	3	Long	48	42	4#3@12"	57	205	262	177	0.795	0.520	1.528
WSDOT	Int	4	Long	48	42	4#3@12"	57	205	262	177	0.795	0.550	1.445
WSDOT	Ext	1	Trans	24	48	2#3@12"	33	118	151	178	1.387	0.900	1.541
WSDOT	Ext	2	Trans	24	48	2#3@12"	33	118	151	178	1.387	0.860	1.613
WSDOT	Ext	3	Trans	24	48	2#3@12"	33	118	151	98	0.764	0.880	0.868
WSDOT	Ext	4	Trans	24	48	2#3@12"	33	118	151	98	0.764	0.880	0.868
WSDOT	Ext	1	Long	48	24	None	0	110	110	132	1.412	0.780	1.810
WSDOT	Ext	2	Long	48	24	None	0	110	110	132	1.412	0.750	1.882
WSDOT	Ext	3	Long	48	24	None	0	110	110	59	0.631	0.650	0.971
WSDOT	Ext	4	Long	48	24	None	0	110	110	59	0.631	0.630	1.002

Table 3.6 Calculation of Shear Code Ratios

is possible that differences in the way the dynamic analyses were conducted had a significant effect on the results.

- At location 4, the present study resulted in a much lower code ratio than did the WSDOT study, presumably for the same reasons as given above for the g-rating.
- As with the static analyses, inclusion of the axial load in the flexural strength calculations increased the computed strength by approximately 50 percent, and reduced the code ratio by approximately 33 percent.

Considerable differences existed in the code ratios calculated in the two studies. The principal trends that can be seen are as follows:

- The ratio between the UW code ratio and the WSDOT Code Ratio was always higher in the lower column lift. This implies that the present study attributed to the lower columns a relatively higher load or lower strength than did the WSDOT study.
- The largest differences arose in the interior girders in the longitudinal direction and in the external columns in the transverse direction, in both cases in the lower column lift.

CHAPTER 4

DISCUSSION

4.1 STRUCTURAL SAFETY

Background

Structural safety is usually discussed in a probabilistic context. The loads, l, and strengths, r, of a structure are treated as random variables, and a third variable, z, is defined as the difference between the first two. That is

$$z = r\text{-}l$$

The variable z is therefore random, and the states of failure and no failure are described by $z<0$ and $z>0$, respectively. The probability of failure then depends on the statistics of z, and if the variables concerned are independent and normally distributed, the critical measure is the safety index, β, defined as

$$\beta = \frac{\mu_z}{\sigma_z} = \frac{\text{mean value of } z}{\text{standard deviation of } z}$$

A large β means that failure is improbable.

This formal analysis of safety is the basis for modern design codes, such as the recently published AISC LRFD Specification for steel structures. The target safety index used in the new code can be calibrated against those inherent in previous codes that have generated satisfactory designs to ensure that designs under the different codes will represent similar levels of safety.

This approach is useful if the issues on which safety depends are distributed randomly. However, a brief review of notable structural failures, and in particular failures of bridges, suggests that collapses have occurred most often as a result of gross errors, in either design or construction. The statistical approach is meaningful only if such gross errors can be excluded with certainty, but their exclusion is not a trivial matter, since many are errors of omission. For example, a structure might prove satisfactory when analyzed

and designed in two dimensions, but unless it is also considered as a three dimensional entity, potentially damaging response in torsion will not be revealed.

The statistical approach is also difficult to apply to dynamic loading where the criteria for failure are much more elusive than for monotonic loading. In this situation design codes tend to rely heavily on prescriptive requirements concerning attributes (such as confining steel in reinforced concrete) that are known to lead to qualitatively favorable behavior, but about which quantitative statements cannot readily be made.

The spirit of this inquiry is therefore to seek general measures of response and to attempt to identify areas that might be considered gross errors in the light of contemporary engineering knowledge. Such an inquiry must include estimates of the loading on the structure in terms of the probable ground motion, the distribution and magnitude of the resulting internal forces, and the resistance of the structure.

Issues for Investigation

The inquiry can be broken into different issues:

- the adequacy of the original design,
- the success of the original construction in fulfilling the design objectives,
- changes over time in the state of the structure and in the evidence of its adequacy, and
- changes in understanding of structural behavior and design requirements.

The original design was executed during the 1950s. The Uniform Building Code of the time contained specific, if minimal, seismic design requirements. In the 1953 AASHO Specifications, the only reference to earthquake loading was in Section 3.2.1, which required that

> *"Structures shall be proportioned for the following loads and forces where they exist:*
>
> *(1)* ...
> *(5)* *Other forces when they exist, as follows:*
> *Longitudinal ..., ... and earthquake forces."*

Seismic load magnitudes and design procedures were not specified. However, the wind loading requirement for the Alaskan Way Viaduct amounted to 0.037W, where W is the weight of the superstructure. Therefore, the original design should have led to some lateral resistance.

The adequacy of the original construction must be judged from construction records and subsequent evidence. The cursory inspection by the UW researchers revealed some evidence of poor concrete quality, but its extent did not constitute a gross error. WSDOT records should be checked to ensure that bar placement was correct.

Concrete continues to gain strength with time, so there is a strong probability that the strength of the concrete in the viaduct is significantly above the specified 3,000 psi. By contrast, the reinforcement is likely to have the same strength, or less, if it has corroded. No evidence of major corrosion problems was apparent during the inspection, although cracks were seen in many locations. Mill certificates should show the original strength of the bars used.

Inferences about the original design and construction could be made from the viaduct's performance since it was built, because it has now been subject to 35 years of gravity loading and one significant earthquake. Most of the cracks in the viaduct would have been expected in a reinforced concrete structure and did not suggest distress caused by gravity or seismic loading. The WSDOT reported no major changes in condition due to the 1965 earthquake. These observations may be construed as positive; however, they are at odds with the predicted performance of some of the connection details (Section 4.4). This contrast signifies an area of uncertainty.

Advances in the profession's understanding of seismic behavior and design represent the most important changes since the 1950s. Requirements for ductile detailing to ensure suitable response constitute a major new design issue that was not considered at the time the viaduct was constructed. Therefore, the adequacy of the viaduct depends strongly on the need for such details, and in turn that need depends on the magnitude and duration

of the expected loading. Recent evidence suggests that the region is susceptible to major subduction earthquakes of long duration, albeit at return periods of approximately 500 years.

Major Areas of Uncertainty

The state of the structure after a 35-year traffic load test suggests that the original design and construction, modified as the material strengths varied with time, were adequate for gravity loads. This statement is particularly important in light of the many bays of the structure to which that loading has been applied.

By contrast, the evidence concerning resistance to major earthquake loading is restricted to one event. A problem with a connection led to Achilles' downfall, and the collapses of many structures during earthquakes have been traced to the same cause. Therefore, it is reasonable to concentrate on the probable behavior of details in the viaduct. Three such critical details are the splices in the piles, the reinforcement splices at the base of the columns, and the anchorage of the bottom cross beam reinforcement. All three are inadequate by contemporary design standards, but their deficiencies are only manifested when the load reaches the threshold at which inelastic response is induced, and the paucity of indicative cracking suggests that that threshold has not yet been reached. The areas in which crucial uncertainties exist can therefore be identified as those that influence the possibility of the details' failure, namely:

- the cyclic load-deflection characteristics of the connection details,
- the ground motion to be expected, and
- the interaction between the soil, the foundations, and the superstructure.

4.2 GEOTECHNICAL ASPECTS

Input Motion

The WSDOT analyses used the input motion recommended in a 1986 Hart-Crowser study for use on the Seattle Transit Access project near the Alaskan Way Viaduct. The

researchers evaluated the propriety of using this motion for the Alaskan Way Viaduct by reviewing the methods and results of the Hart-Crowser study and comparing the geotechnical characteristics of the Seattle Transit Access site with those of the two Alaskan Way Viaduct sections.

Three types of earthquakes can be expected in the Pacific Northwest; these are located at the interface between the North American Plate and the Juan de Fuca plate, within the North American Plate, and within the Juan de Fuca Plate.

The seismicity in the North American Plate is associated with faults in the top of the plate, which produce shallow earthquakes. These faults are largely undetected and are under the residual glacial till in the area. The occurrence of these shallow earthquakes is rare, and a maximum figure of 7.5 on the Richter scale has been recorded in the North Cascade region. Such earthquakes usually include extensive aftershocks, which damage weakened structures.

The earthquakes in the Juan de Fuca Plate are usually due to fracture from plate bending in the subduction under the North American Plate. These are deep earthquakes with few aftershocks. Most recent seismic events in Seattle have resulted from this plate bending, and magnitudes of 7.5 are expected with a return period of 30-50 years.

The tendency of one plate sliding under another to stick creates the circumstances under which a plate suddenly slips. This is the situation as the Juan de Fuca Plate subducts under the North American Plate. The slip-stick mechanism could produce earthquakes of great magnitudes, 8 to 9, in the slip zone off the western Washington coast. Such subduction earthquakes would be felt in the Puget Sound area. The evidence for these earthquakes has been inferred from geological and botanical evidence of drowning during a quake that could have occurred in the 17th Century and the Indian lore reflected in the Swan's log of the 19th Century. The return period has been inferred to be 400 to 500 years.

The ground motions considered in this study correspond to the deep earthquakes experienced in this area. This report is also relevant to the less certain, shallow earthquakes because the magnitudes and durations are much the same. A subduction earthquake in the Pacific could produce ground motions in Seattle that were similar in intensity to the deep and shallow events. The difference would be in the duration. Twenty seconds is a typical duration for the deep and shallow events, whereas the duration of the subduction earthquake might be measured in minutes.

This study did not consider long-duration motions. It is possible that longer duration earthquakes could cause damage to the viaduct that was not revealed in this study.

Foundation Stiffness

The researchers evaluated the foundation stiffnesses used in the WSDOT analyses by reviewing available geotechnical information and the foundation stiffness recommendations presented in the intra-departmental memo. Very little information was available from which to directly compute these foundation stiffnesses. The review of available information was supplemented by a limited number of analyses. Of interest for the dynamic response of the Alaskan Way Viaduct were the stiffnesses in horizontal translation (in two directions where appropriate), vertical translation, and rocking modes of vibration.

Review of the horizontal translational stiffness involved development of p-y curve characteristics of the soils at the sites of the two Alaskan Way Viaduct sections. The p-y curves were used as input into an analysis of the response of single, laterally-loaded piles with the computer program COM625, a modified version of COM624 developed at the University of Washington. COM625 differs from COM624 in that it can account for nonlinear pile bending behavior; however, this feature was not employed in this evaluation. The single pile stiffness was then used to estimate an equivalent pile group stiffness.

Both the vertical translation and rocking stiffnesses of the pile groups depend on the vertical translational stiffnesses of individual piles. Because the response of the structure is

not particularly sensitive to these stiffnesses, and because there was insufficient information from which to compute these stiffnesses, they were not considered further.

Foundation Capacities

Foundation capacities were not explicitly addressed in the WSDOT report. However, they are very important and may influence the interpretation of the results of the dynamic analyses. The structural capacities of the foundation elements themselves were also not addressed, though they are also of concern, particularly, the composite piles used to support the WSDOT sections. The splices used to connect the timber and concrete portions of the composite piles appeared to be incapable of resisting the bending moments that would be induced in them during strong earthquake shaking. Failure of these splices could have a devastating impact on the performance of the viaduct, regardless of how well the superstructure performed.

4.3 STRUCTURAL ANALYSES

Significance of Differences

A series of detailed studies were performed to examine the differences between the WSDOT and UW analyses (Section 3.3) and to determine whether they were significant to the seismic performance of the structure. To perform these studies, the researchers developed entirely independent models. These independent models were developed by a graduate student under faculty supervision. The graduate student study model was less complicated than the UW model. It did not use the three-level joint system to model the deck system. Instead, the deck was modeled with T-beams, and deck displacements were sometimes constrained to develop rigidity in the slab. In addition, some variations of these models did not include the mass of the pile cap. Discussions with WSDOT personnel indicated that these later models were very similar to the model used in the WSDOT study. These simpler models closely matched the periods, frequencies, and mode shapes for all modes reported in the WSDOT study.

These studies clearly showed that the major differences noted above could be attributed to two factors that were different in the UW models, described in Section 2.3, and the WSDOT study. First, the three-level deck system used in the UW model produced a greater deck bending stiffness. This stiffness tended to shorten the periods, and it suppressed some of the deck bending action noted in the higher modes. The second difference was the mass of the pile cap and the location of the foundation springs. This mass was included in the UW models of this study but was not included in the WSDOT study. This mass is not trivial because it approaches 50 percent of the mass of the rest of the structure. The additional mass tended to lengthen the periods of the first few modes, and it introduced the column leg bending modes shown in mode 4 of Figures 3.3 and 3.5.

Although the suitability of these modeling assumptions is arguable, the discussion is irrelevant because the comparison also clearly showed that the differences between the models were not significant to the evaluation of the seismic behavior of the viaduct. There are several reasons for this finding.

1. The UW model included more than ten higher modes with periods of 0.2 seconds to 0.25 seconds. Thus, the higher modes reported in the WSDOT study had similar periods as the higher modes for the basic model of this study.
2. While there were a large number of these higher modes, they contributed little to the translational seismic response of the viaduct frames. As shown in Tables 3.1 and 3.2, approximately 95 percent of the mass for translational movement was effective in the first three modes of vibration. The higher modes would be expected to affect local behavior, but should have little effect on the overall response and base shear of the structure. These higher modes would be very important in an evaluation of vertical response, but seismic design and analysis have not advanced to the point of comonly considering vertical acceleration.

3. Other factors could be extremely important to the seismic performance of the viaduct frames and are worthy of more detailed discussion than the observed differences in the dynamic modes. In particular, natural periods would be very sensitive to the spring stiffness used for translation of the foundation. A 10 percent change in the spring stiffness would produce an observable change in the dynamic properties, and a 50 percent change would alter them dramatically. These translational foundation springs might act almost as base isolators, and might protect the structure from the higher accelerations in the first few modes. As a result, the stiffness of these springs are as important as the isolator stiffness in isolated systems. Unfortunately, the spring stiffness was not accurately known, so dynamic response would vary greatly with this uncertain parameter. On the other hand, the dynamic properties would not be nearly so sensitive to the stiffness of the rotational springs, because dramatic changes in rotational stiffness would be needed to change the dynamic properties significantly.

4. There were very few typical frames. Some had outrigger columns, and others had approach ramps or tapered deck geometry. In addition, it appeared possible that critical elements might deteriorate or fail at moderately small acceleration levels. This deterioration could dramatically change the dynamic characteristics and potential for damage.

Variations in the Models to Simulate Specific Behavior

To evaluate the influence of foundation flexibility and of outrigger columns, two additional sets of analyses were performed. The results of these analyses were compared to the results of the basic models of the typical Seattle section.

Researchers performed the first set of analyses to investigate the influence of foundation flexibility. The stiff springs at the foundation of the basic model attract considerable bending moment to the base, and it is highly questionable that this large

moment could be developed. First, the piles appeared to penetrate into the cap a short distance, with no ties or reinforcement. Tension failure of the pile or perhaps tension pull-out of the pile from the cap could limit this moment capacity. Second, the available information suggested that the piles might be spliced just below the pile cap, and the splice might not be suitable to develop a large foundation moment (Section 3.2). Third, the short lap splice (less than 20 diameters) of the columns at the pile cap could also limit the moment capacity. The combined effect of these factors suggests that this column base moment capacity could be lost early during an earthquake, and this could dramatically change the dynamic characteristics and the potential for seismic damage.

An analysis was performed using the Seattle model member sizes and geometry, but the rotational springs at the foundation were replaced by pins. The dynamic characteristics of this frame are shown in Table 4.1, and the first four mode shapes are shown in Figures 4.1 and 4.2. The calculated periods were much greater than were calculated for the basic model (Table 3.2). Higher modes played a slightly greater role in the seismic response of the frames under these conditions, since the participating mass was somewhat larger in the higher modes. Larger deflections of the frame were computed, so there was greater potential for damage due to secondary effects such as pounding. However, the greatest problem with this change in the model may have related to the redistribution of moments and forces in the frame. The moments at the top of the first story columns increased dramatically, as did the moments and shears in the beams and second story columns. This raises the possibility of severe damage to a portion of the structure that is relatively protected by the foundation stiffness of the basic models.

A number of the bents had outrigger columns to permit changes to the roadway geometry or clearance for the street or rail traffic below the viaduct. These outriggers could dramatically change the dynamic characteristics of the structure. Because of the lost

BASE FORCE REACTION FACTORS

Mode #	Period (sec)	X Direction	Y Direction	Z Direction	X Moment	Y Moment	Z Moment
1	1.744	.122E+02	.288E-03	-.312E-03	-.239E-01	.565E+03	-.287E+03
2	1.497	-.278E-03	.123E+02	-.175E-02	-.559E+03	.135E+00	.109E+04
3	1.318	-.540E-02	-.581E-02	-.287E-03	.254E+00	-.189E+00	-.700E+03
4	.255	-.247E+01	.643E-02	.685E-01	.178E+01	.174E+02	.584E+02
5	.255	-.145E+00	-.239E-02	-.273E+00	-.643E+01	.264E+02	.387E+01
6	.255	.185E-01	-.370E-02	-.268E-01	-.210E+01	.184E+01	.386E+02
7	.255	-.470E-01	.589E-02	.312E-01	.203E+01	-.240E+01	.408E+02
8	.232	.159E-01	.205E+01	-.550E-01	.494E+02	-.179E-01	.179E+03

PARTICIPATING MASS - (percent)

Mode #	X Direction	Y Direction	Z Direction	X Sum	Y Sum	Z Sum
1	93.352	0.000	0.000	93.352	0.000	0.000
2	0.000	94.668	0.000	93.352	94.668	0.000
3	0.000	0.000	0.000	93.352	94.668	0.000
4	3.824	0.000	0.003	97.176	94.668	0.003
5	0.012	0.000	0.047	97.189	94.668	0.050
6	0.000	0.000	0.000	97.189	94.668	0.050
7	0.001	0.000	0.001	97.191	94.668	0.051
8	0.000	2.625	0.002	97.191	97.293	0.053

Table 4.1 Dynamic Properties of Pinned-Base Model

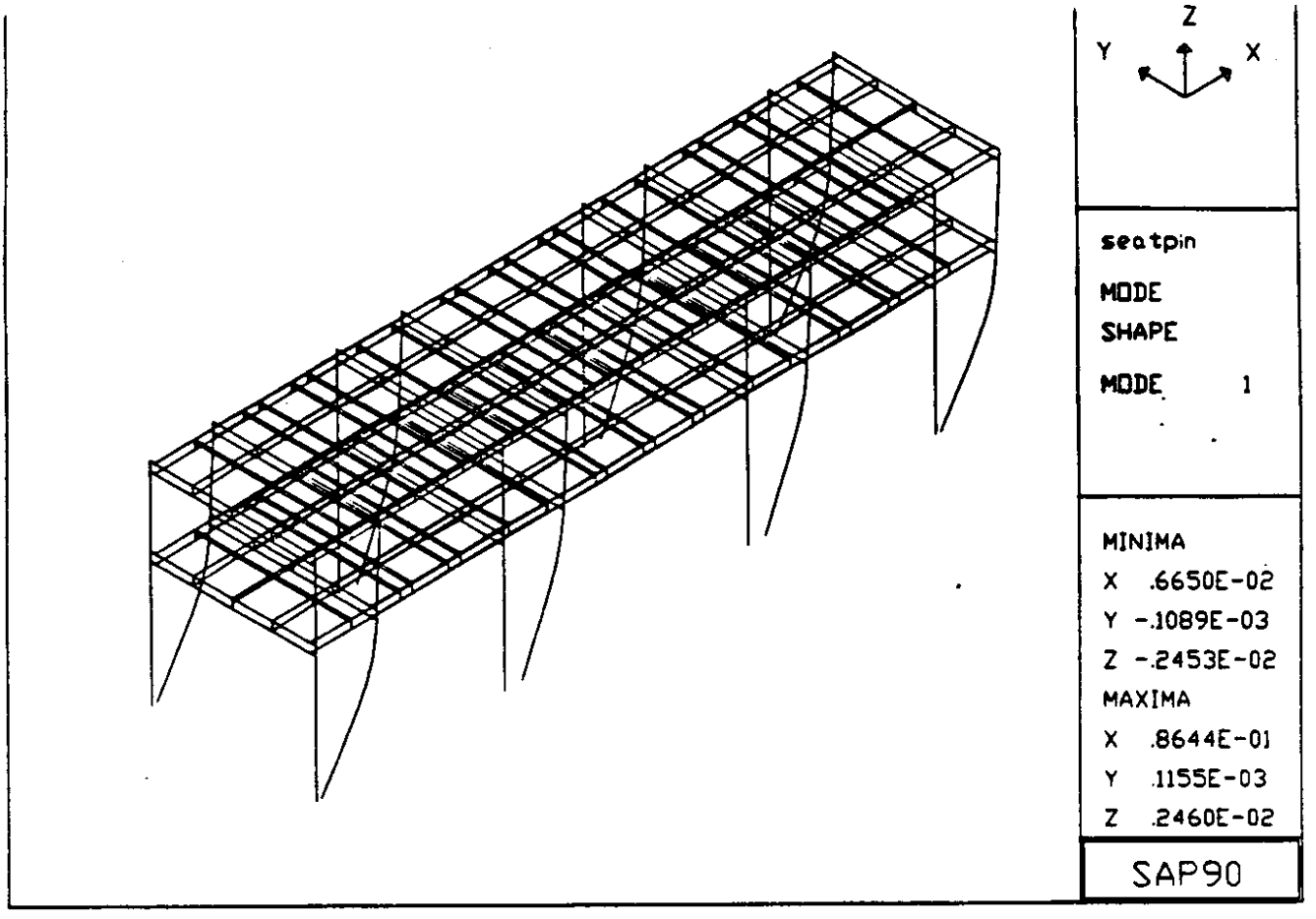

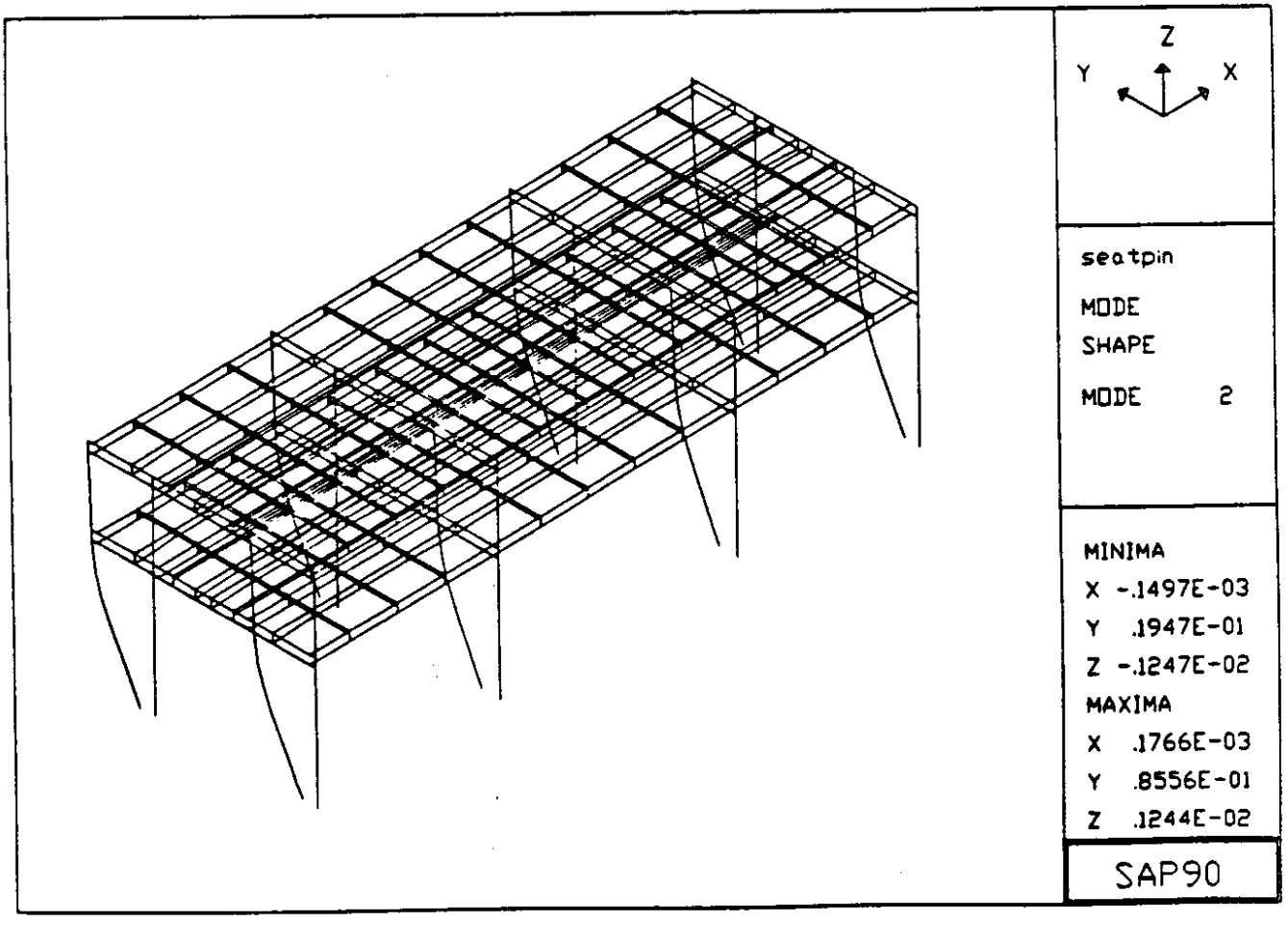

Figure 4.1. Mode Shapes 1 and 2 of Pinned-Base Model

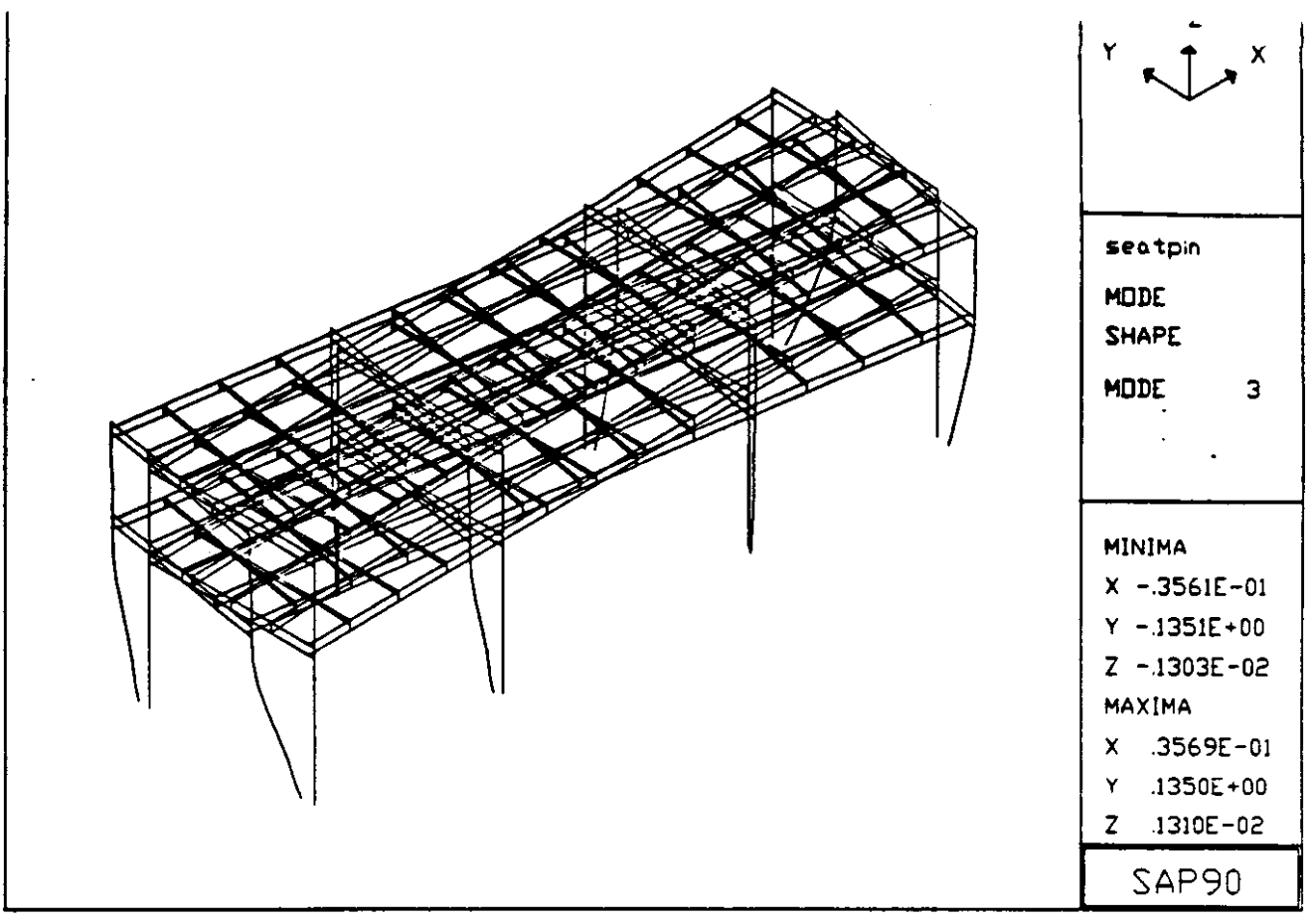

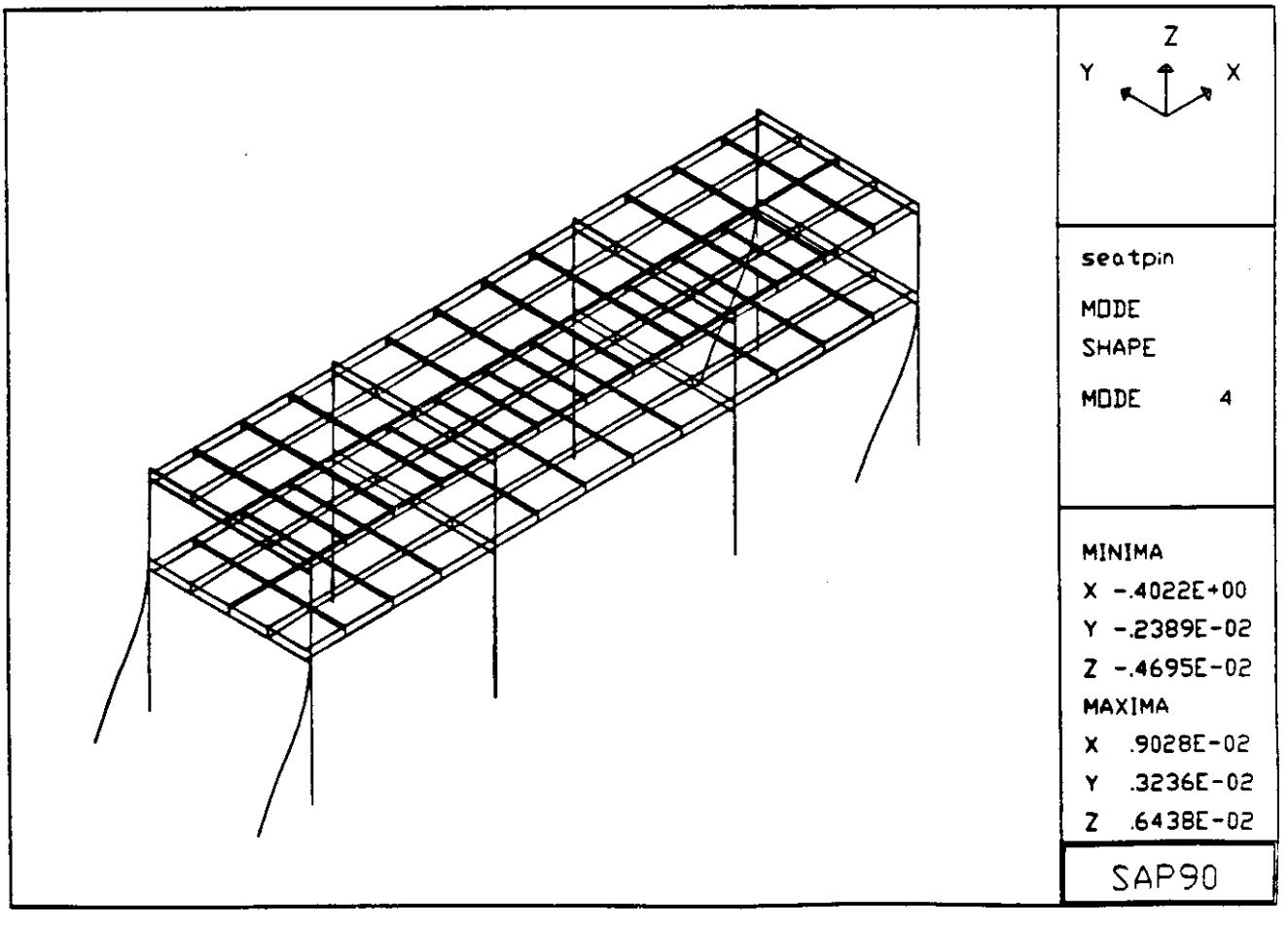

Figure 4.2. Mode Shapes 3 and 4 of Pinned-Base Model

symmetry, dynamic response could be very different than that noted for the typical sections. The geometry change would also affect the ability of the frame to transfer bending moments within the frame. Therefore, an outrigger model was analyzed.

The outrigger model used the same geometry as the basic Seattle section, but a single column was extended outward in a transverse direction by 10 ft. This extension was smaller than some noted over the length of the bridge. Further, it occurred only with one column. The computed dynamic properties for the first eight modes are illustrated in Table 4.2, and the first four mode shapes are shown in Figures 4.3 and 4.4.

The outrigger column increased the calculated periods slightly over the values calculated for the basic Seattle model, but the increase in period was small. The mode shapes were significantly different, however. First, the loss of symmetry had a visible effect on the first several modes. The deformation was no longer purely in the longitudinal direction in the first mode, since there was a slight transverse component. Similarly the transverse mode (Mode 2) had a longitudinal component. The torsional mode aggravated the deformation on the outrigger column, and this led to a nonuniform distribution of forces in the structure.

Other variations in the model could have been considered but were not analyzed in detail because of the limited time available for this study. In particular, the effect of approach lanes and variable deck width may be important. Also, several sections of the viaduct with different construction were not analyzed but could be significant. One section with very tall slender concrete piers toward the north end of the viaduct could have been quite critical. The columns appeared to be very light when the height of the frame was considered, and the lateral load frames were incomplete. These other frames should be analyzed.

BASE FORCE REACTION FACTORS

Mode #	Period (sec)	X Direction	Y Direction	Z Direction	X Moment	Y Moment	Z Moment
1	1.181	.124E+02	-.107E+03	.117E-01	.500E+01	.565E+03	-.292E+03
2	1.124	-.113E+00	-.125E+02	-.202E-02	.560E+03	-.505E+01	.106E+04
3	.975	.102E+00	-.738E+00	-.234E-03	.326E+02	.453E+01	-.782E+03
4	.251	.120E+01	-.113E-01	.976E-01	.188E+01	-.426E+02	.864E-01
5	.241	.191E+01	.191E-01	-.485E+00	-.877E+01	-.639E+02	-.547E-02
6	.240	.132E+00	.329E-01	.573E+00	.169E+02	-.588E+02	-.162E+02
7	.240	-.662E-01	.183E-01	-.117E+00	.216E-01	.140E+02	.433E+02
8	.226	.542E+00	-.151E+00	-.143E+01	-.406E+02	-.243E+03	-.729E+01

PARTICIPATING MASS - (percent)

Mode #	X Direction	Y Direction	Z Direction	X Sum	Y Sum	Z Sum
1	95.926	0.007	0.000	95.926	0.007	0.000
2	0.002	96.526	0.000	95.934	96.534	0.000
3	0.006	0.339	0.000	95.940	96.872	0.000
4	0.890	0.000	0.006	96.830	96.872	0.006
5	2.273	0.000	0.147	99.102	96.873	0.153
6	0.011	0.001	0.204	99.113	96.873	0.357
7	0.003	0.000	0.009	99.116	96.873	0.365
8	0.183	0.014	1.268	99.299	96.888	1.633

Table 4.2 Dynamic Properties of Outrigger Model

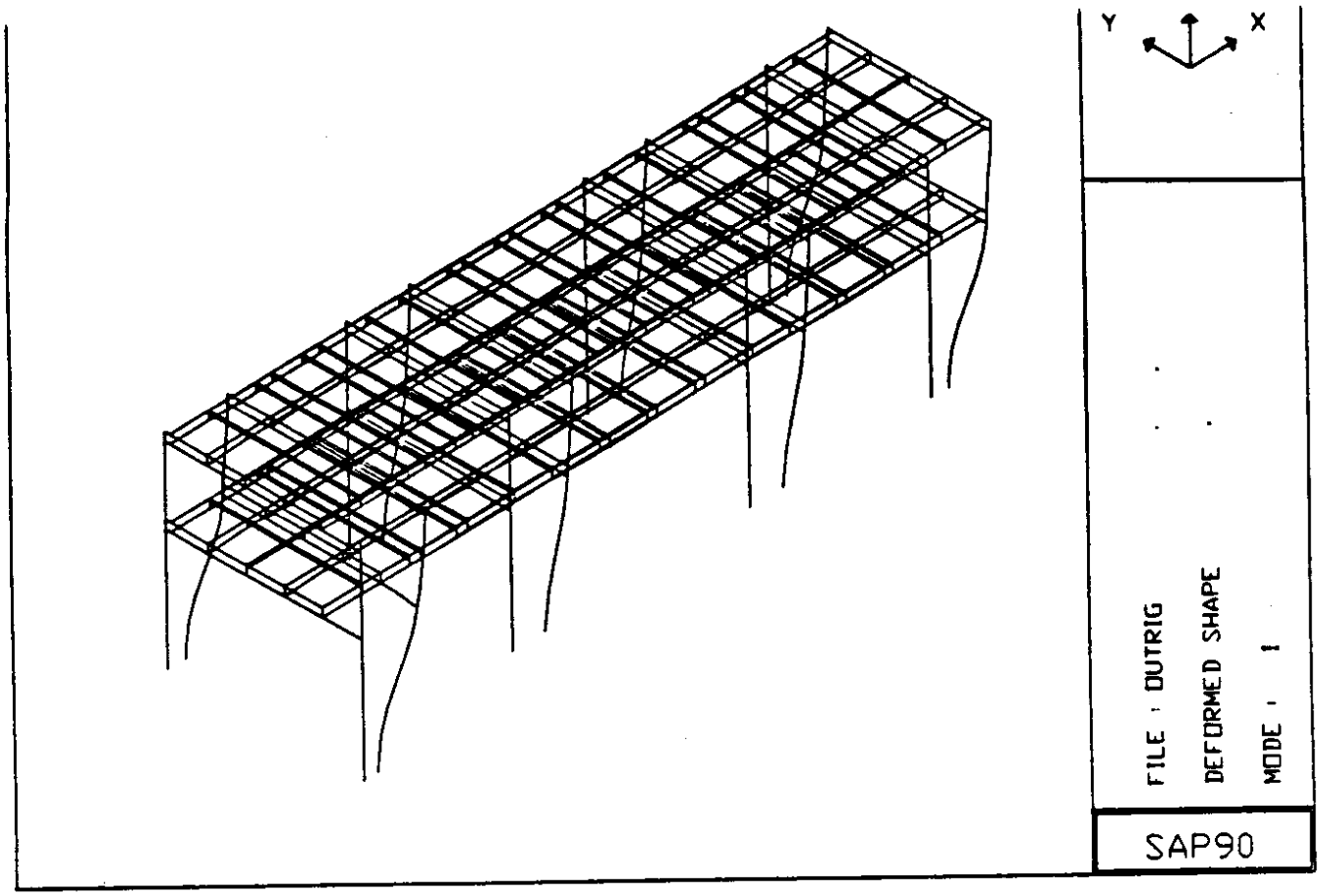

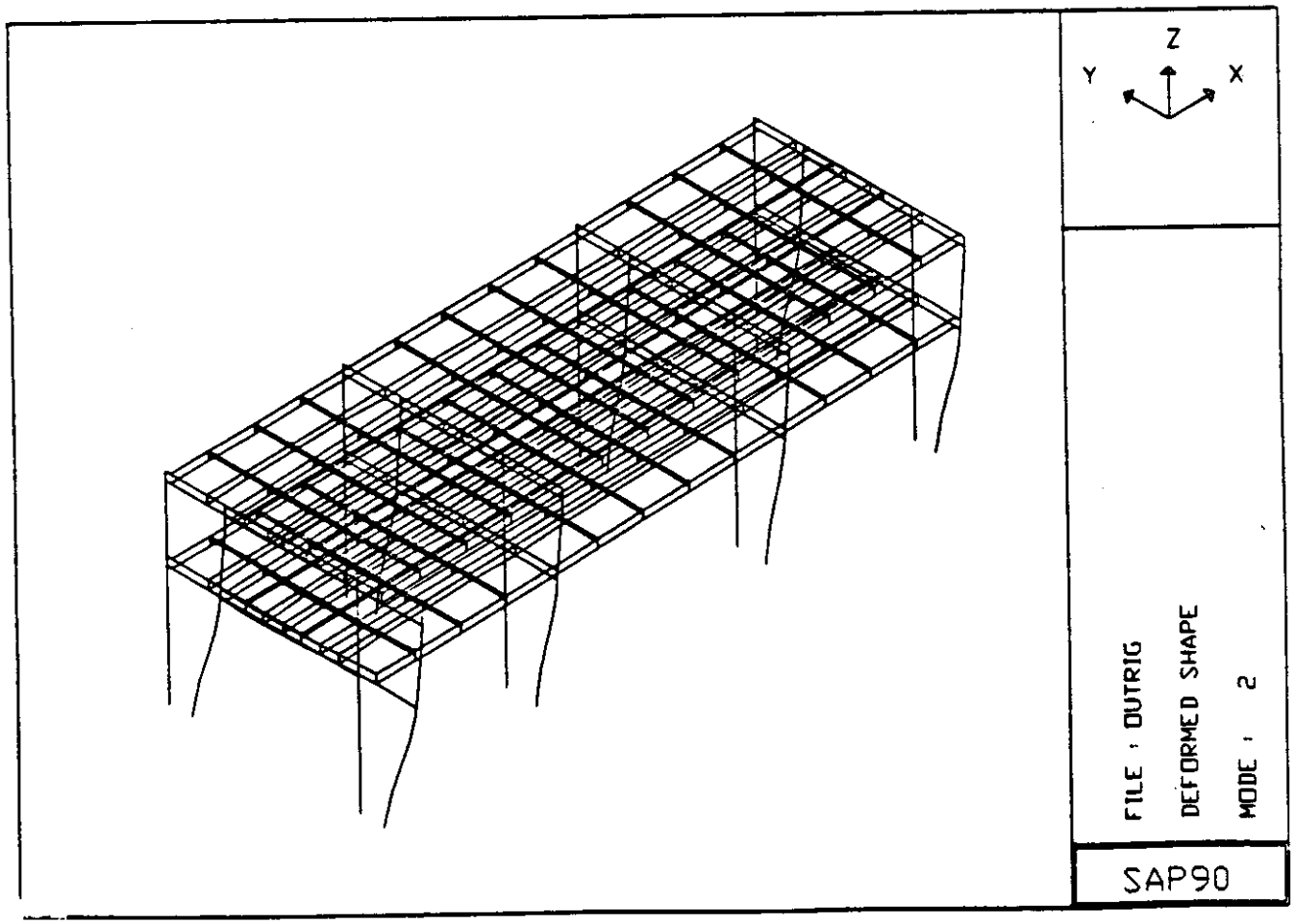

Figure 4.3. Mode Shapes 1 and 2 of Outrigger Model

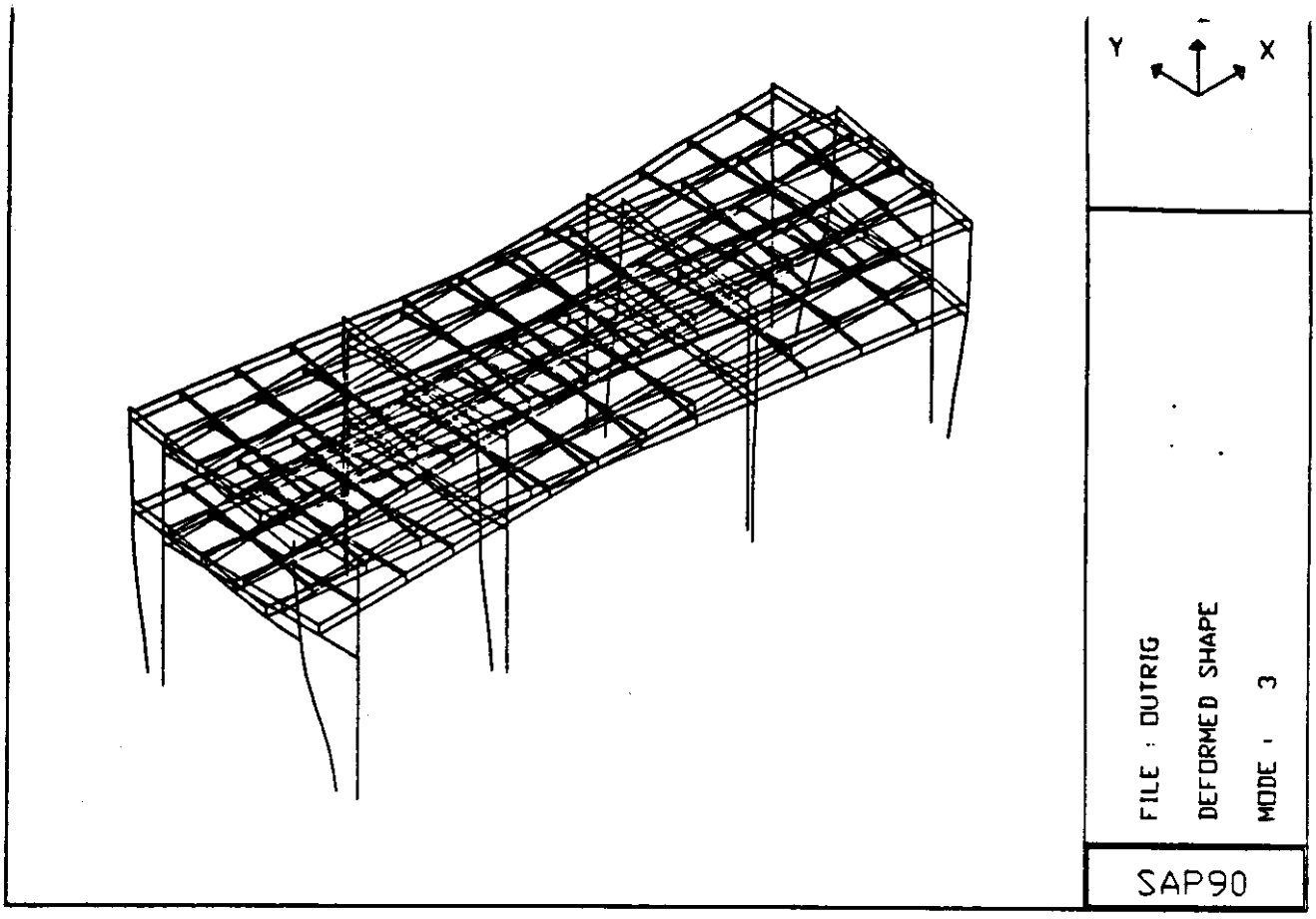

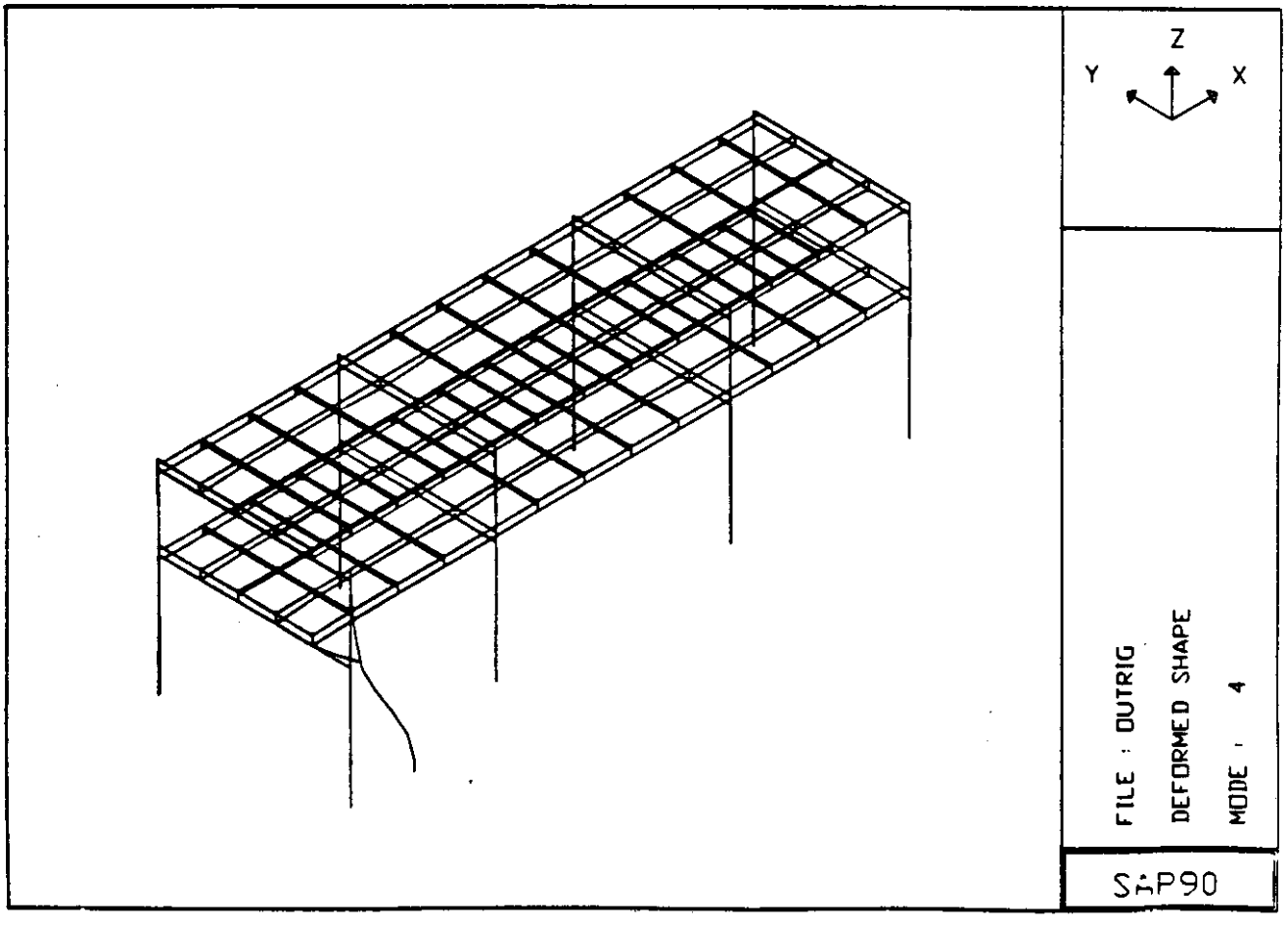

Figure 4.4. Mode Shapes 3 and 4 of Outrigger Model

Static Analysis of WSDOT Section

The analytical models were used to estimate bending moments and shear forces. In the first analysis, the basic WSDOT model was arbitrarily loaded with 800 kips of transverse load at the top deck and 400 kips at the bottom deck. The loads were applied over the length of the deck, and they distributed themselves to each frame in proportion to the frame stiffness. Note that the flexibility of the transverse foundation spring contributed significantly to the relative frame flexibility. Figure 4.5 shows the moment diagrams for an interior and end frame (interior frame is on the top) with this arbitrary loading. The moment diagrams for the two frames were similar in shape, but the bending moments were 55 percent to 120 percent larger in the interior frame than in the end frame because of its greater frame stiffness. The maximum column bending moment was 3,765 kip-ft and 2,030 kip-ft for interior and end frames, respectively. The maximum column shear force were 195 kips and 105 kips for interior and end frames, respectively.

Spectral Analysis of Basic WSDOT Section

The frames were also analyzed with the soft soil spectral loading used in the WSDOT study. The modal contributions were combined with the Complete Quadratic Combination Method. The spectrum was applied simultaneously in the longitudinal and transverse directions, although members are usually checked separately in the two directions. As a result, the member capacities for these orthogonal bending moments and shears were checked separately. Figures 4.6 and 4.7 show the bending moments and shear forces caused by the transverse spectral excitation for the interior and end bents of the basic WSDOT section model. The maximum values of column moment and shear are shown in the figure. The maximum bending moments and shear force in the transverse girders of the end bents were approximately 2,230 kip-ft and 146 kips, respectively. The maximum bending moments and shear force in the transverse girders of the interior bents were approximately 2,620 kip-ft and 215 kips, respectively.

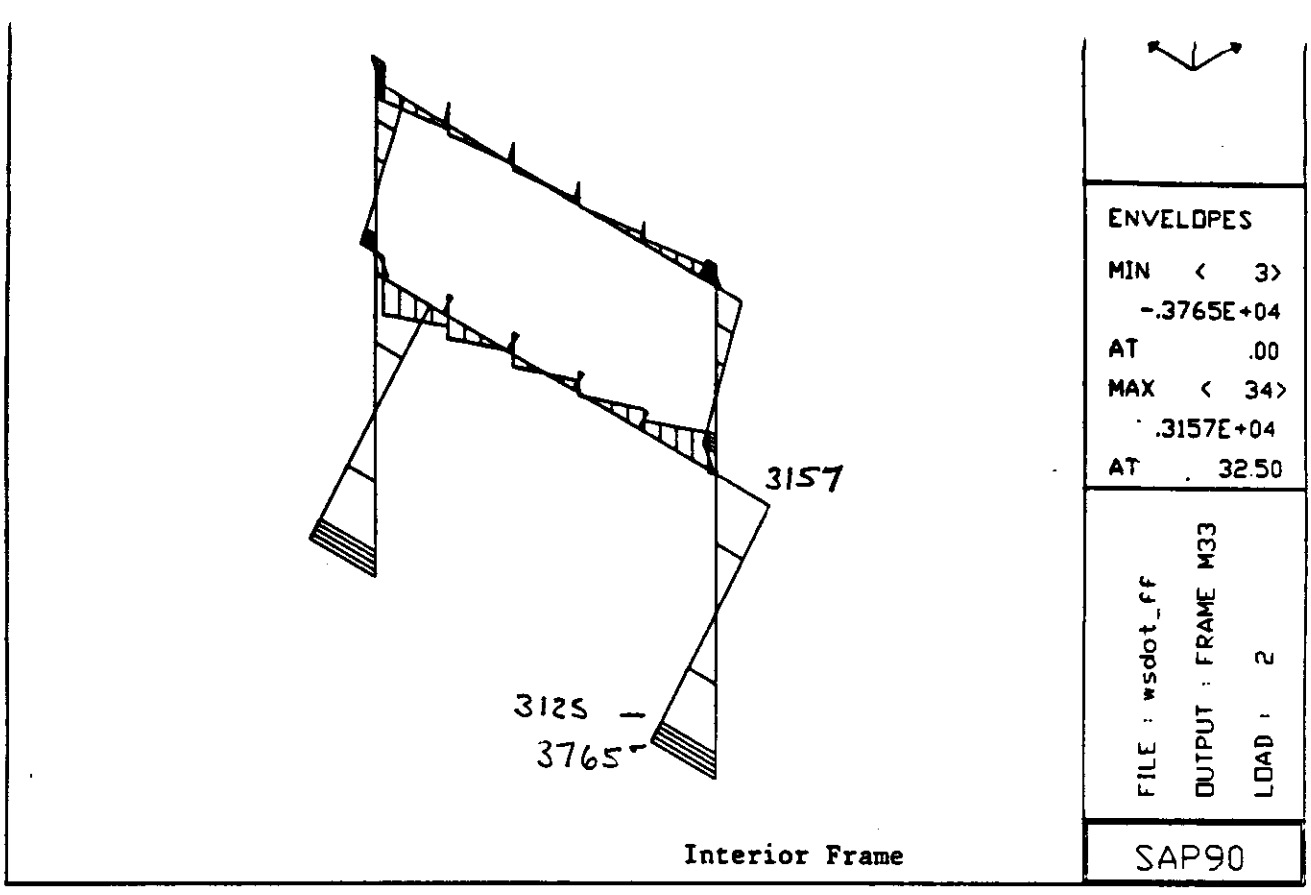

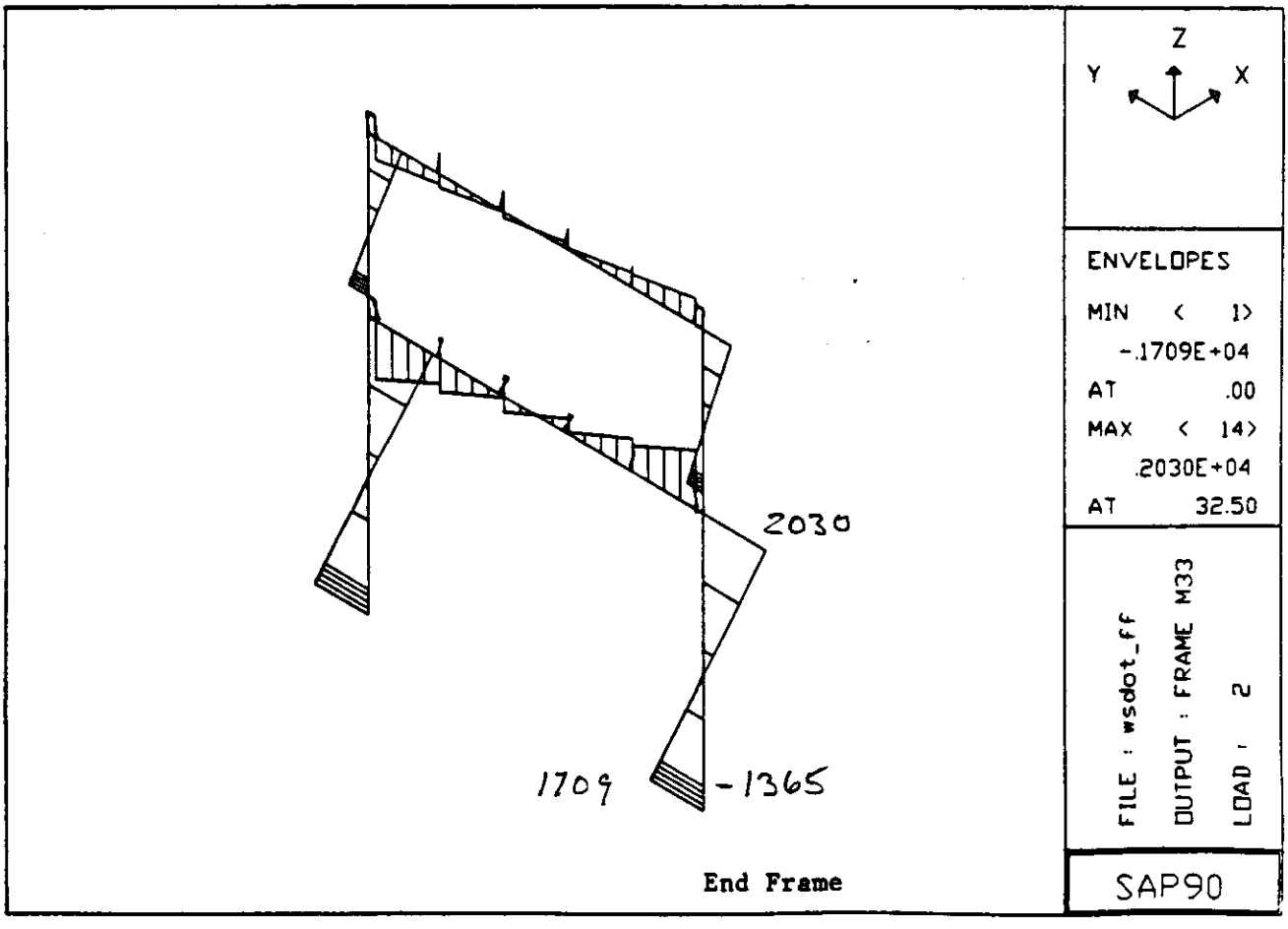

Figure 4.5. Moment Diagrams for WSDOT Section Model with Applied Forces

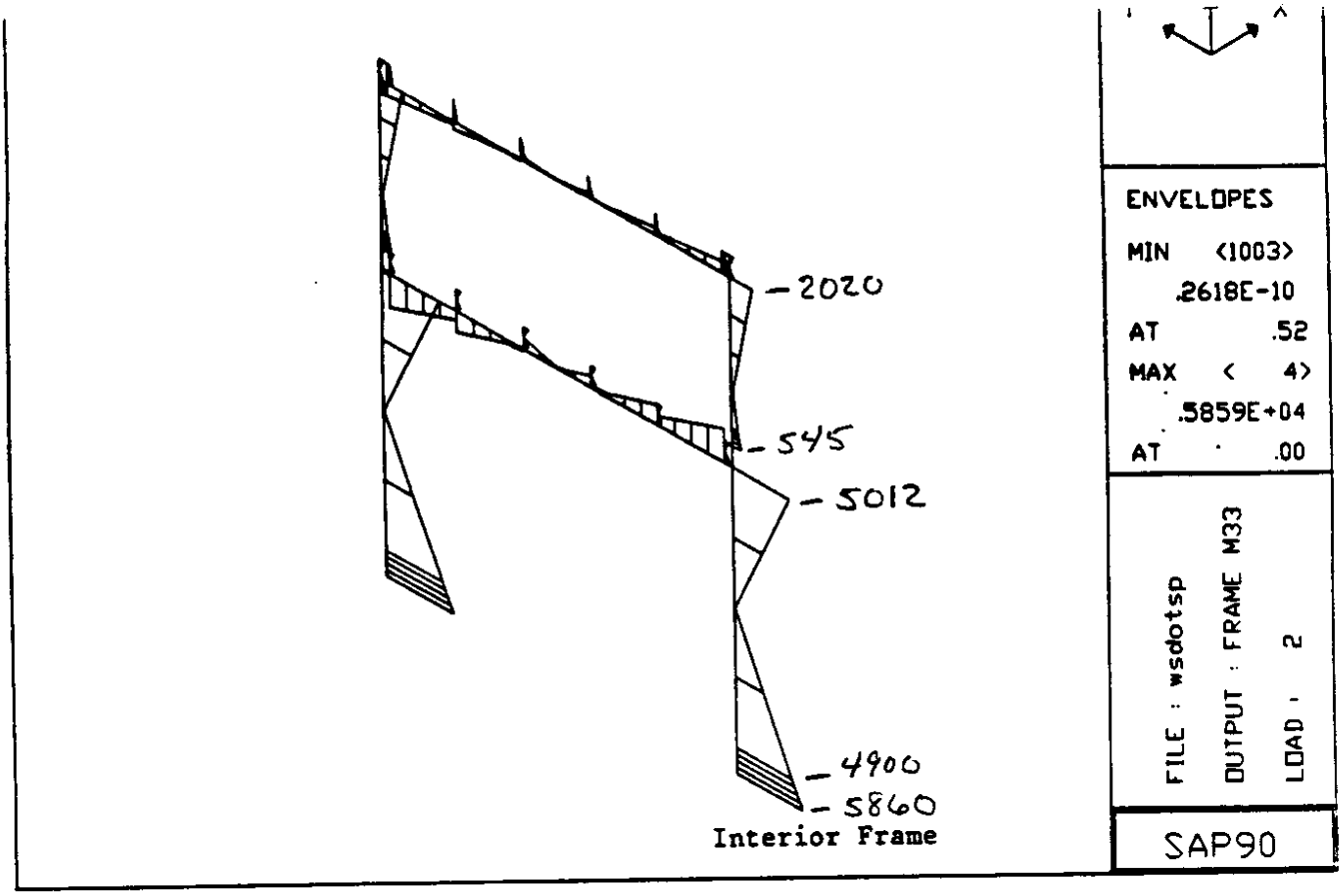

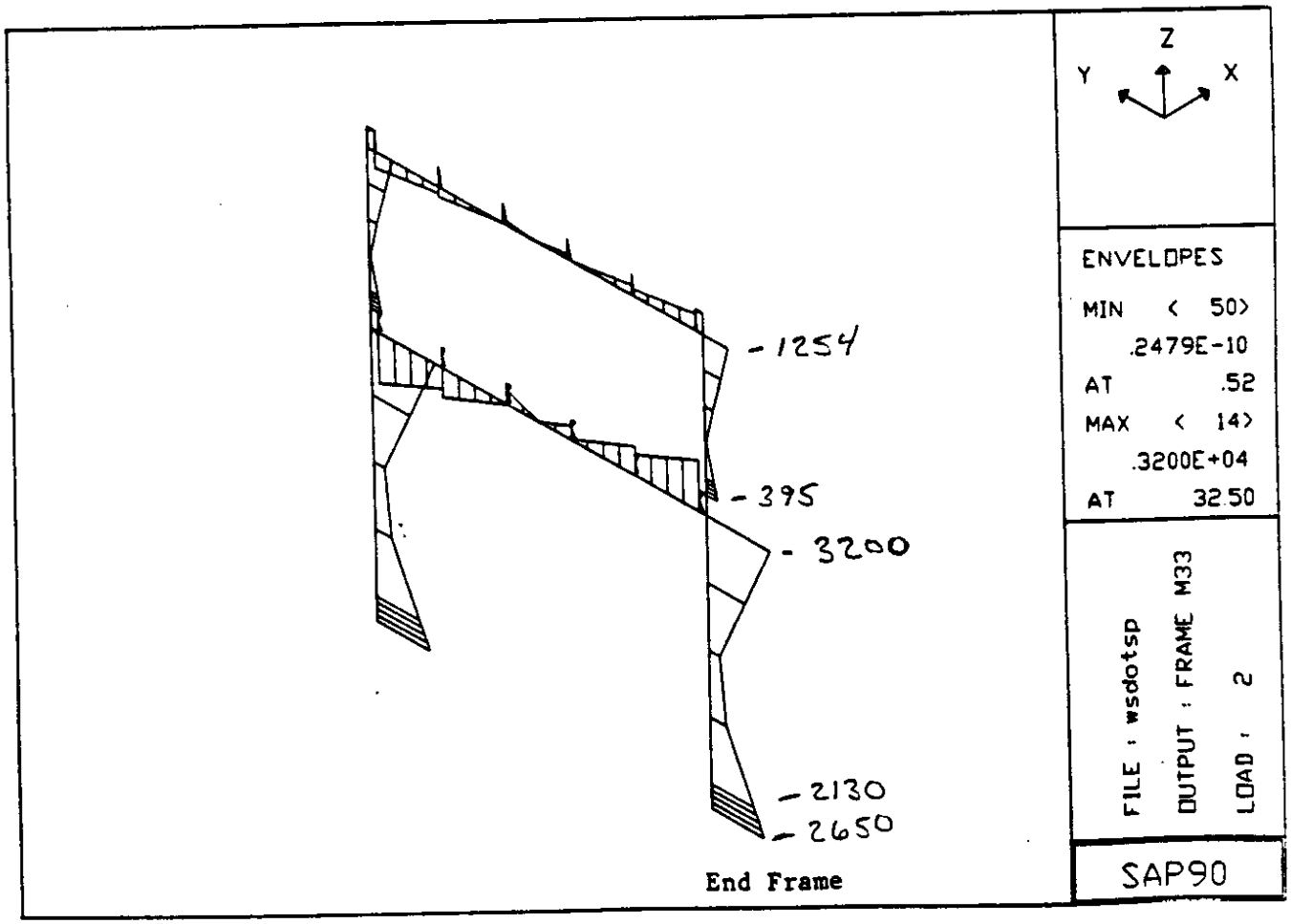

Figure 4.6. Transverse-Loading Moment Envelopes for WSDOT Section Model from Spectral Analysis

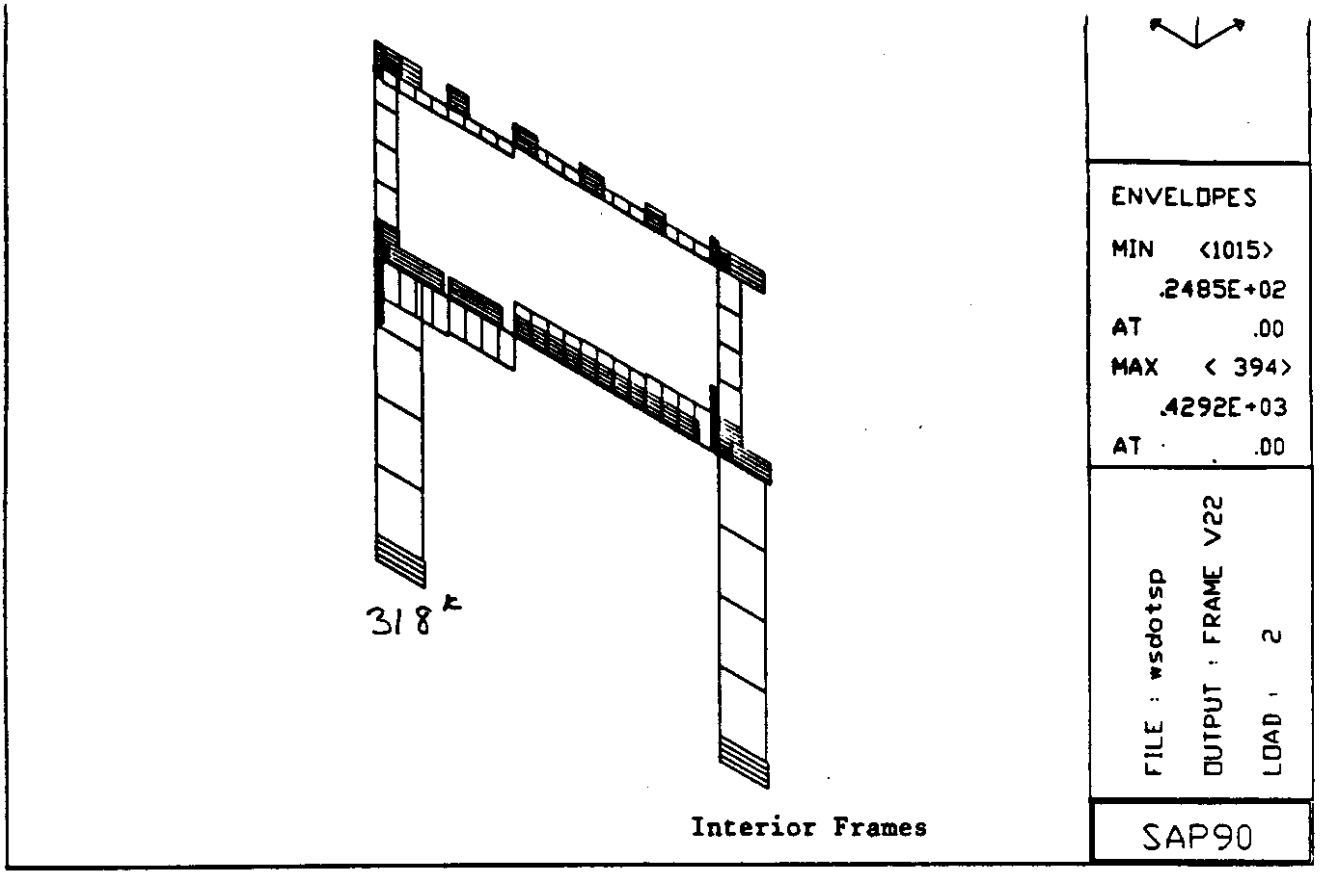

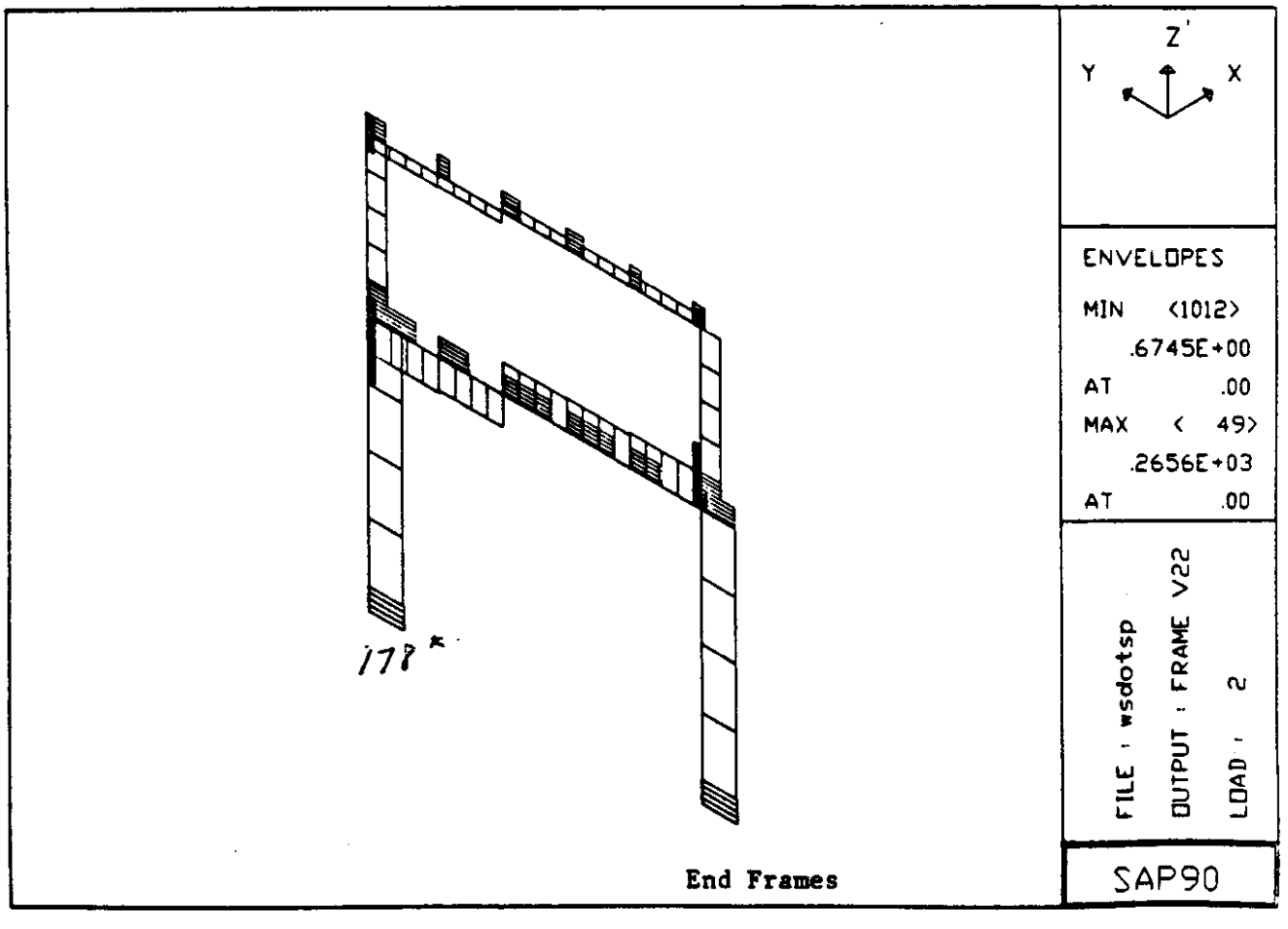

Figure 4.7. Transverse-Loading Shear Envelopes for WSDOT Section Model from Spectral Analysis

Figure 4.8 shows the bending moments in the longitudinal frame due to the longitudinal spectral loading. The top portion of this figure shows the in-plane bending moments of the girder, and the transverse moments in the column. The transverse moments in the column are shown because of SAPLOT's plot component separation mechanism. The bottom portion of Figure 4.8 shows the in-plane moments of the columns created by the longitudinal loading. The maximum shear forces were 332 kips and 132 kips in the columns of the interior and end bents, respectively. The maximum bending moments and shear force in the longitudinal edge girders were approximately 3,040 kip-ft and 124 kips, respectively.

Spectral Analysis of the Basic Seattle Section

Spectral analyses were also performed on the basic Seattle model. The plots of the moment and shear envelopes are omitted because they looked so similar to those of the WSDOT model. However, the maximum values will be summarized. The maximum transverse bending moments were 3,230 kip-ft and 5,460 kip-ft for the columns of the end and interior bents, respectively. The moments at the base of the pile caps were 6,050 kip-ft and 2,650 kip-ft, respectively. The maximum in-plane shear forces were 173 kips and 338 kips for the columns of the interior and end bents, respectively. Comparison of these numbers to the basic WSDOT model shows that the interior frames took a slightly larger portion of the transverse inertial loading with the Seattle model than with the WSDOT model. The shear and bending moments of the girders of the transverse bents were 166 kips and 2,620 kip-ft for the end bent and 299 kips and 4,310 kip-ft for the interior bents.

The longitudinal spectral loading caused maximum bending moments of 2,060 kip-ft and 5,480 kip-ft in the end and interior columns of the longitudinal frames. The longitudinal shear forces were 127 kips and 320 kips for the end and interior columns, respectively. The maximum bending moment and shear force in the longitudinal edge girder were 3,050 kip-ft and 126 kips, respectively.

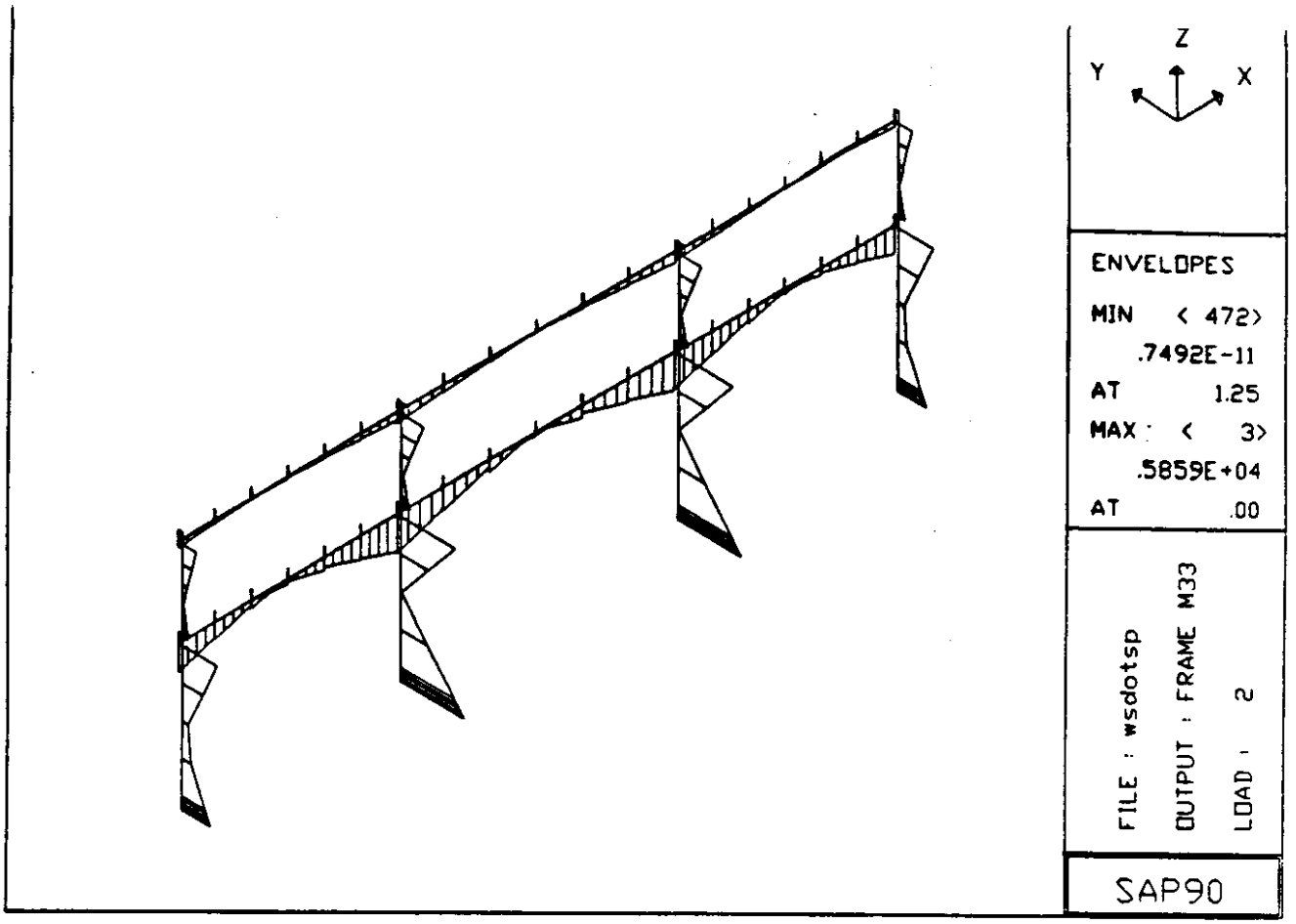

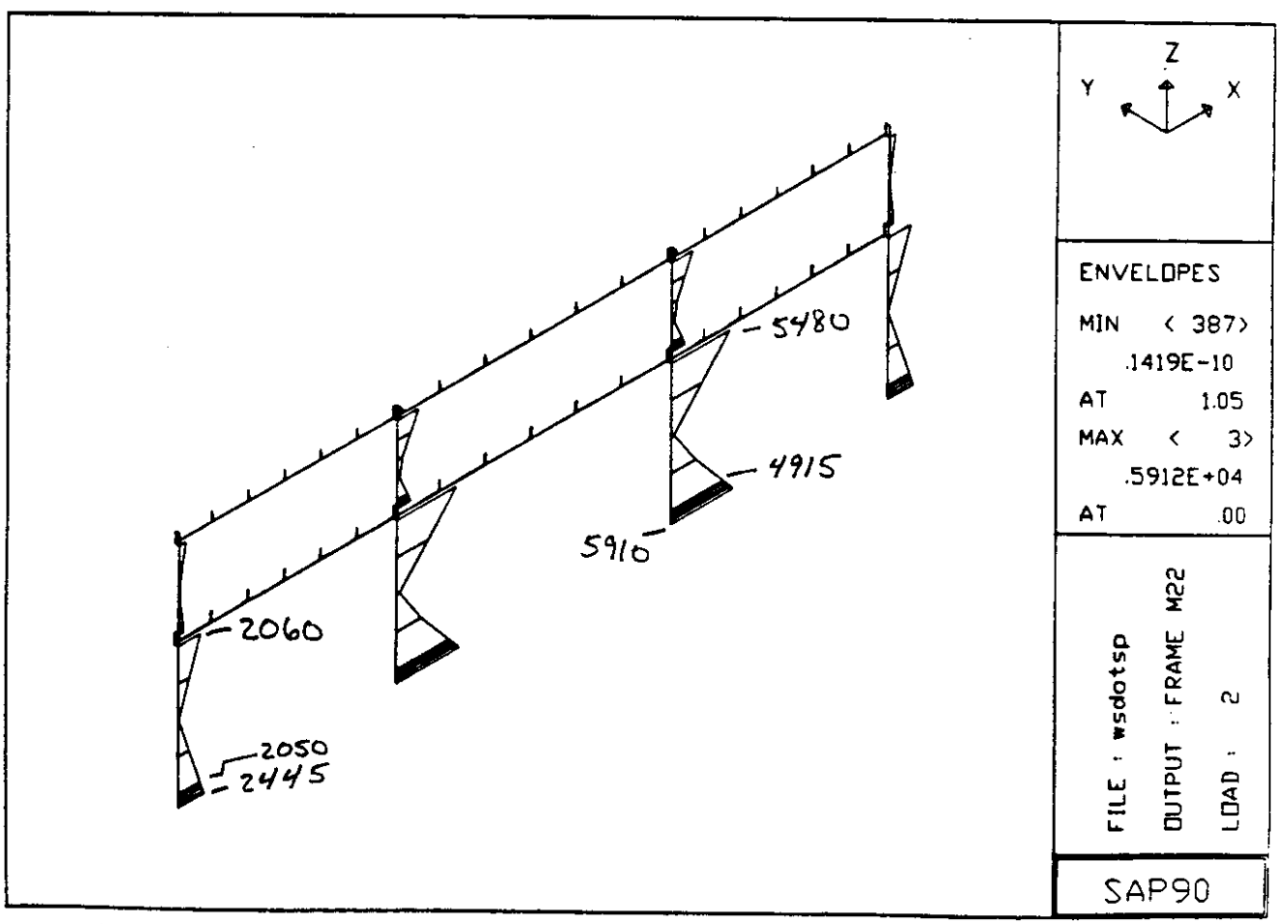

Figure 4.8. Longitudinal-Loading Moment Envelopes for WSDOT Section Model from Spectral Analysis

Spectral Analysis of the Pinned-Base Section

Spectral analyses were performed on the pinned-base model. The moment diagrams are different for this model, and so bending moment envelopes for transverse and longitudinal loading are shown in Figures 4.9 and 4.10, respectively. The shear forces at the pile cap were significantly smaller in the pinned-base model than in the Seattle section model. The maximum shear was 127 kips for a column in an end bent and 229 kips for the interior locations. Bending moments were obviously zero at these locations, and the combined effect was that the pinned base tended to protect the foundation from excessive load and possibly from further damage. However, the pinned base dramatically increased the potential for damage in other parts of the structure. The maximum in-plane bending moment for a column in an end bent was 4,340 kip-ft, and in an interior bent, the maximum was 7,910 kip-ft. These were approximately 35-45 percent larger than those calculated for the Seattle section models. These results suggest that, if flexural capacity were lost at the base, other damage might occur at other locations shortly thereafter.

Bending moments and shear forces in the transverse girders of the end bents were increased to 3,160 kip-ft and 197 kips because of the pinned base. Girders in interior bents had maximum moments of 5,390 kip-ft and shears of 368 kips. Longitudinal bending caused similar increases in the pinned base model for the interior columns, since the maximum moment was 9,530 kip-ft. The difference was probably caused by the dramatic reduction in the end column stiffness due to the loss of rotational restraint and the more flexible foundation springs.

Spectral Analysis of the Outrigger Section

Spectral analyses were performed on the outrigger model. There were some unique features of the force and moment distributions of this model, so some of the moment and shear diagrams are included for this model for comparison with previous figures. The maximum shear and moment in the outrigger columns were 169 kips and 3,190 kip-ft for

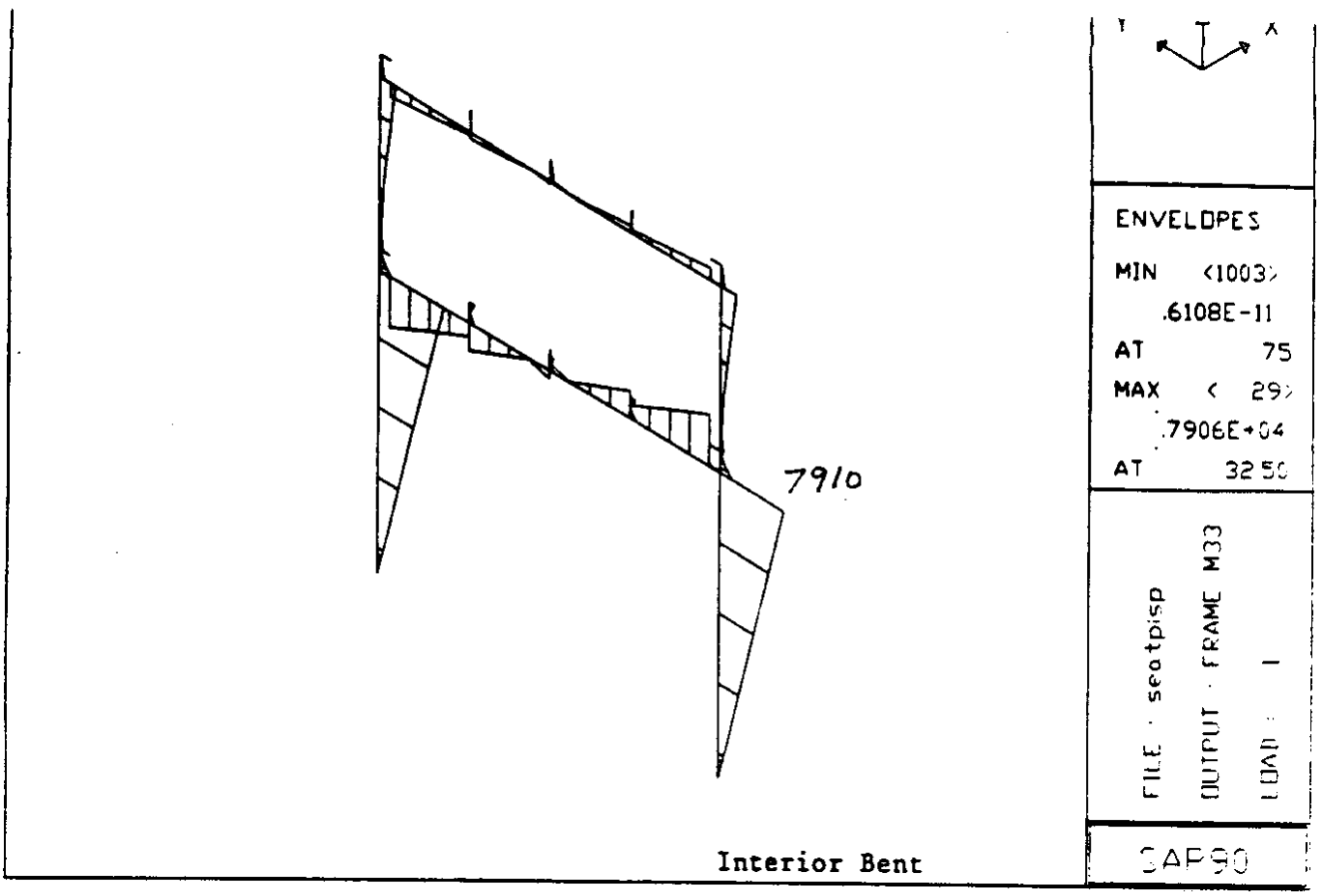

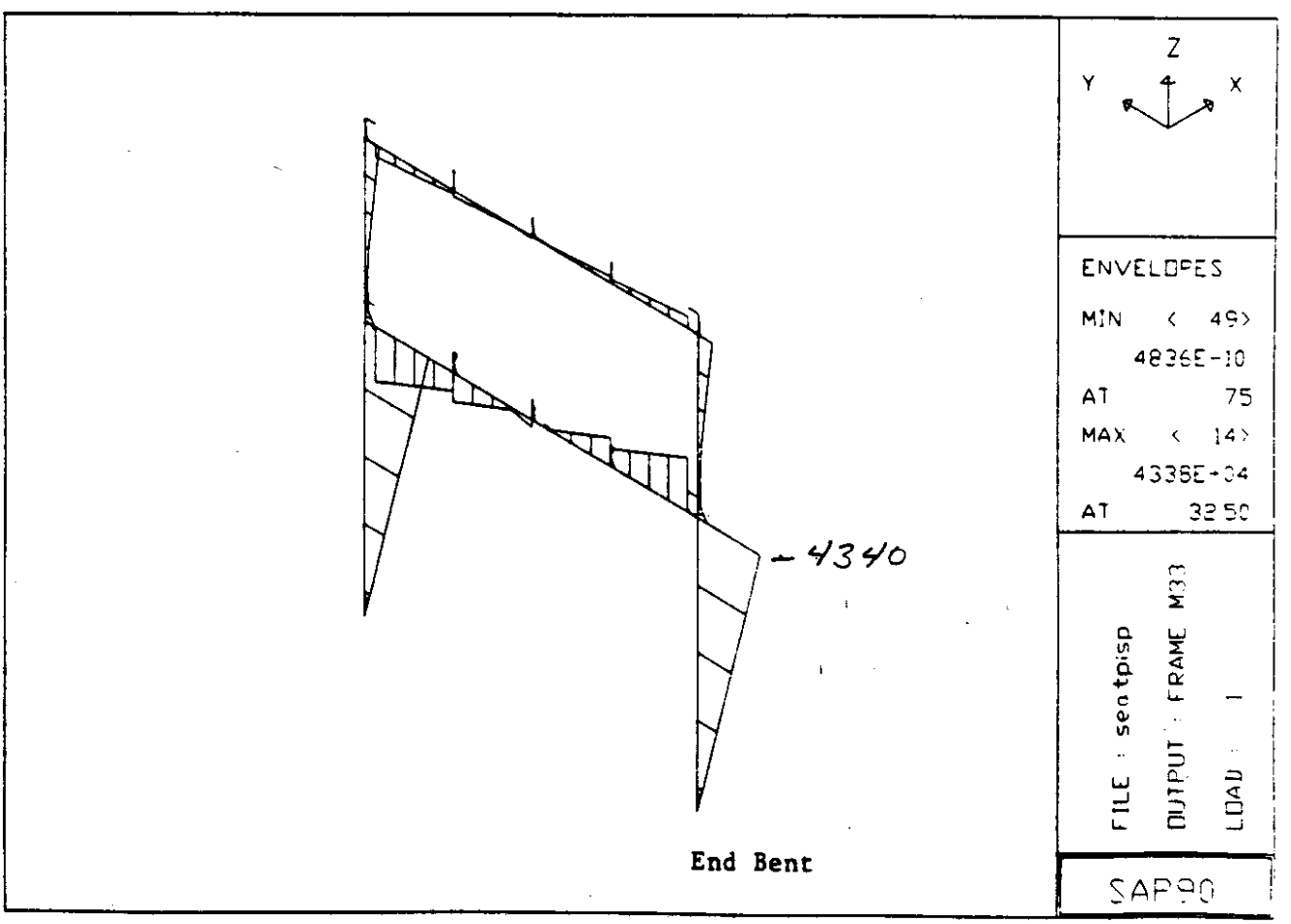

Figure 4.9. Transverse-Loading Moment Envelopes for Pinned-Base Model from Spectral Analysis

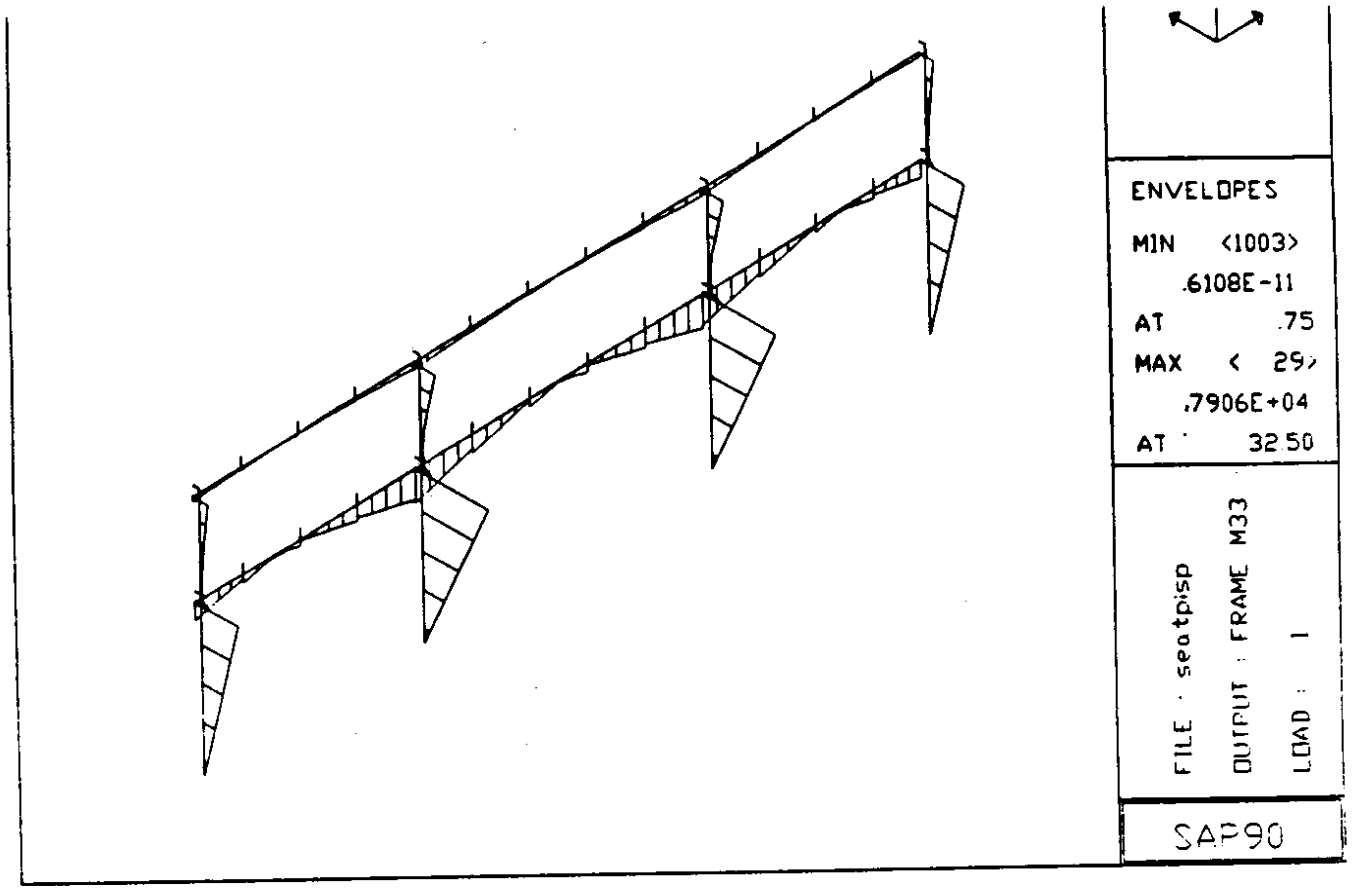

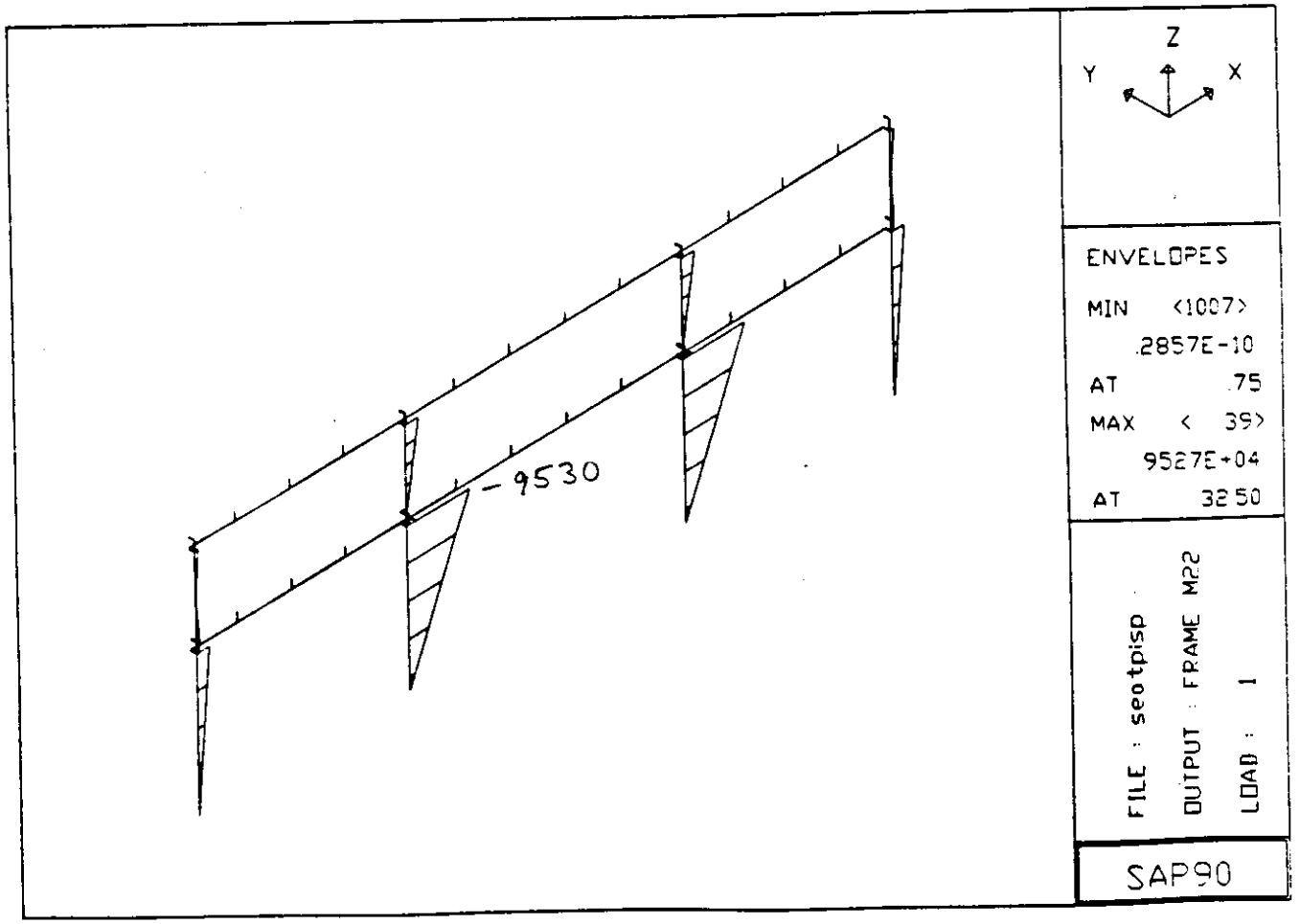

Figure 4.10. Longitudinal-Loading Moment Envelopes for Pinned-Base Model from Spectral Analysis

transverse loading and 100 kips and 1,780 kip-ft for longitudinal loading. Comparison of these numbers to those of the basic Seattle model show that the offset column was far less effective in resisting longitudinal loading than the normal symmetric frame. This can also be seen from the bending moment envelopes of Figures 4.11 and 4.12. The presence of an outrigger column placed increased demands on the interior bents. The columns of the interior bents had maximum shear forces and bending moments of 332 kips and 5,630 kip-ft for transverse loading, and 346 kips and 5,910 kip-ft for longitudinal loading. Similar changes were noted for the moments transferred by the pile up to the pile foundation.

In general, the single outrigger forced larger bending moments and shear forces into the columns and pile foundations of the interior bents. The outrigger bent took larger bending moments and shear forces for transverse loading, and smaller forces and moments for longitudinal loading. As a result, it reduced the transverse loading of the far end bent and increased the longitudinal loading for the same exterior bent. The differences caused by the single outrigger were about 5 to 10 percent. These differences were not terribly large, but they could have a significant effect in a relatively brittle structural system, since they might force damage and premature failure of the more heavily-loaded elements.

4.4 REQUIRED AND COMPUTED STRENGTHS

Although efforts were made to conduct the present study on the same basis as the WSDOT one, differences in assumptions may explain some of the differences between the UW and WSDOT analyses. Some of the differences include the following:

1. In calculating force demands with spectral analyses, the WSDOT considered biaxial bending caused by earthquake loads of 100 percent in one direction combined with 30 percent loading in the orthogonal direction. The UW analyses considered loading in one direction at a time; biaxial bending was not considered.

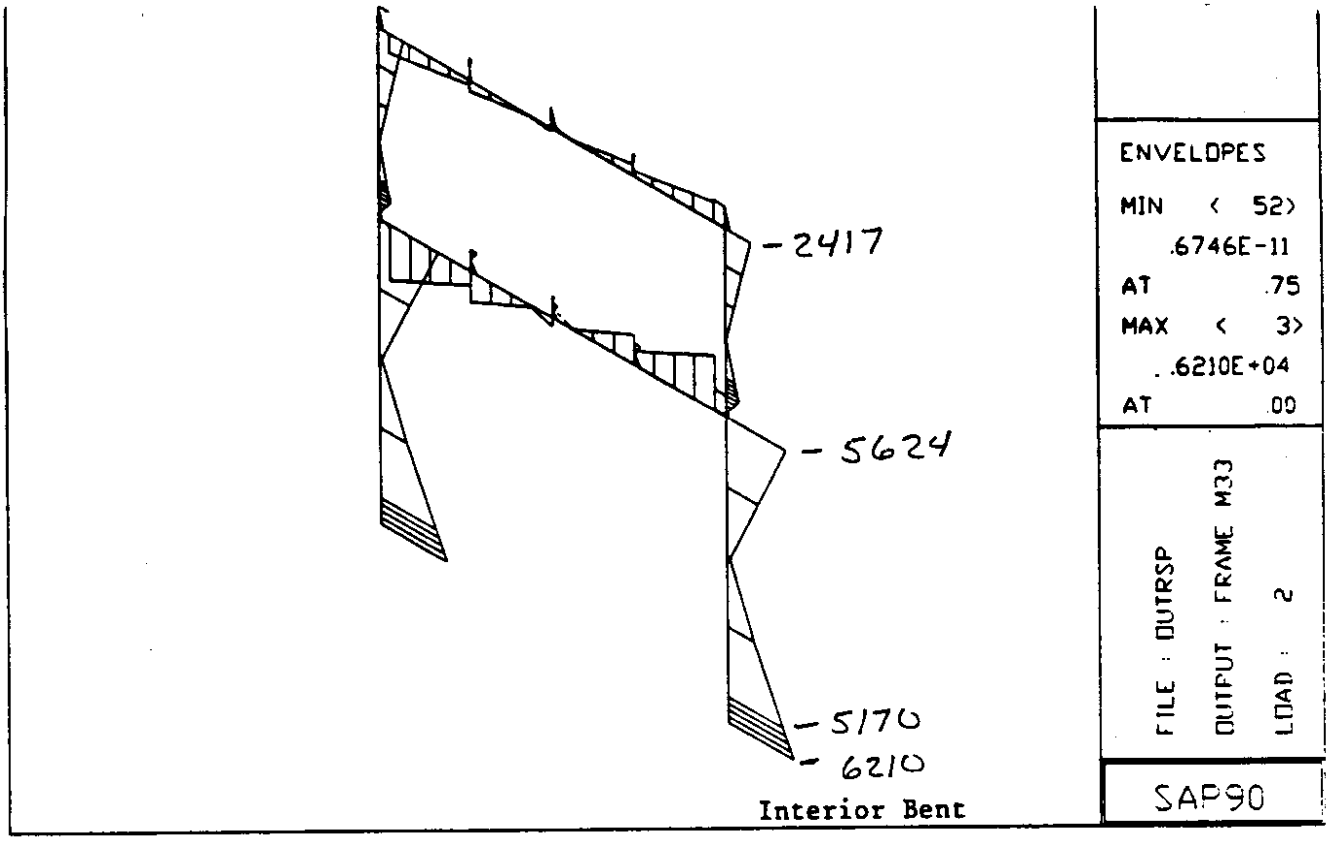

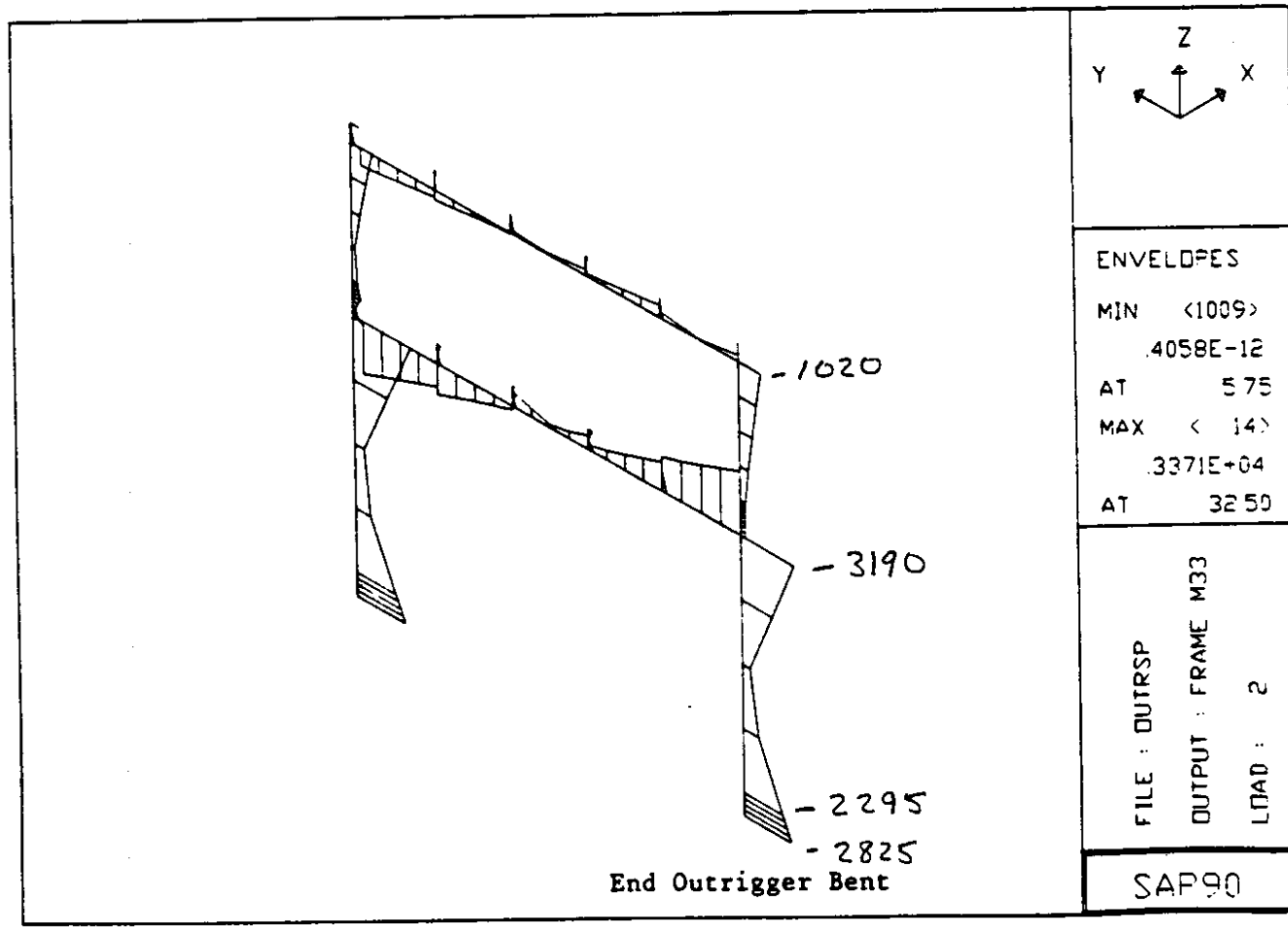

Figure 4.11. Transverse-Loading Moment Envelopes for Outrigger Model from Spectral Analysis

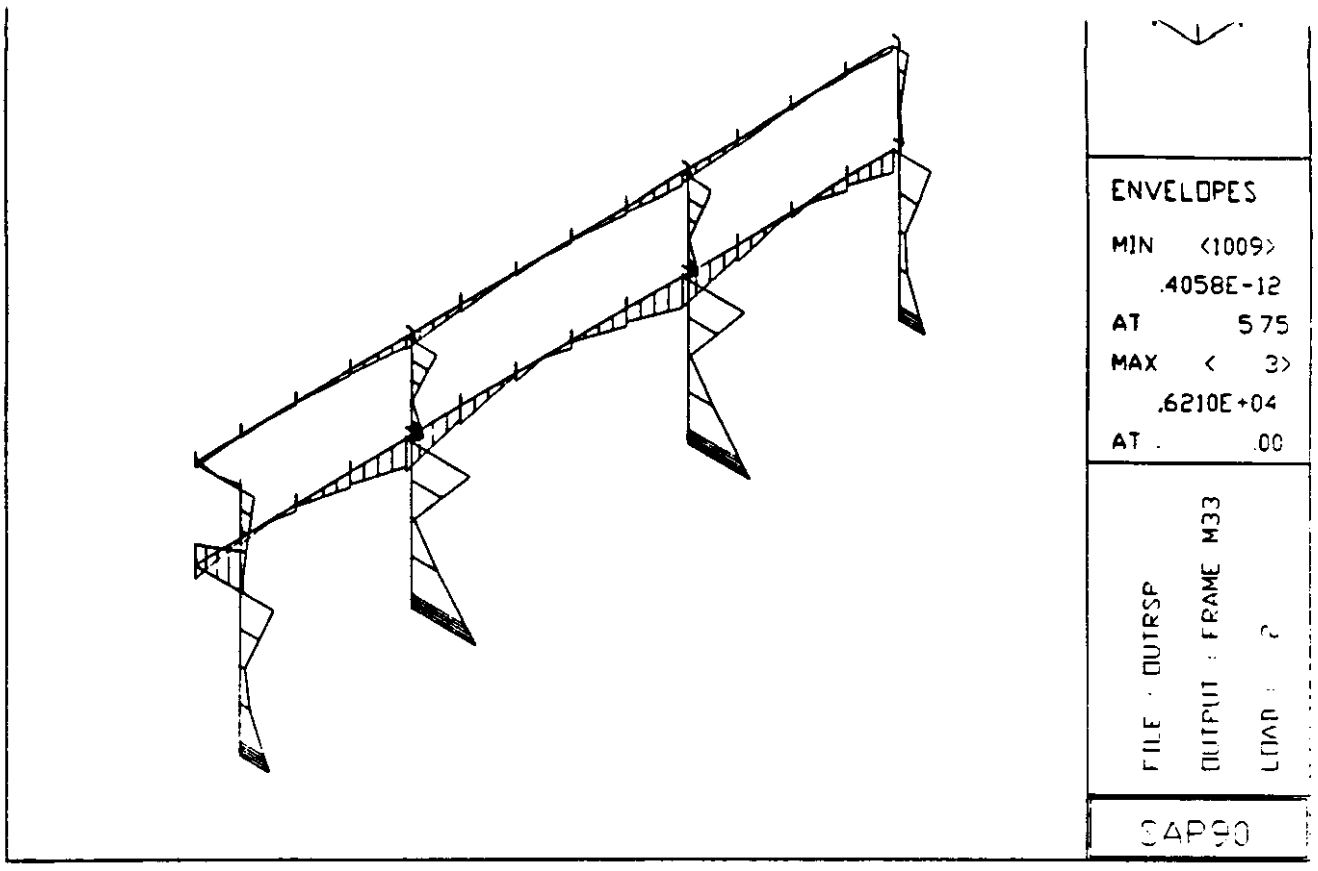

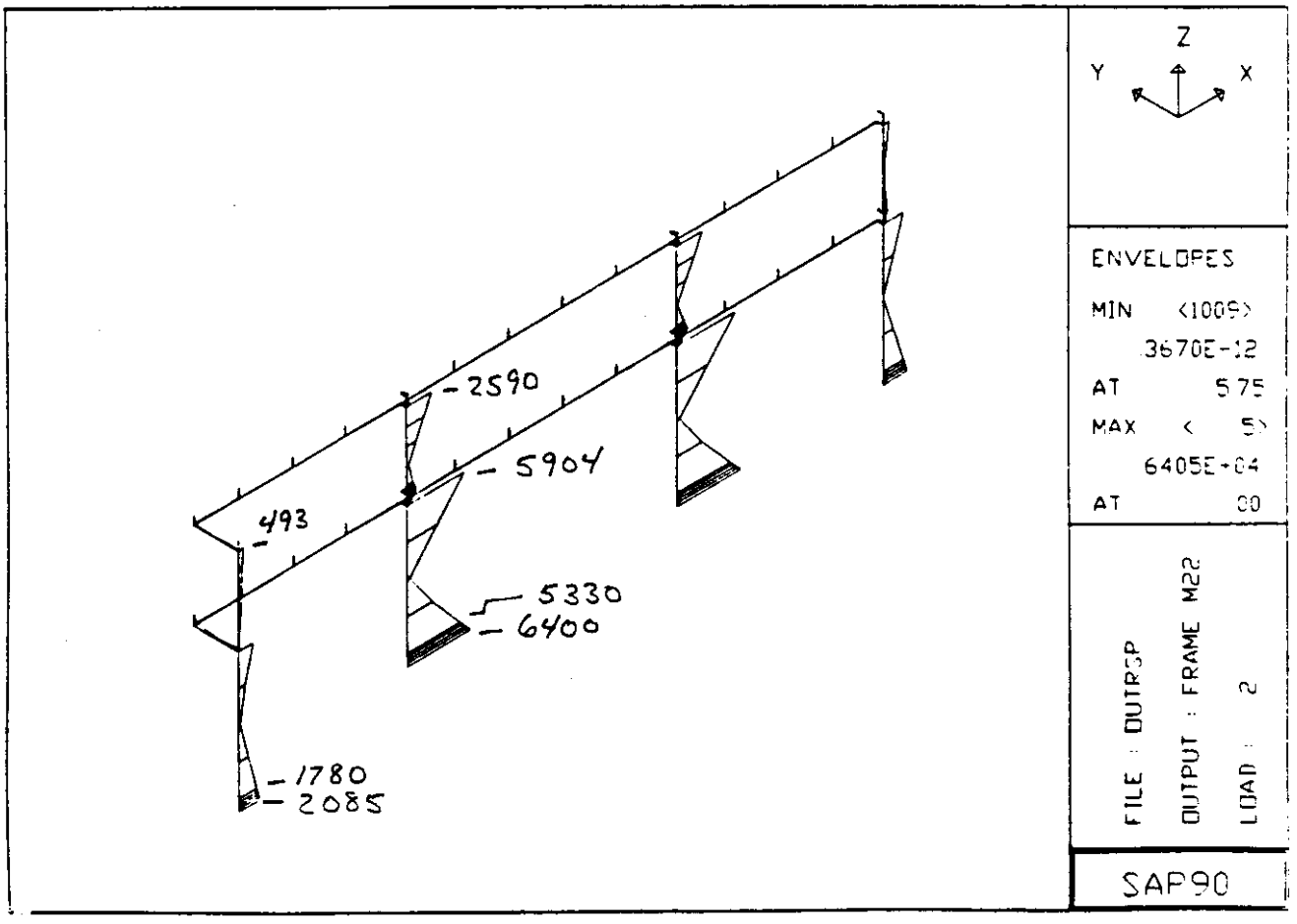

Figure 4.12. Longitudinal-Loading Moment Envelopes for Outrigger Model from Spectral Analysis

2. In calculating forces caused by static loads, the WSDOT engineers distributed loads to each frame according to its tributary area. The UW engineers distributed the loads to each frame according to its stiffness.

3. In calculating column capacities, the WSDOT assumed that axial forces in the columns were caused by the dead load minus the seismic load. The UW researchers computed strength for both dead load only and for zero axial load. Figure 4.13 shows that the computed column strength was approximately 60 percent higher if axial load was taken into account. This occurred because the axial load on the column was relatively small (corresponding to about 400 psi, or $0.133f'_c$ with the nominal material strengths), and the column was in the tension-controlled part of the interaction diagram. However, if this higher strength were to be relied on, the reductions in axial load caused by rocking and vertical accelerations would have to be included in the analysis.

Both sets of assumptions are reasonable. Comparison of the WSDOT and UW g-ratings and code ratios shows the extent that they vary with the analytical assumptions. However, despite the differences in results, both studies came to the same conclusion; the capacity of the viaduct is likely to be inadequate in the event of a large earthquake.

Additional factors, not considered in the WSDOT analyses, may be important. The influence of material strength, column details, inelastic behavior, joint shear and reinforcement development will now be discussed.

Nominal Versus Actual Material Properties

The nominal material strengths were assumed to be f'_c=3,000 psi and f_y=40 ksi, in accordance with the WSDOT assumptions and the strengths that were believed to have been specified at the time. Because shear strength varies only with the square root of concrete strength, shear strengths are less sensitive to material strength differences than are flexural and axial strengths. The strength of the reinforcement remains open to question.

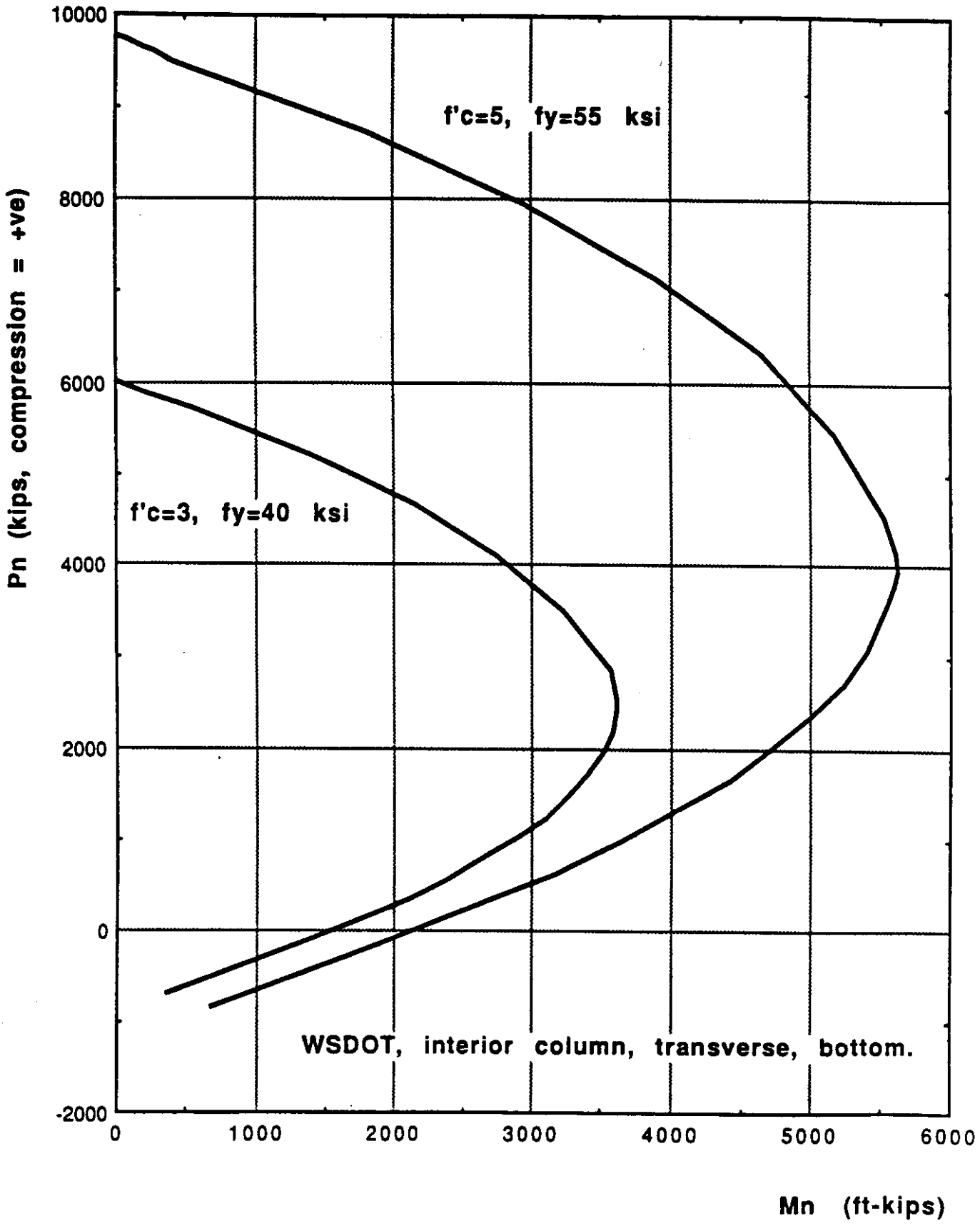

Figure 4.13. Moment-Axial Load Interaction Diagram

The 1953 AASHO Design Specifications recognized four reinforcing steel grades: structural, intermediate, hard, and rail. The first three were subsets of the general descriptor "billet steel." The Materials section of the 1953 AASHO Specification required that Billet Steel bars conform to the requirements of AASHO Materials Specification M 31-52, and that the deformations satisfy ASTM A-305-50 T. M 31-52 was not available, but the corresponding ASTM standard for Billet Steel bars (A 15-50 T) was. Its minimum tensile requirements for deformed bars are as follows:

GRADE	F_y(ksi)	F_u(ksi)
Structural	33	55
Intermediate	40	70
Hard	50	80

Section 3.4.12 of the Design Specification contained a footnote requiring that, if the allowable stresses for the intermediate (and by implication, higher) grades are used, then the contract for the structure should state so, and the grade required should also be noted on the plans. No such notation was found on the plans for the viaduct, implying that the steel was structural grade. However, the set of plans was not complete, so it is possible that a notation existed on a sheet not available to the researchers. However, the WSDOT study assumed a yield strength of 40 ksi, corresponding to intermediate grade, so, for the sake of consistency, that value was used here also.

Indirect evidence of strength was available from tests conducted on bars taken from the old I-90 floating bridge, which was constructed in the same era. Two sets of tests were conducted on 1.125-inch square bars, one by Wiss Janney and Elstner (three specimens), and the other by the University of Washington (two specimens). The results were as follows:

TEST	F_y(ksi)	F_u(ksi)
WJE	54.2	82.2
UW	48.0	77.2

Again, no grade notation was found on the few floating bridge plans made available to the testing agencies, so the steel was assumed to be structural grade.

Another area of uncertainty existed over bar sizes. ASTM A 15-50 T recognizes only bars #2-#11 inclusive, yet the WSDOT section of the viaduct used #13 and #17 bars, and the Seattle section used bars up to 2 inch square. Further research will be necessary to establish the governing specifications and the properties of such bars.

Concrete continues to gain strength after 28 days, and it almost certainly had a strength greater than 3,000 psi, even at 28 days. Intermediate grade reinforcing, with a specified yield of 50 ksi, was available at the time, in which case an average true strength of 55 ksi would be plausible. Two complete interaction diagrams for an interior column in a transverse frame are shown in Fig. 4.13. One was constructed with the nominal strengths, and the other, with f'_c=5,000 psi and f_y=55 ksi. The latter strengths were chosen to represent the upper end of the likely range of material strengths.

The column flexural strength with the stronger materials was about 40 percent higher than with the assumed strengths without the axial load and 30 percent higher with the axial load. Most of this difference arose from the greater steel strength.

Column Details

The most serious defects in the detailing of the structure were the light ties and the short splice lengths. The light tie steel would provide little resistance to buckling of the main bars, particularly if it was secured by 90° bends that did not penetrate the column core. As soon as the cover spalled, the ties would start to unwind and provide little confinement.

If shear cracks formed in the exterior columns because of longitudinal loads, they could miss the ties. The column shear strength would then be derived from the concrete alone, and the behavior would be brittle. The same would be true if the cover spalled from one of the interior columns, releasing the ties.

The connections between the longitudinal girders and the columns were also a source of concern. The inertial forces were largely induced in the deck, and the resistance came from the columns. Thus, axial tension would exist in some of the cross beams where they connected to the column. The girder-column joint regions contained little joint shear reinforcement, so tension from the cross-beam could create a horizontal tension field of sufficient magnitude that a vertical crack could form and the longitudinal girder could start to separate from the column. No calculations were made on this postulated mode of failure, but it warrants attention in any more detailed study.

Inelastic Behavior

The response modification factors were assumed to be 1.0 in the analyses, in accordance with the WSDOT study assumptions. This number implies that response would remain elastic at all times and that no advantage can be taken of the benefits of inelastic action. This assumption is conservative, since even a small amount of stable inelastic action would lead to significant reductions in required strength.

Joint Shear

Joint shear capacity was calculated for several joints. In the interior transverse frames, the cross beams contained two #17 bars in the bottom and two #17 plus two #6 in the top, which continued into the column. Maximum joint shear was therefore induced by negative bending. If f_y=40 ksi, the joint shear stress would be $2.9\sqrt{f'_c}$ if the whole column area was deemed effective in resisting shear. This would be much lower than the $12\sqrt{f'_c}$ permitted on a joint of the same geometry that contained contemporary confinement reinforcing. Beams without shear reinforcement are considered to have a shear strength of $2\sqrt{f'_c}$. The joint contained very little shear steel, so a strength between $2\sqrt{f'_c}$ and $12\sqrt{f'_c}$

seemed appropriate, most likely towards the lower end of the range. During the visual inspection of the viaduct, fine joint shear cracks were seen in some girder-column joints, oriented in the direction associated with negative bending. They were consistent with joint-shear calculations. Joint shear would be unlikely to be a problem in the positive moment sense because the bottom bars would have such poor anchorage that they would be unlikely to reach their yield strength.

The longitudinal direction posed a more grave problem. The girders were attached to the columns so that their inside faces were flush, so the area available for resisting joint shear, according to ACI 318, would be much smaller. The three #17 top bars created a joint shear stress of 426 kips/735 in^2 = $10.6\sqrt{f'_c}$. This would be close to the limit for a properly reinforced joint and would seriously exceed the capacity of the existing ones.

Bond and Splice Lengths

Splice lengths in the structure were generally 20 bar diameters. They were therefore much shorter than those specified for seismic-resistant structures today. Furthermore, there was little confinement steel to maintain their integrity once a crack had initiated. In large bars, the development length is proportional to the bar area rather than its diameter, in which case the splice length, which is directly related to the development length, is no longer proportional to bar diameter. While 24 bar diameters is the minimum for small bars, it is inadequate for large ones.

Requirements for development and splice length are presently in a state of flux, so an incontrovertible definition of the lengths needed is not possible. However, Table 4.3 shows development lengths for #11, 13, and 17 bars for various plausible values of f'_c and f_y, calculated with the 318-89 ACI requirements. They are all significantly longer than the 20 bar diameters used in the viaduct, in some cases by nearly an order of magnitude.

Recent research on bond has demonstrated the importance of good confinement in a splice or anchorage region. Such confinement was clearly lacking in the Alaskan Way

ALASKAN WAY VIADUCT - BAR DEVELOPMENT LENGTHS						
Bottom bar development length (in)						
Bar #	11					
Dia.	1.375					
Area	1.56					
fy	40	45	50	55	60	
f'c						
3000	136	153	169	186	203	
3500	126	141	157	173	188	
4000	117	132	147	161	176	
4500	111	125	138	152	166	
5000	105	118	131	144	158	
5500	100	113	125	138	150	
Bar #	13					
Dia.	1.625					
Area	2.07					
fy	40	45	50	55	60	
f'c						
3000	180	202	225	247	270	
3500	167	187	208	229	250	
4000	156	175	195	214	234	
4500	147	165	184	202	220	
5000	139	157	174	192	209	
5500	133	149	166	183	199	
Bar #	17					
Dia.	2.125					
Area	3.55					
fy	40	45	50	55	60	
f'c						
3000	309	347	386	424	463	
3500	286	321	357	393	428	
4000	267	301	334	367	401	
4500	252	283	315	346	378	
5000	239	269	299	329	358	
5500	228	256	285	313	342	

Table 4.3 Development Lengths

Viaduct, so the splices would probably fail if they were subjected to inelastic cyclic load reversals. Splices occurred within a potential plastic hinge region in the columns at locations 1 and 3.

Anchorage of bars at the ends of members is also important. In this respect, two regions were of particular concern. First, the bottom bars in the main cross beams were #17, yet they continued into the columns for a maximum of only 45 inches. This is only 15 percent of the length required by ACI 318-89. Even if those requirements are somewhat conservative, it is likely that the bars would pull out before they reached yield. If the bottom bars pulled out, a crack would open up at the column face, across which the concrete could carry no shear. All the shear (approximately 400 kips) would then fall on the two #17 top bars in dowel action. They would be unable to carry this load. In addition, the positive moment strength of the joint would be lost.

The second region of concern was the longitudinal girders. They were reinforced with #17 bars top and bottom. There were six #17 top bars, all placed in a single plane in the top of the curb, with virtually no confinement reinforcement, as shown in Fig. 4.14. This arrangement could create significant splitting forces in the plane of weakness. Furthermore, three of the bars did not pass through the column, so they would be useless for resisting seismic forces. Any longitudinal forces induced in them would create torsion in the cross beam where it joined the column. This region is already one of potential distress, as described previously. Last, the bottom reinforcement, also #17, was spliced about 1.5 girder depths from the column and so was in a potential plastic hinge zone.

Sequence of Collapse — Transverse

Simple calculations were done to evaluate the most likely sequence of collapse in the transverse direction. This direction was chosen because the information from the Loma Prieta earthquake suggested that in all the freeway structures in San Francisco and Oakland, regardless of orientation, much more damage was inflicted transversely than longitudinally.

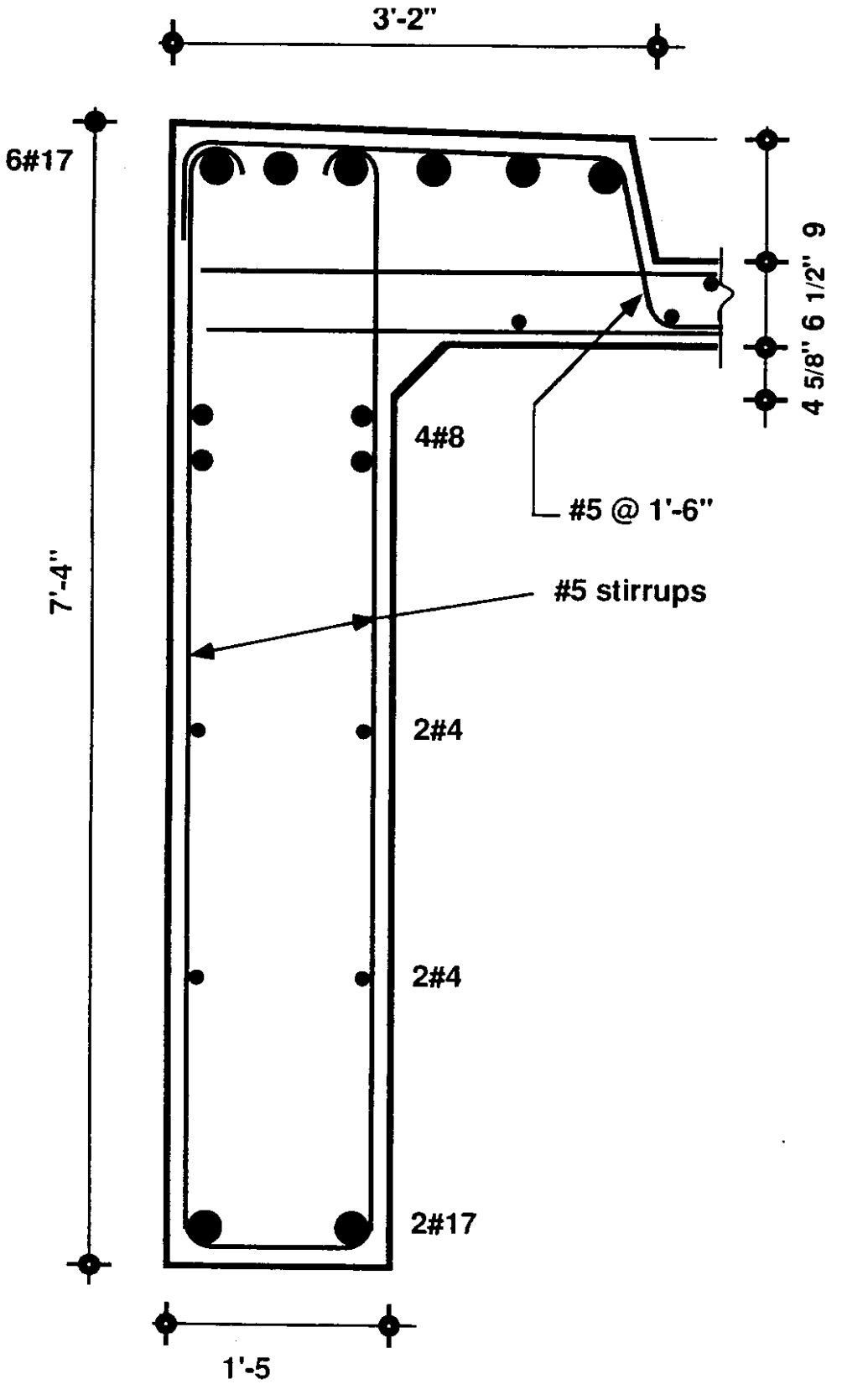

Figure 4.14. Section of Longitudinal Girder

The reasons for this behavior are not clear, although some engineers have suggested that lack of coherency of ground motion along the length of the structures may have reduced their potential for damage.

The negative and positive moment strengths, M_n, of the interior cross beams would be 1,418 and 1,587 ft-kips if the bars reached f_y=40 ksi. Because the moments in the columns at locations 2 and 3 would both have to be equilibriated by the cross-beam moment, a g-rating of 8.6 percent was established for the cross beam, as shown in Table 4.4, assuming a strength reduction factor, ϕ, of 1.0. This g-rating would reduce to 6.0 percent if ϕ=0.7.

The bottom #17 cross beam bars were embedded for only 45 inches in the column. Assuming that the concrete strength was 5,500 psi and f_y=40 ksi, the required development length for a #17 bar would be 228 inches, of which only 20 percent would be available. The bars would then start to debond at a stress of approximately 8 ksi, giving a real moment strength, M_n, of approximately 315 ft-kips, and a g-rating of 1.7 percent (ϕ=1.0) or 1.2 percent (ϕ=0.7).

The moment strength of the column at location 1 would also be reduced, in light of the short splice (28 inches) in the #11 bars there. However, the g-rating of the cross-beam would still be significantly lower than that of the column at location 1, even in the latter's down-graded form.

The bar force at which debonding would start cannot be predicted with certainty. The characteristics of the #17 bars (lug pattern, etc) were not known, and some effects of confinement would be likely, since the cross-beam was much narrower than the column. However, even if the development length were one half of that required by ACI, debonding would still occur at a structural acceleration of 0.034g.

Such a low predicted strength suggests that the joint should have sustained damage in the 1965 Seattle earthquake, yet no cracks were seen at that location during the visual

Interior frame			
No debonding			
Element	Mn(P)	M(1g)	g-rating
			(phi=1.0)
Column loc 1	2664	15060	17.7%
Column loc 2	3100	12628	24.5%
Lower Cross beam	1587	18348	8.6%
Column loc 3	3100	5720	54.2%
Column loc 4	3537	5720	61.8%
Upper Cross beam	1587	5720	27.7%
Interior frame			
Debonding			
Element	Mn(P)	M(1g)	g-rating
			(phi=1.0)
Column loc 1	750	15060	5.0%
Column loc 2	3100	12628	24.5%
Lower Cross beam	315	18348	1.7%
Column loc 3	3100	5720	54.2%
Column loc 4	3537	5720	61.8%
Upper Cross beam	315	5720	5.5%

Table 4.4 Influence of Debonding on g-Rating

investigation, and WSDOT reported that its post-earthquake inspection crews saw none either. This evidence suggests that either the detail is much stronger than conventional analysis implies, or that the applied loads were small. The strength of the connection would be best determined by physical testing, whereas the applied loads can only be estimated from a more detailed study of the soil-foundation-structure system.

In these calculations, the concrete strength was assumed to be 5,500 psi, but the steel yield stress was 40 ksi. If the steel was in fact stronger, debonding would become even more likely to precede yield, although the load at which debonding started would be unchanged.

CHAPTER 5

RECOMMENDATIONS/IMPLEMENTATION

The decision to improve the seismic performance of the Alaskan Way Viaduct would undoubtedly be an expensive one. Thus, repairs should be made judiciously. Unfortunately, the extent of the inadequacies were only investigated in a preliminary manner during this study. Further research is required to more clearly assess the vulnerability of the Alaskan Way Viaduct.

5.1 CRITERIA

The criteria by which safety of the structure is to be judged must be agreed upon. Should the structure be repaired to withstand current AASHTO seismic criteria? Should the criteria be similar to those used to evaluate the viaducts in California? How do the California evaluation procedures rate the Alaskan Way Viaduct?

5.2 GEOTECHNICAL INFORMATION

More information on subsurface soil conditions and on existing foundation conditions is needed to improve geotechnical estimates of soil and foundation response. Further investigation of subsurface geometry and material properties, and of the actual foundation details, including their strength, is also necessary. Better definition of subsurface conditions will allow improved prediction of site-specific ground response. Reliable evaluation of foundation stiffnesses may involve full-scale field testing. Investigation of vulnerable foundation elements, such as the composite pile splices in the WSDOT section, may also be required. These investigations are required to more accurately model the response of the structure to earthquake loads.

5.3 DETAILS

The poor detailing of the structure suggests that response modification factors should be low, but they may be greater than the conservative estimate of 1.0. However,

unless some of the more vulnerable details are tested, reliable estimates are impossible. These tests should be coordinated with California studies, where possible, to prevent duplication of effort and increase the efficiency of the investigation. The selection of details to be tested should follow more detailed analysis and review of tests by other investigators.

5.4 MATERIAL PROPERTIES

Concrete and steel samples should be obtained from the structure so that calculations can be based on actual properties rather than nominal, and thus, conservative, ones.

5.5 ATYPICAL FRAMES

The influence of atypical frames must also be investigated by further analysis and, if necessary, by testing. The particular analyses to be performed will depend on the details of the atypical frames. Structural drawings of atypical frames were not reviewed in this preliminary study.